Journal: ACP
Title: Simulating the SOA formation of isoprene from partitioning and aerosol phase reactions in the presence of inorganics
Author(s): R. L. Beardsley and M. Jang
MS No.: acp-2015-820
MS Type: Research article

To the editor and referees,

We appreciate the time you spent reviewing our manuscript and providing comments. We have responded to each of the comments and modified the manuscript to reflect this. Below we have listed the referee comments with the associated response and updated sections to the manuscript listed directly after each comment. We have also copied the entire modified manuscript and supplemental information including figures (with track changes shown) to the end of this document. A few of the comments led to modifications of large sections of the manuscript and in these cases we provide line numbers associated with the copied manuscript instead of copying the entire section. We feel the manuscript is improved and we hope that our responses meet your expectations. Thanks again for your time and input.

Sincerely,

Ross L. Beardsley and Dr. Myoseon Jang

Anonymous Referee #1

General comments:

1. **Referee's Comment:**
   "*It is not clear in the introduction section what the authors are trying to accomplish in this paper. There are in fact many models that already exist which model the formation of isoprene SOA including aqueous reactions and OS formation etc...(McNeill et al., 2012; Pye et al., Gaston et al., 2014, and likely others.). In this case, what is the issue which the authors are trying to address? Is there a clear deficiency in these other models that their model can improve upon? Is there missing chemistry for isoprene in other models? Although there are some places in the paper that hint at what the point of this paper is, it is far from clear and would benefit from stating these facts up front rather than buried somewhere in the paper.*"

   Response:

   There have been some recent model studies that employ uptake coefficients predicted as a function of inorganic aerosol composition to simulate the aqueous phase reactions of isoprene photooxidation products, such as the study by McNeill et al. (2012) in which the photochemical box model GAMMA was used to predict aqueous phase SOA production in the presence of deliquesced ammonium sulfate, and Pye et al. (2013) in which the aqueous phase, heterogeneous uptake of IEPOX and methacrylic acid epoxide (MAE) were added to CMAQ. These approaches focus on a few chemical species utilizing

empirically determined uptake coefficients or effective Henry's constants (when available), and set branching ratios to estimate OS formation. They require parameters for each compound, which is why they focus on compounds such as IEPOX and glyoxal whose individual SOA formation have been experimentally investigated due to contributing a significant amount to ambient and chamber generated SOA and being used as tracers for aqueous phase SOA formation. While, the aqueous phase SOA formation of these compounds contribute significantly to the overall SOA mass production of isoprene, they do not account for the majority of the mass production. Although most isoprene photooxidation products are highly volatile, they are also highly reactive allowing for the formation of oligomers through aqueous phase reactions, but also through organic-organic oligomerization reactions and partitioning of later generation products. Surratt et al. (2006) measured the composition of isoprene SOA under varying NO_x conditions with and without effloresced inorganic seed and in the presence of deliquesced, acidified ammonium sulfate seeds, and found oligomers contributed a large fraction of the total SOA mass in all cases. A number of other studies have also observed organic-organic oligomerization in isoprene SOA, including Nguyen et al. (2010) who measured oligomers after an hour of isoprene ozonolysis without inorganic seed with 'the absolute majority' of detected peaks corresponding to highly oxidized oligomers. The formation of a wide range of high MW products from isoprene oxidation in the absence of an inorganic aqueous phase demonstrates the importance of organic-organic oligomerization reactions. Furthermore, these studies show that a large number of compounds are contributing to SOA mass even if there individual contributions are small. For example, Nguyen et al. (2010) assigned 1000 peaks with only a small fraction corresponding to known products. This is also the case in the presence of inorganic acids. In Surratt et al. (2006), the presence of acidified ammonium sulfate seeds led to 3.6 times more SOA mass, but 2-methyltetrols and C_5 alkene triols, which are proposed to be major products of aqueous phase reactions, contribute only 0.46% and 0.06% to the total SOA mass. Additionally, a matrix-assisted laser desorption ionization mass spectrometer was employed to determine the range of *m/z* of the SOA products, and the product distributions were similar for low NO_x isoprene SOA in the presence of dry ammonium sulfate seed and liquid acidified ammonium sulfate seed. Similarly, in Edney et al. (2005) 2-methylglyceric acid and 2-methyltetrols only made up 6% of the SOA in the presence of acidic inorganic seed with a majority of the SOA mass being unidentified. Therefore, while the aerosol phase products of IEPOX and glyoxal are viable tracer species due to their high concentrations and distinct fragmentation signatures, the aqueous phase SOA formation of these products is not fully representative of the total mass from isoprene SOA formation. The photooxidation of isoprene produces a wide range of highly reactive products (epoxides, carbonyls) that can form SOA products through a number of aerosol phase reactions.

UNIPAR utilizes the near-explicit Master Chemical Mechanism (MCM) to estimate the SOA formation of all of the known isoprene photooxidation products through partitioning, inorganic aqueous phase reactions (hydration, acid-catalyzed, OS formation), and organic-organic oligomerization reactions. The lumping structure of

SVOC utilized by UNIPAR was developed to be representative of the thermodynamic properties and particle phase chemistry of organic compounds. All of known products of isoprene photooxidation products from MCM are lumped as a function of VOC/NO_x using the individual chemical structures from the Master Chemical Mechanism, which allows for estimation of vapor pressure and chemical reactivity in aerosol phase accretion reactions. In previous work, the aerosol phase reactivity of various model carbonyls with acidic inorganic seed was measured in a flow reactor and the aerosol growth was used to establish a predictive model for the aerosol phase rate constant, $k_{AR,i}$, of each species (i). In the absence of inorganic seeds or in the organic layer of a liquid-liquid phase separated (LLPS) aerosol, the same predictive model is used to estimate $k_{AR,i}$, but the terms associated with inorganic aerosol approach zero and it is just a function of the reactivity of i. This allows UNIPAR to simply predict the SOA formation of isoprene and other VOCs for varying aerosol composition (organic only, mixed inorganic-organic, LLPS in-or). In this way, UNIPAR exploits the individual product structures provided by the explicit gas model, but does not require the explicit model to be run online. The gas phase concentrations are scaled to VOC/NO_x and the SOA formation is determined as a function of the properties of the partitioning species and the size and composition of the aerosol phase.

The distribution of isoprene's lumped stoichiometric mass coefficients ($\boldsymbol{\alpha}$) in UNIPAR highlights the potential SOA mass contribution of other reactive isoprene products. Table 1 shows the combined $\boldsymbol{\alpha}$ of IEPOX, glyoxal, and methylglyoxal along with the summed $\boldsymbol{\alpha}$ of all other isoprene products with one or more aldehyde and/or epoxide for a range of initial VOC/NO_x. It is clear that while the individual contribution of other products may not be as large as that of IEPOX or glyoxal, the total contribution of other reactive species can be as great or greater than the contribution from those few species.

VOC/NOx	100	62.5	50	33	25	16	12.5	8
IEPOX+GLY+MGLY	0.02	0.03	0.04	0.06	0.08	0.10	0.11	0.11
OTHER M, F, VF	0.28	0.31	0.32	0.34	0.34	0.34	0.34	0.31

Table 1. Summed stoichiometric mass coefficients from UNIPAR of IEPOX, glyoxal and methylglyoxal, and all other reactive species (one or more carbonyl/epoxide) as a function of VOC/NO_x ratio (ppbC/ppb). The reaction begin with sunrise and the reaction time is determined based on the model protocol (near 1PM).

Modification to manuscript:

The introduction has been modified in order to clarify the purpose of this work and how it relates to previous model studies of isoprene SOA formation from aqueous phase reactions. The changes can be seen in **Sect. 1 (Page 3, Line 29 – Page 4, Line 19)** in the modified manuscript with track changes (at end of this document), and have been copied below.

"More recent studies have modeled aqueous phase SOA production using empirically determined uptake coefficients or effective Henry's constants (when available) to estimate reactive uptake of major isoprene products, such as IEPOX and glyoxal, in the inorganic aqueous phase (Marais et al., 2016; McNeill et al., 2012; Pye et al., 2013; Woo and McNeill, 2015). For example, McNeill et al. (2012) developed the box model GAMMA to predict the aqueous SOA production of isoprene in the presence of deliquesced ammonium sulfate. Pye et al. (2013) modified the regional Community Multi-scale Air Quality model to include the heterogeneous uptake of IEPOX and methacrylic acid epoxide. While these models greatly improve the predictions of isoprene SOA formation over classical partitioning models, SOA formation of these known products via aqueous phase reactions is not fully representative of total isoprene SOA formation. Edney et al. (2005) measured the composition of isoprene SOA in the presence of acidic inorganic seed, and methylglyceric acid and 2-methyltetrols, which are tracer species for aqueous phase reactions, made up only 6% of the total SOA mass with the majority of the products being unidentified. Furthermore, highly oxidized oligomers comprise the majority of isoprene SOA even in the absence of an inorganic aqueous phase (Nguyen et al., 2010; Surratt et al., 2006) due to aerosol phase reactions in organic-only aerosol. The photooxidation of isoprene produces a large number of highly reactive products (epoxides, carbonyls) that will react even in the absence of an inorganic aqueous phase to produce the large fraction of high molecular weight (MW) species. Therefore, while the high contribution of the aqueous phase products of IEPOX and similar compounds make them ideal tracers, they are not fully representative of isoprene SOA as is demonstrated by the large number of high MW products and lack of mass closure in isoprene composition studies even in the absence of an inorganic aqueous phase.

In this study, the Unified Partitioning-Aerosol Phase Reaction (UNIPAR) model, which was previously developed and applied to aromatic VOCs (Im et al., 2014), was updated and expanded to model the SOA formation of isoprene in the presence of low VOC/NO_x (due to the high sensitivity to $[H^+]$ in the low NO_x regime) and aerosol acidity using natural sunlight. UNIPAR predicts SOA formation from gas-particle partitioning, and oligomerization reactions in both organic-only aerosol and the inorganic aqueous phase using a lumping structure that was developed to be representative of the thermodynamic properties and chemical reactivity of oxidized products in the aerosol phase. The model was validated using outdoor chamber data from isoprene photooxidation experiments with and without acidic inorganic seeds."

2. **Referee's Comment:**

"*The paper is also generally overly complex and disorganized. A number of equations can be in the supplemental information rather than in the main paper, and the same can be said for the explanation of these equations. It is not quite clear why the authors would use so many different parameters to describe acidity of the aerosol, and then try to investigate the effect of these parameters on SOA yield. At the end of the day it may be*

the particle pH that is important for aqueous reactions, but all the other parameters used will also affect the particle pH. For example, LWC affects the acidity, as does the "free sulfate". Because of this, it is not possible to understand what is actually controlling what process. I would suggest that the authors use one term that describes acidity and in particular the particle pH. The paper would be made much clearer if it was organized in such a way as to separately describe the effects of pH, LWC and sulfate (because SO4 is responsible for OS and also effects the pH) on the SOA yield, rather than the manner which it is done currently."

Response:

The model description has been modified and the full derivation of model equations has been moved to the supplemental information with only necessary equations being shown in the manuscript. The modifications span multiple sections (**Sect. 3.3 and 3.3.1**) and are too long to copy here so please refer to **Page 9, Line 26** – **Page 12, Line 9** in the updated manuscript copied at the end of this document.

Referee #2 asked a similar question regarding the discussion of particle acidity and separating the discussion of each effect. Please refer to the response to Referee #2's Major Comments 1a-1d (one response for 4 comments).

3. **Referee's Comment:**
"Some experiments were conducted with acidic particles. It is unclear how relevant these particles are to the ambient atmosphere. The authors need to compare their aerosol acidities with what might be expected in the atmosphere. The same can be said for the range of VOC/NOx used in these experiments."

Response:

In the acidic seeded experiments of this study, H_2SO_4 solution was nebulized into the chamber to generate inorganic seed. Although, pure H_2SO_4 seeds are initially more acidic than typical ambient inorganic aerosol, NH_4^+ generated from the chamber walls and the formation of OS quickly begin to neutralize the H_2SO_4. Furthermore, since the isoprene SVOC and inorganic aerosol form a single homogeneously mixed aerosol phase, the growth of SOA mass will dilute $[H^+]$ (mol/L aerosol). In order to determine if the acidity of these experiments is relevant to ambient particles, the pH of our experimental aerosol can be compared to that of the S.E. U.S as was measured by Guo et al. (2015). The measured mean pH in the S.E. US, which is known to have highly acidic aerosol, was 0.94 with a minimum and maximum of -0.94 and a 2.23, respectively. In experiment SA1 of this study, the pH starts at -0.70 and steadily increases throughout the experiment to finally reach 1.35. In experiment SA2, the pH ranges from -0.72 to 0.65. Therefore, the acidity of the aerosol in this study are representative of regions of the ambient environment with acidic aerosol.

The range of high VOC/NO_x (ppbC/ppb) used in these experiments, or low NO_x or 'NO_x limited' conditions, are typical of rural or areas down wind of urban centers (Finlayson-Pitts and Pitts, Jr., 1993). Pun et al. (2003) measured the 24-hr average VOC/NO_x ratio within Atlanta and found it to always be greater than 5.5 and range from 5.6-8.4. As the plume moves downwind from the city, this ratio will increase as NO_x decays more rapidly than VOCs meaning that NO_x limited conditions will dominate this area, which is infamous for isoprene derived SOA. Low NO_x conditions are especially relevant for isoprene SOA as isoprene is a biogenic VOC whose emission will be highest in rural areas and highly forested areas, such as the S.E. U.S. (similar to conditions of this study) and the Amazon (very low NO_x).

Modification to manuscript:

The relevance of our experiments to ambient aerosol has been reflected in the updated manuscript at the end of the document and is copied below.

From **Sect 4.1, Page 15, Lines 10-16**

"The predicted pH is relatively stable in the first hour of the experiment because the effects of decreasing RH (and LWC) and increasing [NH_4^+] counteract each other, but once SOA formation starts pH increases rapidly due to titration by NH_3 produced from the chamber walls, the consumption of [SO_4^{2-}] by OS formation, and the dilution of [H^+] by SOA mass. Overall, the predicted pH starts at -0.73 and increases to 0.65 at the end of the experimental run, which is within the range of ambient aerosol pH measured by Guo et al. (2015) in the S.E. U.S (mean: 0.94, min: -0.94, max: 2.23)."

From **Sect 4.2, Page 16, Lines 11-13**

"However, very little investigation has been performed on isoprene SOA formation within the low NO_x regime (VOC/NO_x > 5.5 and NO_x > 0 ppb) of this study, which is typical of rural areas downwind of urban centers (Finlayson-Pitts and Pitts, Jr., 1993)."

Specific comments:

4. **Referee's Comment:**
"**Pg 33135, line 23-24:** *If it is acidity of some sort which is required for aqueous reactions to occur how does one explain the OM_AR being the dominant contributor (65%) to experiments without any SA seed particles? For that matter, how is an experiment without any seed particles relevant to the ambient atmosphere? The authors are relying upon nucleation of isoprene products to make particles, which only occurs here because they are using ppm levels of isoprene in their chamber. This will not occur in the real atmosphere, and so the authors must explain the utility of such experiments without any pre-existing seed particles.*"

Response:

The purpose of the isoprene-NO_x photooxidation experiments in the absence of inorganic seed is to test the model prediction of organic-organic oligomerization reactions. As was discussed in our response to Comment #1, oligomers have been detected in SOA from the oxidation of isoprene and many other volatile organic compounds (VOC) in the absence of an inorganic seeded aqueous phase. The volatility of isoprene photooxidation products means that partitioning cannot account for the SOA mass resulting in the absence of inorganic seed or the in the presence of effloresced (dry) inorganic seed, but the reactivity of these species due to the presence of carbonyls and epoxides allows for organic-organic oligomerization reactions to occur. In the absence of a aqueous inorganic phase, UNIPAR estimates the aerosol phase reaction rate of each compound using the same parameterization (Eq 7 in the manuscript), but the inorganic associated terms (LWC, [H+]) approach zero and the reaction rate is predicted as a function of the reactivity of the partitioning species.

Although isoprene concentrations will not be high enough in the ambient atmosphere for self-nucleation to occur, there may be areas in which sub-micron aerosol are dominated by organics or more typically where the inorganic and organic layers of the aerosol are liquid-liquid phase separated (LLPS). In either case, there would be an aerosol liquid phase with highly concentrated organics that can interact and engage in organic only aerosol phase reactions. In our experiments, there are low levels (~1 µg/m3) of preexisting seed (M_o) even after pre-cleaning that allow for the initial absorption of isoprene SOA products. Theoretically, we could introduce an organic seed but there is no reason to believe that a single component organic seed would be any more representative of actual atmospheric processes. Performing isoprene photooxidation experiments in the absence of inorganic seed provides a simple means of evaluating our model for these organic-organic reactions.

Modification to manuscript:

This has been clarified in the updated manuscript at the end of the document and is copied below.

From **Sect 4.1, Page 13, Lines 3-20**:

"The experiments performed in the absence of inorganic seed (ISO1 and ISO2) are used to test the prediction of organic-only oligomerization by UNIPAR. SOA formation is reasonably predicted in the absence of an inorganic aqueous phase for both experimental conditions with a maximum SOA yield ($Y_{SOA} = \Delta OM_{exp}/\Delta Iso$) of 0.025 and 0.007 for ISO1 and ISO2, respectively. These SOA yields are similar to those of reported literature values for isoprene in the absence of acidic seeds (Dommen et al., 2006). The model marginally overestimates the SOA formation in beginning of each chamber run, but the modeled OM_T falls within the range of error of OM_{exp} once the rate of SOA formation stabilizes and reaches a maximum. OM_{AR} makes up the majority of OM_T (>65% in ISO1 and ISO2). This is in agreement with the work of Nguyen et al. (2010) and Surratt et al. (2006) who analyzed the composition of isoprene SOA formed in the absence of an

inorganic aqueous phase and found that the majority of SOA mass was from oligomeric structures. Furthermore, UNIPAR predicts that the approximately 70% of the OM_T is from lumping group $3OS_p$-M, of which more than 93% of the mass contribution is organic peroxides (MCM products C510OOH (~40%), C57OOH (~27%), C58OOH (~15%) and HMACROOH(11%), structures shown in Fig. S7 of the SI). This is close to the measurements of Surratt et al. (2006), in which 61% of the total mass in the absence of seeds is from organic peroxides."

5. **Referee's Comment:**
"**Pg 33134, lines 1-4:** *It has already been shown (minerath et al., 2008, barsanti et al...) that functional groups such as alcohols and aldehydes are likely to react too slow under realistic atmospheric conditions to make much OS. Including them here may be inducing more OS than is realistic. The authors need to justify including them here.*"

Response:

Minerath et al. (2008) investigated the bulk phase formation of OS from simple alcohols and stated that 'it appears that these reactions are kinetically infeasible for low temperature upper tropospheric SOA' and for lower tropospheric SOA 'it appears that the aerosol acidity is rarely high enough such that these reactions are likely to be responsible' for OS in SOA. However, bulk phase investigations may not be representative of actual aerosol processes, and many studies have measured the OS formation of alcohols and aldehydes in the aerosol phase (Eddingsaas et al., 2012; Liggio et al., 2005; Li et al., 2015a; Zhang et al., 2012). E.g., Eddingsaas et al. (2012) measured OS formation from alcohols in SOA from particle-phase sulfate esterification of multi-functional alcohols, and concluded that esterification is likely faster for the complex alcohols typical of VOC photooxidation than for the simple alcohols investigated in Minerath et al. (2008). Therefore, we still predict the OS formation of all three functional groups within UNIPAR since they have all been found to form OS in studies of particle phase processes. The increased tendency of epoxides to form OS is accounted for in our model since epoxides have 2 potential reaction sites instead of one for alcohols and aldehydes.

Modification to manuscript:

The citation for the OS from alcohols has been updated to include Eddingsaas et al. (2012).

From **Sect 3.3.2, Page 13, Lines 1-2**:

"The functional groups that have been shown to form *OS* are alcohols (Eddingsaas et al., 2012; Li et al., 2015b; Minerath et al., 2008; Zhang et al., 2012), aldehydes (Liggio et al., 2005), and epoxides (Surratt et al., 2010)."

6. **Referee's Comment:**

"**Pg 33124, lines 5-8:** *a mechanistic reason(s) for these facts should be included here if possible. Pg 33124, lines 4: "lowly" is poor grammar. This is also written throughout the paper and should be changed accordingly.*"

Response:

The reasons for higher sensitivity at low VOC/NO_x conditions have been added to the manuscript and the modified sentence is copied below. The use of 'lowly' has been removed throughout.

Sect 1, Page 3, Lines 7-9

"In the presence of high NO_x, SOA formation will depend on the ratio of NO_2 to NO with isoprene SOA yields being be lower at low NO_2/NO due to RO2 reacting with NO to produce more volatile products (Kroll et al., 2006; Surratt et al., 2010)."

7. **Referee's Comment:**
"**Pg 33125, lines 3-4**: *poor grammar in this last line. Make it two sentences.*"

Response:

The manuscript has been modified and the second half of the last line was determined to be unnecessary and was removed.

Modification to manuscript:

Sect 1, Page 4, Lines 29-31

"The model was validated using outdoor chamber data from isoprene photooxidation experiments with and without acidic inorganic seeds."

8. **Referee's Comment:**
"**Pg 33126, first paragraph:** *there is no mention of the issue of semi-volatile gas-phase wall losses. This is a recent area of concern for chamber studies and should at least be mentioned.*"

Response:

SVOC wall loss was mentioned previously in Sect. 4.4 (Model sensitivity, uncertainty, and limitations). A few additional lines have also been added.

Modification to manuscript:

Sect 4.4, Page 21, Lines 20-27:

"A number of recent studies have found that the loss of gas phase vapors to chamber walls can compete with gas-particle partitioning (Matsunaga and Ziemann, 2010; Zhang et al., 2014, 2015). Vapor wall loss was not accounted for in this study and thus the experimental SOA mass may be low biased. However, based on the conclusions of Zhang

et al. (2015), the high volatility of isoprene products likely results in gas-particle partitioning outcompeting vapor wall loss in chambers with a large ratio of volume to surface area."

9. **Referee's Comment:**
"**Pg 33127, line 2:** *insert "the" after "on" Pg 33127, lines 23-27: Some justification or reasoning for selecting these reactivity bins, and how compounds were assigned to these bins would be very useful here.*"

Response:

The typo was corrected (**Page 6, Line 28** in manuscript at bottom of document). A brief description of how the reactivity bins in UNIPAR were developed has also been added, as is shown below.

Modification to manuscript:

Sect. 3.1, Page 7, Lines 21-29

"The reactivity bins were developed based on previous work in which the measured gas-particle partitioning coefficients (K_p) of toluene and α-pinene SOA products were found to deviate from the theoretical value due to higher than expected particle concentrations. The degree of deviation was found to depend on the functionalization of the SOA product (Jang et al., 2002; Jang and Kamens, 2001). The experimental log(K_p) of ketones (S reactivity bin) were found to be only slightly higher than the theoretical value, while the experimental log(K_p) of conjugated aldehydes (M reactivity bin) and the products associated with F and VF reactivity bins were found to be 10-40 times higher and 2 to 3 orders higher, respectively."

10. **Referee's Comment:**
"**Pg 33128, lines 8-10:** *choosing the concentrations of each group based on the maximum HO2/NO ratio seems arbitrary. The composition will be dependent upon a number of factors such as this ratio, and time etc... its not clear why this particular value was selected and what effect this would ultimately have on the final model results.*"

Response:

UNIPAR was developed to be a self-contained module which requires no additional inputs other than those commonly available within current regional and global models. We cannot utilize the near-explicit Master Chemical Mechanism online since it not feasible to do so in a regional model. Since we cannot run an explicit gas phase model online within the current framework, we need to lump the individual products at a set time in order to determine the stoichiometric mass coefficients of each lumping group. In the previous application of UNIPAR to aromatic hydrocarbons, the concentrations of each of the SOA products were lumped when half of the VOC had reacted at each

VOC/NO_x (Im et al., 2014). In this version, we wanted to use a more dynamic method of determining the time of lumping based on different oxidative conditions of each run. The maximum HO_2/NO was chosen as this represents the shift in RO_2 chemistry (and overall gas phase chemistry) where the more oxidized products that contribute to SOA are formed (i.e. IEPOX). Furthermore, the maximum HO_2/NO also typically corresponds with the period in which the majority of SOA formation occurs. The early generation products of isoprene photooxidation (when HO2/NO is low) are highly volatile and unlikely to form SOA. While, this lumping approach with fixed concentration for each initial VOC/NO_x is not as representative of the actual gas phase composition as the use of a fully explicit model would be, it is representative of the gas phase at the time in which most of the SOA are formed and provides a simple solution that fits within the framework of our self-contained model. Overall, we agree with the reviewer in that online explicit gas phase mechanisms could be incorporated within UNIPAR to allow for better prediction of dynamic compositions over atmospheric photooxidation of hydrocarbons, and we plan to test this for chamber simulations in the future. However, the current structure is most suitable for application in large scale models. Although the lumping structure would not be necessary within an online frame in the future, the gas-particle partitioning and reaction rate constants based on the organic molecular structures are still suitable for an explicit SOA model.

11. Referee's Comment:

"**Pg 33129, lines 4-10:** *how similar are the compounds chosen in Bertram et al, to the products of isoprene? Is it valid to use these parameterizations? Also, how well does the UNIPAR model predict the O:C ratio?*"

Response:

Although the parameterizations in Bertram et al.(Bertram et al., 2011) were developed for model compounds with ammonium sulfate seed, the authors tested them for both isoprene SOA and ambient aerosol. These tests show that the parameterizations perform well for isoprene SOA and also for ambient aerosol comprised mainly of oxygenated organics, ammonium, and sulfate and not nitrate or other anions, which is true of the aerosol of this study. O:C was not measured for our experimentally generated SOA, but we compared out model prediction to published isoprene O:C from literature and found that it matched up reasonably well. However O:C will vary between different NO_x and inorganic seed conditions. As is reported in Sect. 4.1 of the manuscript, the literature values of isoprene SOA range from 0.69 to 0.88, while the model predicted O:C range from 0.69-0.98. However, in UNIPAR we do not account for the reduction in O:C that would result from oligomerization, but our predicted O:C are still near literature values.

These parameterizations were applied within UNIPAR because they provide a computationally simple means of predicting the RH of LLPS, ERH and DRH of mixed oxygenated organic/inorganic SOA systems. As with predictions of most SOA

parameters, predicting the RH of these important phase transitions is difficult due to the complexity and unknown nature of many products in mixed systems. Attempts have been made at developing a thermodynamic model for mixed inorganic-organic SOA systems (i.e. AIOMFAC), but these systems have huge uncertainty, are constrained using limited bulk phase liquid data for simple systems, and have large computational requirements (Zuend and Seinfeld, 2012). On the other hand, the Bertram parameterizations were developed empirically using SOA systems, and tested for the SOA similar to those of this study making them the most representative of the systems we are modeling and the most appropriate for our model. If a better approach is developed in the future that meets our requirements, we will revisit our handling of ERH, DRH, and RH of LLPS in UNIPAR.

12. Referee's Comment:

"***Pg33131, equation:*** *This equation and many of the following ones are missnumbered.*"

Response:

Many of the equations have been moved to the supplemental information (based on Comment #13 directly below) and the numbering in the manuscript and the SI have been checked.

13. Referee's Comment:

"**Pg 33133, eq 11:** *it is not clear how this equation was derived. There are too many equations in this section and the text is rather complex and confusing. I suggest simplifying this page and putting it in the supporting info.*"

Response:

The model description has been simplified and many of the equations were removed from the manuscript. The full derivation was added to the supporting information.

Modification to manuscript:

Please refer to **Sect 3.3-3.31 (Page 9, Line 26 – Page 12, Line 9)** and **Sect. S3** in the SI.

14. Referee's Comment:

"**Figure 1:** *It would be useful to have a gas-phase flow chart associated with this one for the aerosol phase....or at least an additional schematic box attached above it.*"

Response:

The figure has been modified. Please refer to new Fig. 1 (**Page 34)** in the updated manuscript at the end of this document to see the changes.

15. Referee's Comment:

"**Figure 2:** *the compound acronyms in the legend need to be described in the caption.*"

Response:

The full names of each of the reactivity bins has been added to the figure caption.

Modification to manuscript:

The caption to Figure 2 has been updated (**Page 37**) and a typo in the legend has been corrected. The new figure caption is copied below.

"Figure 2. The stoichiometric mass coefficients (α_i) of each lumping group at a VOC/NO_x (ppbC/ppb) of 25. The photooxidation products predicted by an explicit gas phase chemical mechanism are lumped as a function of vapor pressure (x-axis, 8 bins) and aerosol phase reactivity (y-axis, 6 bins). The aerosol phase reactivity bins are very fast (VF, α-hydroxybicarbonyls and tricarbonyls), fast (F, 2 epoxides or aldehydes,), medium (M, 1 epoxide or aldehyde), slow (S, ketones), partitioning only (P), organosulfate precursors (OS_P, 3 or more alcohols) and IEPOX products, which were lumped separately to more easily quantify their contribution."

16. Referee's Comment:

"**Figure 3:** *this figure is nearly impossible to read. It must be made bigger and clarified.*"

Response:

The figure was small due to the vertical stacking of the 3 plots. The figures have been reconfigured and made bigger.

Modification to manuscript:

Please refer to the new Figure 3 on **Page 38** of the manuscript at the end of the document.

Anonymous Referee #2

Major Comments:

1. **The role of LWC and [H+] on isoprene SOA formation**

Referee's Comment 1a:

"*The use of [H^+] or fractional free sulfate (FFS) as an indicator of particle acidity is puzzling. It is because particle acidity (pH) represents the hydrogen ion activity in an aqueous solution, which depends not only on [H^+] (in unit of ug/m^3 air or nmol/m^3 air), but also LWC. Using [H^+] as particle acidity is problematic and introduces a lot of confusion in the discussion. For example, p33138 line 12-13, YSOA decreases with increasing RH is a result of increase in pH, instead of reduction in [H^+] (ug/m3 air) as stated in the manuscript. Same argument applies for FFS, which is essentially an ion balance method. Please refer to Hennigan et al. (2015) and Guo et al. (2015) for more discussions on particle acidity. Also, many recent studies have moved beyond ion balance or [H^+], and calculated particle pH when discussing the role of particle acidity on isoprene SOA formation. Therefore, I strongly suggest the authors to use particle pH throughout the manuscript.*"

Referee's Comment 1b:

"*The role of sulfate should be discussed explicitly in the manuscript, considering the following reasons. Firstly, sulfate drives both LWC and particle acidity. Secondly, organosulfate accounts for about 1/3 of total sulfate in the model (p 33136, line 9), which suggests the important role of sulfate as nucleophile. Thirdly, recent ambient measurements have repeatedly observed good correlation between isoprene SOA via IEPOX uptake and sulfate, which suggests that sulfate plays an important role in this process.*"

Referee's Comment 1c:

"*I agree with that particle acidity plays an important role in isoprene SOA formation, especially via IEPOX uptake. However, one needs to be careful when interpreting the effects of particle acidity on isoprene SOA formation from laboratory studies, because sulfate is confounding in many studies. For example, the authors cite Lewandowski et al. (2015) to support the importance of [H^+] (p33142 line 15). However, in Lewandowski et al. (2015), sulfate correlates perfectly with [H^+], so that it is difficult to argue if the yield enhancement is due to [H^+] or sulfate. I strongly suggest that the authors should carefully discuss the confounding effects and provide insights about the role of sulfate, particle acidity (pH), and LWC based on the model simulations.*"

Referee's Comment 1d:

"*The authors should calculate the pH and compare it to ambient measurements in (Xu et al., 2015; Budisulistiorini et al., 2015). Since H2SO4 is used in the study, the particle pH should be lower or comparable with ambient pH. This suggests that isoprene SOA formation (via IEPOX uptake) in this study should not be limited by particle acidity, which is similar to ambient observations.*"

Response to 1a-1d:

In the manuscript $[H^+]$ has units of (mol of $[H^+]$/L of aerosol) and not (mol $[H^+]/m^3$ of air), which seems to the source of the confusion and should have been more clear. Therefore, the pH is simply the negative $\log_{10}$ of the $[H^+]$ used throughout the manuscript, and the discussion on p33138 line 12-13 is correct as increasing the RH does lead to a reduction in $[H^+]$.

Guo et al. (2015) analyzed particle mass concentrations and the associated pH at one site of the Southern Oxidant and Aerosol Study (SOAS). The authors state that 'a simple ion balance or NH_4^+/SO_4^{2-} molar ratio or per-volume-air concentration of aerosol hydronium ion (H^+_{air}) cannot be used as a proxy for pH in the particle,' because it does not account for fluctuations in aerosol liquid water content (LWC) and the impact on pH. We completely agree with the conclusions of this paper, and use the same approach as the authors to calculate particle acidity within UNIPAR. The authors measure the inorganic ion concentration using a PILS-IC, and then input this data into an inorganic thermodynamic model to calculate particle pH. We use exactly the same approach with PILS-IC concentrations of SO_4^{2-} and NH_4^+ input into an inorganic thermodynamic model within UNIPAR. The only difference is that we use inorganic thermodynamic model E-AIM while ISORROPIA-II is used in Guo et al. (2015).

Furthermore, the pH of acidic aerosols in our study fall within the range of pH measured by the authors for the S.E. U.S. In Guo et al. (2015) the median predicted pH was 0.94 with a minimum and maximum pH of -0.94 and 2.23, respectively. While the acidic seeds in our study were created from H_2SO_4 solution before sunrise while RH is high, NH_3 (g) produced from the chamber walls immediately starts to titrate the seeds and increase the pH. Also, the formation of SOA dilutes particle $[H^+]$ as the isoprene SOA are single mixed phase, and the formation of *OS* consumes inorganic SO_4^{2-}. Therefore, our seeds are quickly titrated and are similar in pH to those of the S.E. U.S. For example, the acidic seeds in Experiment SA2 start at a predicted pH of -0.74 and end at pH of 0.63. In order to illustrate this, a new figure (**Figure 4** of the updated manuscript at the end of this document) has been added to the manuscript and copied below.

As can be seen, the pH rapidly increases with the formation of OS and by titration with ammonia. Also, the model does a good job at predicting the OS formation measured by the C-RUV method. Therefore, while the lack of clarification on the units of $[H^+]$ in the original manuscript hindered the interpretation, our approach is in line with the current state of the research regarding particle acidity.

However, we still believe that using fractional free sulfate (FFS) and RH in Figure 6 (of the updated manuscript copied below) instead of pH provides for a clearer visualization of the impact of inorganic composition and LWC on isoprene SOA formation. As stated by Guo et al. (2015), 'measurement of pH is highly challenging, and so indirect proxies are often used to represent particle acidity,' such as the ion-balance method. We provide FFS along with the RH, which are the inputs that the authors of that study used to estimate pH within a thermodynamic model. Measurements of RH, $[SO_4^{2-}]$ and $[NH_4^+]$ are widely available and easy to produce, unlike pH, and can be used to estimate pH

within ISORROPIA or E-AIM. Therefore, we believe our figure and associated discussion more clearly show the dynamics of how isoprene SOA yield relates to $[H^+]$ and LWC, and will be easier to use in future studies by a larger number of research groups.

Modification to manuscript:

The new figure (**Fig. 4** in updated manuscript) can be found on **Page 40** of the updated manuscript at the end of this document.

In addition to adding a figure, the manuscript has been modified to clarify the units of $[H^+]$, to use pH instead of $[H^+]$ where appropriate in the discussion, to compare the range of pH to ambient aerosol, and to more carefully discuss the role of SO_4^{2-}, LWC, and pH.

Sect. 3.2, Page 9, Lines 22-24:

"$[H^+]$ is used to describe particle acidity and has units of mol H^+/L of aerosol. Therefore, $[H^+]$ will change with variation in inorganic composition, LWC and total aerosol mass (SOA). The particle pH is simply the negative log of $[H^+]$."

Sect. 4.2, Page 17, Line 7- Page 18, Line 6:

"Y_{SOA} is also dynamically related to inorganic compositions. SOA formation in the absence of inorganic seed is primarily a function of the characteristics of $i_{m,n}$ and the impact of LWC on isoprene SOA is minimal. However, under ambient conditions SOA will typically be formed in the presence of inorganic aerosol. Variations in the inorganic aerosol composition ($[SO_4^{2-}]$ and $[NH_4^+]$) and RH lead to significant changes in LWC and pH. At high LWC, the total volume of absorptive mass (M_{mix}) increases allowing for hydrophilic $i_{m,n}$ to partition into the aerosol in significant amounts and engage in aerosol phase reaction. Additionally, highly reactive species such as IEPOX will react to rapidly form SOA in the presence of $[H^+]$ (Gaston et al., 2014). In Fig 6 the simulated Y_{SOA} is plotted as a function of the fractional free sulfate (FFS), $([SO_4^{2-}]-0.5[NH_4^+])/[SO_4^{2-}]$, and RH. Unlike pH, which is very difficult to measure, $[SO_4^{2-}]$, $[NH_4^+]$, and RH data are widely available and easy to measure, which is why FFS and RH were used in Fig 6. Using an ion balance such as FFS alone has been shown to be not representative of actual particle pH (Guo et al., 2015), but providing both FFS and RH allow for estimation of pH within an inorganic thermodynamic model and ease of use by future studies.

It is difficult to decouple the effects of $[SO_4^{2-}]$, LWC and pH since $[SO_4^{2-}]$ ultimately influences both LWC and pH, but Fig 6 can be used to help elucidate the influence of these effects in UNIPAR. For AS seed (FFS=0.0), SO_4 is entirely titrated by ammonia and the lowest Y_{SOA} occurs below the ERH. As the RH increases, AS becomes deliquesced and the LWC gradually rises leading to an increase in Y_{SOA}. This is true for the predictions at all small values of FFS due to the increase in the total volume of absorptive mass (M_{mix}) associated with increasing LWC, allowing for hydrophilic $i_{m,n}$ to partition into the aerosol in significant amounts and engage in aerosol phase reactions. However, as the amount of $[NH_4^+]$ decreases (FFS < 0.7, highly acidic), the effect of

increasing LWC reverses, and Y_{SOA} decreases with increasing LWC due to the dilution of $[SO_4^{2-}]$ and the resulting increase in pH. If RH is held constant, varying FFS allows for investigation of the effect of pH on Y_{SOA}. Increasing FFS or decreasing pH at constant RH leads to a rapid increase in Y_{SOA} at all RH due to an increase in the SOA formation from the acid catalyzed reactions of species such as IEPOX. Therefore, $[SO_4^{2-}]$ modulates Y_{SOA} within UNIPAR by controlling LWC and $[H^+]$ which influence $k_{AR,i}$ (Eq. 5). The consumption of $[SO_4^{2-}]$ by OS formation is accounted for in UNIPAR through a reduction in acidity and LWC, but the role of $[SO_4^{2-}]$ in reactive uptake as a nucleophile is not directly accounted for."

2. **Referee's Comment:**
"*Many studies have developed models to evaluate the isoprene SOA formation via different pathways from lab scale to global scale, which should be discussed in the manuscript (Pye et al., 2013; McNeill et al., 2012; Lin et al., 2012; Gaston et al., 2014).*"

Response:

Comment #1 by Referee #1 was very similar. Please find the response to Comment #1 by Referee #1.

3. **Referee's Comment:** "*The photooxidation of VOC is predicted explicitly offline and then the concentrations are set at the peak HO_2/NO ratio. This treatment is problematic since the gas phase composition changes dramatically with time. In Figure S2, modelled O3 and NOx do not agree with the measurements, which are probably due to the gas phase treatment. The authors need to test the sensitivity of modeled SOA to the gas phase treatment. I mean, if setting the gas phase concentrations at a different time, how would the modeled SOA change? I want to point out that the agreement between measured and predicted SOA is mainly due to the tuning parameter y in Eq. (7).*"

Response:

Figure S2 shows the explicit gas phase simulation of our experimental data using the Master Chemical Mechanism v3.2 (MCM) within a kinetic solver. All of the offline gas phase simulations are performed explicitly. Then, using the explicit concentrations of each product from the gas phase simulations, the stoichiometric mass coefficients of each lumping group are calculated at the point of the maximum HO_2/NO. Therefore, the difference between the measured and predicted NO_x and O_3 is not due to the concentrations being fixed in the gas phase simulation, because they aren't, but because of inaccuracy of MCM for our experimental conditions. While MCM is the best available tool for explicit gas phase modeling, it is far from perfect as is discussed in the limitations section of the manuscript. For example, the in the case of aromatic hydrocarbons additional OH radicals must be added in order to fit the VOC consumption. Isoprene does not require addition OH radicals, but possibly still has some error. We use

MCM because it is the best available tool for providing explicit concentrations and product structures that we utilize for lumping.

As far as, when the gas phase concentrations are fixed, we chose the maximum HO_2/NO ratio as it represents a shift in RO_2 chemistry that corresponds with the formation of products that are known to form isoprene SOA. Furthermore, the maximum HO_2/NO corresponds with the period of the majority of the isoprene SOA formation. Therefore, lumping at this time is the most representative of the gas phase composition when SOA is forming (see our response to **Referee #1, Comment #10**). Lumping earlier in the photooxidation or later would yield less and more isoprene mass, respectively, due to the gas phase being composed of less and more oxidized products. We feel the current approach is effective and the best way to represent the gas phase composition at the time of SOA formation. However, we believe that SOA model may be much improved when the gas-phase reactions are explicitly simulated without lumping and applied to online aerosol model in the future.

4. **Referee's Comment:** "*In Eq. (6), do the authors consider the aerosol phase reaction between two species or species in two different bins?*"

Response:

For the determination of reaction rate constant of organics, please also find the responses to Comment #9 from Referee #1. Like RO_2 chemistry, the cross reaction in aerosol phase is complex. The aerosol phase reaction rate is calculated using a self-dimerization reaction approach, and so the amount of OM_{AR} formed from each lumping group in each time step is calculated as the product of the concentration of that lumping group in the aerosol phase ($C_{mix,i}$', mol L^{-1}) and the aerosol phase reaction rate constant, $k_{AR,i}$.

Modification to manuscript:

The description of the equation was modified in the manuscript to add the word 'self-' as is shown below.

Sect. 3.3.1, Page 11, Line 6-7:

"the OM_{AR} formation of $i_{m,n}$ is estimated in UNIPAR assuming a second-order self-dimerization reaction as is shown in Eq. 4,"

5. **Referee's Comment:** "*In the model, OM_{AR} is calculated before OM_p. Does the calculation order affect the model results? It is surprising that even in the absence of seed, OMAR is much larger than OMP (p33135, line 22-24), considering the particle acidity is low without the seed. What are the products in OM_{AR} without seed? Is this conclusion affected by the calculation order of OMAR and OMP?*"

Response:

The order of the OM_{AR} and OM_P module does not significantly affect the model results because the model iterates the concentration of each species in the aerosol phase in each module. The contribution of OM_{AR} in the absence of seeds is attributable to organic-organic oligomerization reactions. Referee #1 asked a similar question and this was discussed in detail in the response to Comment #1 by Referee #1, but in summary, oligomers have been shown to comprise the majority of the SOA mass of isoprene in the absence of inorganic seeds and in the presence of dry inorganic seeds (Nguyen et al., 2010; Surratt et al., 2006). The high volatility of isoprene SOA products means that partitioning cannot account for the SOA mass formation observed, and thus aerosol phase reactions are important even in the absence of a liquid inorganic phase. UNIPAR utilizes the same predictive model (Eq. 7 in the manuscript) to determine the aerosol phase reaction rate constant, $k_{AR,i}$, of each lumping species, *i*, in the absence of seed or in the presence of effloresced inorganic salt, except terms associated with the inorganic liquid phase approach zero, and $k_{AR,i}$ is just a function of the reactivity of *i*.

The prediction that the majority of mass is contributed by aerosol phase reactions in the absence of seed agrees with the measurements of Surratt et al. (2006), in which the majority of SOA mass was from high MW species with 61% of this mass from organic peroxides. For Exp. ISO1, UNIPAR predicts that 70% of the total SOA mass is from lumping group 3OSp-M (products with both a carbonyl and alcohols, Figure S3). At the VOC/NO_x ratio of ISO1 (17), $3OS_p$-M is comprised almost entirely of organic peroxides with the MCM products C510OOH (~40%), C57OOH (~27%), C58OOH(~15%) and HMACROOH(11%) making up approximately 93% (structures shown below). Therefore, the predicted SOA composition of UNIPAR in the absence of seed correlates well with

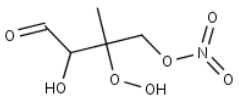

C510OOH

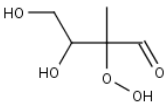

C57OOH

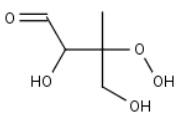

C58OOH

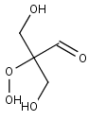

HMACROOH

the measured composition of Surratt et al. (2006) for low NO_x isoprene SOA.

Modification to manuscript:

Sect. 4.1, Page 13, Line 13 – Page 14, Line 20

"The ability of UNIPAR to simulate the SOA formation from isoprene photooxidation in the presence and absence of acidic inorganic seeds under low initial VOC/NO_x was determined through comparison of the simulated OM_T and experimental OM formation (OM_{exp}). All OM_{exp} were corrected for particle wall loss. Fig. 3 shows measured and predicted SOA formation in the presence and absence of SA at initial VOC/NO_x of ~17 for ISO1 and SA1 and 32 for ISO2 and SA2. The experiments performed in the absence of inorganic seed (ISO1 and ISO2) are used to test the prediction of organic-only oligomerization by UNIPAR. SOA formation is reasonably predicted in the absence of an inorganic aqueous phase for both experimental conditions with a maximum SOA yield ($Y_{SOA} = \Delta OM_{exp}/\Delta Iso$) of 0.025 and 0.007 for ISO1 and ISO2, respectively. These SOA

yields are similar to those of reported literature values for isoprene in the absence of acidic seeds (Dommen et al., 2006). The model marginally overestimates the SOA formation in beginning of each chamber run, but the modeled OM_T falls within the range of error of OM_{exp} once the rate of SOA formation stabilizes and reaches a maximum. OM_{AR} makes up the majority of OM_T (>65% in ISO1 and ISO2). This is in agreement with the work of Nguyen et al. (2010) and Surratt et al. (2006) who analyzed the composition of isoprene SOA formed in the absence of an inorganic aqueous phase and found that the majority of SOA mass was from oligomeric structures. Furthermore, UNIPAR predicts that the approximately 70% of the OM_T is from lumping group $3OS_p$-M, of which more than 93% of the mass contribution is organic peroxides (MCM products C510OOH (~40%), C57OOH (~27%), C58OOH (~15%) and HMACROOH(11%), structures shown in Fig. S7 of the SI). This is close to the measurements of Surratt et al. (2006), in which 61% of the total mass in the absence of seeds is from organic peroxides."

6. **Referee's Comment:** "*More model vs measurements plots should be included in order to better evaluate the model performance. For example, the modeled* $[H^+]$ *and* $[SO_4^{2-}]_{OS}$ *should be compared to the measurements (by C-RUV) in the format of time series or scatter plot.*"

Response:

Based on your comment a new Figure was added to the manuscript and was used in the response to Comments 1a-1d above (Fig. 4 in updated manuscript).

Modification to manuscript:

The following discussion of the figure was added to the manuscript,

Sect 4.1, Page 15, Line 1-16

"In addition to OM_T, O:C and $[SO_4^{2-}]_{OS}$ were also predicted using the model. The predicted $[SO_4^{2-}]_{OS}$ is important due to the consumption of SO_4^{2-} that leads to an increase in particle pH and a reduction in LWC. In exp. SA2, $[SO_4^{2-}]_{OS}$ was measured using the C-RUV method allowing for comparison to the model (refer to Sect. 2 for C-RUV method description). Fig. 4 shows time series of the model predicted and measured $[SO_4^{2-}]_{OS}$ along with the total $[SO_4^{2-}]$ and $[NH_4^+]$ measured by the PILS-IC, the measured RH, and the predicted particle pH. Once SOA formation starts, OS quickly forms. The measured $[SO_4^{2-}]_{OS}$ is reasonably well predicted by the model with the predicted value being within the range of error once SOA mass stabilizes. The predicted pH is relatively stable in the first hour of the experiment because the effects of decreasing RH (and LWC) and increasing $[NH_4^+]$ counteract each other, but once SOA formation starts pH increases rapidly due to titration by NH_3 produced from the chamber walls, the consumption of $[SO_4^{2-}]$ by OS formation, and the dilution of $[H^+]$ by SOA mass. Overall, the predicted pH starts at -0.73 and increases to 0.65 at the end of the experimental run, which is within

the range of ambient aerosol pH measured by Guo et al. (2015) in the S.E. U.S (mean: 0.94, min: -0.94, max: 2.23)."

7. **Referee's Comment:** "*OS formation. What's [SO4]? Does it represent the initial SO4 concentration? The calculation of [SO42-]free is confusing. For example, if the seed is NH4HSO4, then all the sulfate should be treated as [SO42-]free and [SO42-]free = 1. However, [SO42-]free is only 0.5 using the algorithm in the manuscript (p33133 line 14). This also applies to the FSS calculation. Also, have the authors compared the OS formation rates in this study to literature values?*"

   Response:

   $[SO_4^{2-}]$ is the total concentration of sulfate in µmol/m^3 at the given time step as is measured by PILS-IC. In the case of the H_2SO_4 experiments, this is the initial $[SO_4^{2-}]$, but in the experiment which began with SO_2(g), $[SO_4^{2-}]$ increases as the SO2 is oxidized in the gas phase to add additional H_2SO_4 (g). In the model we assume that only the SO_4 which is not associated with NH_4 can form OS, which is why we calculate $[SO_4^{2-}]_{free}$. Ranges from 0.0 for $(NH_4)_2SO_4$ to 1.0 for H_2SO_4. Our estimation of OS formation is not kinetically determined, but is calculated as a function of the available SO_4, the number of functional groups that can engage in OS formation (alcohols, aldehydes, and epoxides with epoxides counting twice as much as the other groups), and a weighting parameter that was empirically determined in Im et al. (2014) by fitting the model predicted $[SO_4^{2-}]_{OS}$ to measured value for toluene SOA. The same parameter was applied to predict the $[SO_4^{2-}]_{OS}$ of isoprene SOA and performed well as can be seen in Fig. 4 in the updated manuscript.

8. **SOA yield vs. VOC/NO_x ratio**

   Referee's Comment 8a: "*The authors found that with increasing NOx within the simulation conditions, isoprene SOA yield increases, which seems to be novel and contradicts with previous studies. However, this conclusion is based on the wrong interpretation of previous studies. For example, p33124 line 68 and p33137 line 7-9, the authors claim that "the presence of any significant amounts of NOx will lead to SOA at lower yields than photooxidation under low NOx conditions". This statement is wrong. Both Kroll et al. (2006) (figure 7) and Xu et al. (2014) (figure 6) have shown that isoprene SOA yield has a non-linear relationship with the VOC/NOx ratio and the isoprene SOA yield is higher under intermediate NOx level. With that said, the conclusion in this manuscript is not novel and the conclusion is consistent with previous laboratory studies*"

   Response 8a:

   The sentence "the presence of any significant amounts of NOx will lead to SOA at lower yields than photooxidation under low NOx conditions was indeed too simplified and

incorrect, and has been removed. However, while the non-linear relationship of isoprene SOA yields with VOC/NOx has been shown, there has not been any detailed investigation of the SOA yield in range of VOC/NOx of this study. As is stated in the manuscript, previous studies, including Kroll et al. (2006) and Xu et al. (2014), have primarily investigated isoprene SOA formation in the presence of high NO_x or no NO_x, as is shown in the table below.

	Kroll et al. (2006)						Xu et al. 2014				
Isoprene (ppb)	46.7	43.5	42.7	49.1	42.7	42	97.7	91.4	114.6	105	100
NO_x (ppb)	266	526	129	78	405	745	68.1	114.8	338.2	466.2	738.1
VOC/NO_x (ppbC/ppb)	0.878	0.413	1.655	3.147	0.527	0.282	7.173	3.981	1.694	1.126	0.677

This table shows the VOC/NOx ratio of each of the experiments in those studies performed with NO_x, so the no NO_x OH-initiated experiments are not included. It can be seen that with the exception of 1 experiment from Xu et al. (2014), that all of the runs were high NO_x. Therefore, the majority of the investigation of low NOx isoprene photooxidation was performed in the absence of NO_x, and while the conclusion that the relationship between isoprene and VOC/NO_x ratio is non-linear may not be novel, the detailed investigation of the SOA yield and composition of the SOA for the low NO_x range and in particular, the varying impact of acidity on SOA yield within this range has not presented before to the best of our knowledge.

The manuscript has been updated to reflect this and more clearly represent what is new about this study. The changes are copied below.

Modification to manuscript:

The last line of the introduction has been deleted (**Page 3, Line 10-11** of updated manuscript at the end of this document.)

Sect. 4.2, Page 16, Line 6 – Page 17, Line 6

"Recent studies have investigated the effect of NO_x on the SOA formation of isoprene for the high NO_x regime (VOC/NO_x < 5.5) and in the absence of NO_x (Chan et al., 2010; Kroll et al., 2006; Xu et al., 2014), and found that in the Y_{SOA} of isoprene is non-linearly related to VOC/NO_x with Y_{SOA} being highest at intermediate NO_x conditions (VOC/NO_x = ~2). However, very little investigation has been performed on isoprene SOA formation within the low NO_x regime (VOC/NO_x > 5.5 and NO_x > 0 ppb) of this study, which is typical of rural areas downwind of urban centers (Finlayson-Pitts and Pitts, Jr., 1993). To investigate the influence of the NO_x level on Y_{SOA} in this range, simulations were performed in which the VOC/NO_x ratio was increased incrementally from 10 to 100 with SA seeded SOA without titration and isoprene only SOA. The Y_{SOA} of each simulation are plotted in Fig. 5. Overall, increasing NO_x within this range (decreasing VOC/NO_x) increases Y_{SOA} both with and without acidic seeds, which agrees with the general trend of Kroll et al. (2006) where intermediate NO_x conditions had higher Y_{SOA} than no-NO_x

conditions. However, the degree of the increase in Y_{SOA} with increasing NO_x is different for the isoprene only SOA and the SOA formed in the presence of SA seeds, which has not previously been shown to the best of our knowledge.

Y_{SOA} increases much more rapidly with increasing NO_x in the presence of SA seeds, which is due to an increase in the relative contribution of reactive species. RO radicals produced from the reaction of RO_2 radicals with NO can lead to multifunctional carbonyls via reaction with oxygen and also simple carbonyls such as glyoxal and methylglyoxal through fragmentation of RO radicals. These products are all highly reactive in the aerosol phase and produce OM_{AR}. Furthermore, some late generation RO_2 radicals, whose precursors are formed from the RO pathway (High NO_x), react with HO_2 to form low volatility organic peroxides with alcohol functional groups and an aldehyde ($3OS_p$-M: C510OOH, C57OOH, C58OOH, HMACROOH in MCM, Sect S7). Therefore, increases in NO_x within the simulation condition (VOC/NO_x 10~100) of this study leads to increases Y_{SOA} with higher sensitivity to VOC/NO_x in the presence of inorganic seed. Fig. S5 shows the stoichiometric mass coefficients (α_i) of important products as a function of VOC/NO_x."

Referee's Comment 8b: "*The discussion in section 4.2 is really confusing, which may be caused by the typos in the manuscript. For example, p33137 line 14-15: "Overall, with decreasing VOC/NOx, Y_{SOA} increases in all cases". However, p33137 line 22: "Therefore, increases in VOC/NOx within the simulation condition of this study leads to increases YSOA." There are many typos in the manuscript, which make the discussions very confusing. Most of the equations are mislabeled. For example, it should be Eq. (11) in p33133 line 16, instead of Eq. (10).*"

Response 8b:

We apologize for this typos and they have been corrected.

Referee's Comment 8c: "***p33137 line 10-11.*** *The authors claim that very little investigation has been performed in the low NOx regime (VOC/NOx > 5.5). The authors need to justify why this regime is interesting*"

Response 8c:

Referee #1 asked us (Comment #3) to discuss how relevant the range of VOC/NOx of this study is to the ambient atmosphere, and so we have copied it here.

"The range of high VOC/NO_x (ppbC/ppb) used in these experiments, or low NO_x or 'NO_x limited' conditions, are typical of rural or areas down wind of urban centers (Finlayson-Pitts and Pitts, Jr., 1993). Pun et al. (2003) measured the 24-hr average VOC/NO_x ratio within Atlanta and found it to always be greater than 5.5 and range from 5.6-8.4. As the plume moves downwind from the city, this ratio will increase as NO_x decays more

rapidly than VOCs meaning that NO_x limited conditions will dominate this area, which is infamous for isoprene derived SOA. Low NO_x conditions are especially relevant for isoprene SOA as isoprene is a biogenic VOC whose emission will be highest in rural areas and highly forested areas, such as the S.E. U.S. (similar to conditions of this study) and the Amazon (very low NO_x)."

Modification to manuscript:

From **Sect 4.2, Page 16, Lines 11-13**

"However, very little investigation has been performed on isoprene SOA formation within the low NO_x regime ($VOC/NO_x > 5.5$ and $NO_x > 0$ ppb) of this study, which is typical of rural areas downwind of urban centers (Finlayson-Pitts and Pitts, Jr., 1993)."

Minor Comments:

1. **Referee's Comment:** "***p33126, line 9-11.*** *Briefly describe the C-RUV technique. Can you compare the measured [H+] with model simulation? Later (p33136 line 8), the authors also mention that using C-RUV to measure sulfate, which should be discussed in the method part as well.*"

   Response:

   The colorimetry integrated with a reflectance UV-Visible spectrometer (C-RUV) technique (Li and Jang, 2012) is used to directly measure aerosol acidity without the use of solvents or high temperature extraction techniques, which are known to decompose OS. Particles are sampled onto Teflon-coated glass fiber filters that have been dyed with metanil yellow (MY) as an indicator for proton concentration. The presence of protons causes the filter color to shift from yellow to pink, which is measured with high sensitivity using the UV-Visible spectrometer, and used to estimate $[H^+]$ (mol/L of aerosol) using a calibration curve based on the measured absorbance and the volume of aerosol sampled. In order to estimate the sulfate which formed OS, the actual aerosol $[H^+]$ measured by C-RUV is compared to the $[H^+]$ predicted by a thermodynamic model using the inorganic composition measured by the PILS-IC (Li et al., 2015a). The PILS-IC uses high temperature steam to allow for the impaction of aerosol and subsequent measurement of composition by an IC. The high temperatures of the PILS leads to the decomposition of OS, and thus the $[SO_4^{2-}]$ measured by the PILS-IC is the total concentration ($[SO_4^{2-}] + [SO_4^{2-}]_{OS}$). The difference between the measured $[H^+]$ and the predicted [H+] using the inorganic composition from PILS-IC is attributable to the formation of OS. Thus, $[SO_4^{2-}]_{OS}$ is determined by reducing the measured $[SO_4^{2-}]$ until the measured and predicted $[H^+]$ are the same.

   Modification to manuscript:

Figure 4 (**Page 40)** was added to compare the $[SO_4^{2-}]_{OS}$ predicted by the model and determined using the C-RUV technique. A brief discussion of the use of the C-RUV technique to measure OS was added to experimental methods and copied below.

From **Sect 2, Page 5, Lines 29-Page 6, Line 12**

"The Colorimetry integrated with Reflectance UV-Visible spectrometer (C-RUV) technique (Jang et al., 2008; Li et al., 2015b; Li and Jang, 2012) was used to measure $[H^+]$ (mol L^{-1} aerosol) in experiment SA2. The C-RUV technique utilizes a dyed filter to collect aerosol and act as an indicator for particle acidity. The change in color is measured using a UV-Visible spectrometer in absorbance mode and allows for determination of $[H^+]$ using a calibration curve. Then the amount of $[SO_4^{2-}]$ that forms organosulfates (OS) ($[SO_4^{2-}]_{OS}$) is estimated by comparing the actual particle $[H^+]$ measured by the C-RUV technique to the $[H^+]$ predicted using the inorganic composition from PILS-IC by the inorganic thermodynamic model, E-AIM II (Clegg et al., 1998). OS are reversible in the high temperature water droplets of the PILS system and so the measured $[SO_4^{2-}]$ is the total sulfate including OS. Therefore, by reducing the amount of $[SO_4^{2-}]$ input into E-AIM II until the predicted $[H^+]$ matches the actual value measured by C-RUV, the amount of $[SO_4^{2-}]_{OS}$ can be estimated. A more detailed explanation of the use of the C-RUV technique to estimate OS in SOA can be found in (Li et al., 2015b). A more complete description of the experimental design and chamber operation can be found in Im et al. (2014)."

2. **Referee's Comment:** "***p33128, line 1.*** *Have the authors considered the salting-in and salting-out effects of glyoxal and methylglyoxal (Waxman et al., 2015; Kampf et al., 2013)?*"

Response:

While we are aware of the recent work regarding the salting-in and salting-out effects of glyoxal and methylglyoxal, these effects have not been directly input into our model. As with any model development, we must decide what to include and what not to include into our model based on the current overall progress of research in our field. While these effects are really interesting and important for the understanding of atmospheric SOA formation, the research into these effects is not complete and the effects are not yet fully understood. Waxman et al. (2015) state that "additional measurements need to be made for other water-soluble organic molecules such as IEPOX and methyl tetrol, and further work on mixed salt solutions should be performed to confirm whether (the parameterization provided) presents a good approximation over a wider parameter space of mixed salt solutions." Based on this, we have waited to add these effects to UNIPAR, but we will revisit the implementation of salting effects once they have been more comprehensively investigated.

Modification to manuscript:

A line has been added to Sect. 4.4 (Model sensitivity, uncertainty, and limitations) to document that the model does not account for this (copied below).

Sect. 4.4, Page 21, Line 26-31

"Another new development in the SOA formation is the discovery of the salting-in and salting-out of glyoxal and methylglyoxal (Waxman et al., 2015). While these effects are very interesting and likely influence the SOA formation of these species, they are not yet included within UNIPAR. The topic will be reconsidered for application within our model once these effects have been more comprehensively investigated for a wider range of relevant water-soluble organic molecules and inorganic aerosol compositions."

3. **Referee's Comment:** "***p33131, line 3.*** *Why do the authors use the prime over Cmix,i?*"

Response:

$C_{mix,i}$ is the concentration in μg/m3, while $C'_{mix,i}$ is the concentration in mol/L of aerosol.

Modification to manuscript:

From **Sect. 3.3.1, Page 11, Line 6-10:**

"Once $C_{mix,i}$ (μg m^{-3}) is determined for each Δt, the OM_{AR} formation of $i_{m,n}$ is estimated in UNIPAR assuming a second-order self-dimerization reaction as is shown in Eq. 4, where $C'_{mix,i}$ is the aerosol phase concentration of $i_{m,n}$ in mol L^{-1} of aerosol and $k_{AR,i}$ (L mol^{-1} s^{-1}) is the aerosol phase reaction rate of each $i_{m,n}$."

4. **Referee's Comment:** "***p33137, line 22.*** *What's C510OOH? It seems to represent a peroxide instead of peroxynitrate.*"

Response:

The structure of C510OOH and the other compounds of high concentration in lumping group $3OS_p$-M are shown below and have been added to the supplemental information.

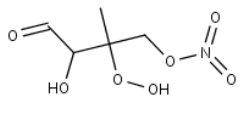

C510OOH

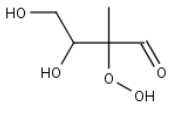

C57OOH

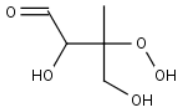

C58OOH

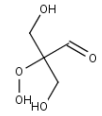

HMACROOH

This has be clarified in the manuscript.

Modification to manuscript:

From **Sect. 4.2, Page 16, Line 25-Page 17, Line 2**

"RO radicals produced from the reaction of RO_2 radicals with NO can lead to multifunctional carbonyls via reaction with oxygen and also simple carbonyls such as glyoxal and methylglyoxal through fragmentation of RO radicals. These products are all highly reactive in the aerosol phase and produce OM_{AR}. Furthermore, some late generation RO_2 radicals, whose precursors are formed from the RO pathway (high NO),

react with HO_2 to form low volatility organic peroxides with alcohol functional groups and an aldehyde ($3OS_p$-M: C510OOH, C57OOH, C58OOH, HMACROOH in MCM, Sect S7)."

5. **Referee's Comment:** "***p33138, line 1-5****. Would the effect of LWC on SOA formation change once you take into account the salting-in and salting-out of glyoxal and methylglyoxal? For example, increasing RH not only provides more absorbing medium, but also change the aqueous phase concentrations and hence affect the partitioning.*"

   Response:

   If the salting-on of glyoxal and salting-out of methylglyoxal were added to the model, the effect of LWC may change slightly since decreasing the LWC may increase the partitioning of glyoxal, but would also decrease the concentration of methylglyoxal (and the rest of the water soluble organics). Therefore, depending on the relative contribution of glyoxal compared to the other isoprene photooxidation products, the relationship between LWC and SOA formation could be slightly different, but as was mentioned in the response to minor comment 2 above, we will not be adding these effects to UNIPAR until the understanding is more comprehensive and constrained.

6. **Referee's Comment:** "***p33139, line 4****, subscript "i" after MF*"

   Response:

   This was corrected.

7. **Referee's Comment:** "*It should be 10^6 instead of 10^{-6}.*"

   Response:

   This was corrected.

References

Bertram, A. K., Martin, S. T., Hanna, S. J., Smith, M. L., Bodsworth, A., Chen, Q., Kuwata, M., Liu, A., You, Y. and Zorn, S. R.: Predicting the relative humidities of liquid-liquid phase separation, efflorescence, and deliquescence of mixed particles of ammonium sulfate, organic material, and water using the organic-to-sulfate mass ratio of the particle and the oxygen-to-carbon elemental ratio of the organic component, Atmos Chem Phys, 11(21), 10995–11006, doi:10.5194/acp-11-10995-2011, 2011.

Chan, A. W. H., Chan, M. N., Surratt, J. D., Chhabra, P. S., Loza, C. L., Crounse, J. D., Yee, L. D., Flagan, R. C., Wennberg, P. O. and Seinfeld, J. H.: Role of aldehyde chemistry and NOx concentrations in secondary organic aerosol formation, Atmos Chem Phys, 10(15), 7169–7188, doi:10.5194/acp-10-7169-2010, 2010.

Clegg, S. L., Brimblecombe, P. and Wexler, A. S.: Thermodynamic Model of the System H+−NH4+−SO42-−NO3-−H2O at Tropospheric Temperatures, J. Phys. Chem. A, 102(12), 2137–2154, doi:10.1021/jp973042r, 1998.

Dommen, J., Metzger, A., Duplissy, J., Kalberer, M., Alfarra, M. R., Gascho, A., Weingartner, E., Prevot, A. S. H., Verheggen, B. and Baltensperger, U.: Laboratory observation of oligomers in the aerosol from isoprene/NOx photooxidation, Geophys. Res. Lett., 33(13), L13805, doi:10.1029/2006GL026523, 2006.

Eddingsaas, N. C., Loza, C. L., Yee, L. D., Chan, M., Schilling, K. A., Chhabra, P. S., Seinfeld, J. H. and Wennberg, P. O.: α-pinene photooxidation under controlled chemical conditions-Part 2: SOA yield and composition in low- and high-NOx environments, Atmospheric Chem. Phys., 12(16), 7413–7427, doi:10.5194/acp-12-7413-2012, 2012.

Edney, E. O., Kleindienst, T. E., Jaoui, M., Lewandowski, M., Offenberg, J. H., Wang, W. and Claeys, M.: Formation of 2-methyl tetrols and 2-methylglyceric acid in secondary organic aerosol from laboratory irradiated isoprene/NOX/SO2/air mixtures and their detection in ambient PM2.5 samples collected in the eastern United States, Atmos. Environ., 39(29), 5281–5289, doi:10.1016/j.atmosenv.2005.05.031, 2005.

Finlayson-Pitts, B. J. and Pitts, Jr., J. N.: Atmospheric Chemistry of Tropospheric Ozone Formation: Scientific and Regulatory Implications, J. Air Waste Assoc., 43(8), 1091–1100, doi:10.1080/1073161X.1993.10467187, 1993.

Gaston, C. J., Riedel, T. P., Zhang, Z., Gold, A., Surratt, J. D. and Thornton, J. A.: Reactive Uptake of an Isoprene-Derived Epoxydiol to Submicron Aerosol Particles, Environ. Sci. Technol., 48(19), 11178–11186, doi:10.1021/es5034266, 2014.

Guo, H., Xu, L., Bougiatioti, A., Cerully, K. M., Capps, S. L., Hite, J. R., Carlton, A. G., Lee, S.-H., Bergin, M. H., Ng, N. L., Nenes, A. and Weber, R. J.: Fine-particle water and pH in the southeastern United States, Atmospheric Chem. Phys., 15(9), 5211–5228, doi:10.5194/acp-15-5211-2015, 2015.

Im, Y., Jang, M. and Beardsley, R. L.: Simulation of aromatic SOA formation using the lumping model integrated with explicit gas-phase kinetic mechanisms and aerosol-phase reactions, Atmos Chem Phys, 14(8), 4013–4027, doi:10.5194/acp-14-4013-2014, 2014.

Jang, M. and Kamens, R. M.: Characterization of Secondary Aerosol from the Photooxidation of Toluene in the Presence of NOx and 1-Propene, Environ. Sci. Technol., 35, 3626–3639, doi:10.1021/es010676+, 2001.

Jang, M., Czoschke, N. M., Lee, S. and Kamens, R. M.: Heterogeneous Atmospheric Aerosol Production by Acid-Catalyzed Particle-Phase Reactions, Science, 298(5594), 814–817, doi:10.1126/science.1075798, 2002.

Jang, M., Cao, G. and Paul, J.: Colorimetric Particle Acidity Analysis of Secondary Organic Aerosol Coating on Submicron Acidic Aerosols, Aerosol Sci. Technol., 42(6), 409–420, doi:10.1080/02786820802154861, 2008.

Kroll, J. H., Ng, N. L., Murphy, S. M., Flagan, R. C. and Seinfeld, J. H.: Secondary Organic Aerosol Formation from Isoprene Photooxidation, Environ. Sci. Technol., 40(6), 1869–1877, doi:10.1021/es0524301, 2006.

Liggio, J., Li, S.-M. and McLaren, R.: Heterogeneous Reactions of Glyoxal on Particulate Matter: Identification of Acetals and Sulfate Esters, Environ. Sci. Technol., 39, 1532–1541, doi:10.1021/es048375y, 2005.

Li, J. and Jang, M.: Aerosol Acidity Measurement Using Colorimetry Coupled With a Reflectance UV-Visible Spectrometer, Aerosol Sci. Technol., 46(8), 833–842, doi:10.1080/02786826.2012.669873, 2012.

Li, J., Jang, M. and Beardsley, R. L.: Dialkylsulfate formation in sulfuric acid-seeded secondary organic aerosol produced using an outdoor chamber under natural sunlight, Environ. Chem. [online] Available from: http://dx.doi.org/10.1071/EN15129 (Accessed 17 November 2015a), 2015.

Li, J., Jang, M. and Beardsley, R. L.: Dialkylsulfate formation in sulfuric acid-seeded secondary organic aerosol produced using an outdoor chamber under natural sunlight, Environ. Chem., doi:10.1071/EN15129, 2015b.

Marais, E. A., Jacob, D. J., Jimenez, J. L., Campuzano-Jost, P., Day, D. A., Hu, W., Krechmer, J., Zhu, L., Kim, P. S., Miller, C. C., Fisher, J. A., Travis, K., Yu, K., Hanisco, T. F., Wolfe, G. M., Arkinson, H. L., Pye, H. O. T., Froyd, K. D., Liao, J. and McNeill, V. F.: Aqueous-phase mechanism for secondary organic aerosol formation from isoprene: application to the southeast United States and co-benefit of SO2 emission controls, Atmos Chem Phys, 16(3), 1603–1618, doi:10.5194/acp-16-1603-2016, 2016.

Matsunaga, A. and Ziemann, P. J.: Gas-Wall Partitioning of Organic Compounds in a Teflon Film Chamber and Potential Effects on Reaction Product and Aerosol Yield Measurements, Aerosol Sci. Technol., 44(10), 881–892, doi:10.1080/02786826.2010.501044, 2010.

McNeill, V. F., Woo, J. L., Kim, D. D., Schwier, A. N., Wannell, N. J., Sumner, A. J. and Barakat, J. M.: Aqueous-Phase Secondary Organic Aerosol and Organosulfate Formation in Atmospheric Aerosols: A Modeling Study, Environ. Sci. Technol., 46(15), 8075–8081, doi:10.1021/es3002986, 2012.

Minerath, E. C., Casale, M. T. and Elrod, M. J.: Kinetics Feasibility Study of Alcohol Sulfate Esterification Reactions in Tropospheric Aerosols, Environ. Sci. Technol., 42(12), 4410–4415, doi:10.1021/es8004333, 2008.

Nguyen, T. B., Bateman, A. P., Bones, D. L., Nizkorodov, S. A., Laskin, J. and Laskin, A.: High-resolution mass spectrometry analysis of secondary organic aerosol generated by ozonolysis of isoprene, Atmos. Environ., 44(8), 1032–1042, doi:10.1016/j.atmosenv.2009.12.019, 2010.

Pun, B. K., Seigneur, C. and White, W.: Day-of-Week Behavior of Atmospheric Ozone in Three U.S. Cities, J. Air Waste Manag. Assoc., 53(7), 789–801, doi:10.1080/10473289.2003.10466231, 2003.

Pye, H. O. T., Pinder, R. W., Piletic, I. R., Xie, Y., Capps, S. L., Lin, Y.-H., Surratt, J. D., Zhang, Z., Gold, A., Luecken, D. J., Hutzell, W. T., Jaoui, M., Offenberg, J. H., Kleindienst, T. E., Lewandowski, M. and Edney, E. O.: Epoxide Pathways Improve Model Predictions of Isoprene Markers and Reveal Key Role of Acidity in Aerosol Formation, Environ. Sci. Technol., 47(19), 11056–11064, doi:10.1021/es402106h, 2013.

Surratt, J. D., Murphy, S. M., Kroll, J. H., Ng, N. L., Hildebrandt, L., Sorooshian, A., Szmigielski, R., Vermeylen, R., Maenhaut, W., Claeys, M., Flagan, R. C. and Seinfeld, J. H.: Chemical composition of secondary organic aerosol formed from the photooxidation of isoprene, J. Phys. Chem. A, 110(31), 9665–9690, doi:10.1021/jp061734m, 2006.

Surratt, J. D., Chan, A. W. H., Eddingsaas, N. C., Chan, M., Loza, C. L., Kwan, A. J., Hersey, S. P., Flagan, R. C., Wennberg, P. O. and Seinfeld, J. H.: Reactive intermediates revealed in secondary organic aerosol formation from isoprene, Proc. Natl. Acad. Sci. U. S. A., 107(15), 6640–6645, doi:10.1073/pnas.0911114107, 2010.

Waxman, E. M., Elm, J., Kurtén, T., Mikkelsen, K. V., Ziemann, P. J. and Volkamer, R.: Glyoxal and Methylglyoxal Setschenow Salting Constants in Sulfate, Nitrate, and Chloride Solutions: Measurements and Gibbs Energies, Environ. Sci. Technol., 49(19), 11500–11508, doi:10.1021/acs.est.5b02782, 2015.

Woo, J. L. and McNeill, V. F.: simpleGAMMA v1.0 – a reduced model of secondary organic aerosol formation in the aqueous aerosol phase (aaSOA), Geosci. Model Dev., 8(6), 1821–1829, doi:10.5194/gmd-8-1821-2015, 2015.

Xu, L., Kollman, M. S., Song, C., Shilling, J. E. and Ng, N. L.: Effects of NOx on the Volatility of Secondary Organic Aerosol from Isoprene Photooxidation, Environ. Sci. Technol., 48(4), 2253–2262, doi:10.1021/es404842g, 2014.

Zhang, H., Worton, D. R., Lewandowski, M., Ortega, J., Rubitschun, C. L., Park, J.-H., Kristensen, K., Campuzano-Jost, P., Day, D. A., Jimenez, J. L., Jaoui, M., Offenberg, J. H., Kleindienst, T. E., Gilman, J., Kuster, W. C., de Gouw, J., Park, C., Schade, G. W., Frossard, A. A., Russell, L., Kaser, L., Jud, W., Hansel, A., Cappellin, L., Karl, T., Glasius, M., Guenther, A., Goldstein, A. H., Seinfeld, J. H., Gold, A., Kamens, R. M. and Surratt, J. D.: Organosulfates as Tracers for Secondary Organic Aerosol (SOA) Formation from 2-Methyl-3-Buten-2-ol (MBO) in the Atmosphere, Environ. Sci. Technol., 46(17), 9437–9446, doi:10.1021/es301648z, 2012.

Zhang, X., Cappa, C. D., Jathar, S. H., McVay, R. C., Ensberg, J. J., Kleeman, M. J. and Seinfeld, J. H.: Influence of vapor wall loss in laboratory chambers on yields of secondary organic aerosol, Proc. Natl. Acad. Sci., 111(16), 5802–5807, doi:10.1073/pnas.1404727111, 2014.

Zhang, X., McVay, R. C., Huang, D. D., Dalleska, N. F., Aumont, B., Flagan, R. C. and Seinfeld, J. H.: Formation and evolution of molecular products in α-pinene secondary organic aerosol, Proc. Natl. Acad. Sci., 112(46), 14168–14173, doi:10.1073/pnas.1517742112, 2015.

Zuend, A. and Seinfeld, J. H.: Modeling the gas-particle partitioning of secondary organic aerosol: the importance of liquid-liquid phase separation, Atmospheric Chem. Phys., 12(9), 3857–3882, doi:10.5194/acp-12-3857-2012, 2012.

Simulating the SOA formation of isoprene from partitioning and aerosol phase reactions in the presence of inorganics

R. L. Beardsley[1] and M. Jang[1,*]

[1]{Department of Environmental Engineering Sciences, University of Florida, P.O. Box 116450, Gainesville, FL 32611, USA}

Correspondence to: M. Jang (mjang@ufl.edu)

Abstract

The secondary organic aerosol (SOA) produced by the photooxidation of isoprene with and without inorganic seed is simulated using the Unified Partitioning Aerosol Phase Reaction (UNIPAR) model. Recent work has found the SOA formation of isoprene to be sensitive to both aerosol acidity ([H+], mol/L) and aerosol liquid water content (LWC) with the presence of either leading to significant aerosol phase organic mass generation and large growth in SOA yields (Y_{SOA}). Classical partitioning models alone are insufficient to predict isoprene SOA formation due to the high volatility of ~~the~~ photooxidation products and ~~the~~ sensitivity of their mass yields to variations in inorganic aerosol composition. UNIPAR utilizes the chemical structures provided by a near-explicit chemical mechanism to estimate the thermodynamic properties of the gas phase products, which are lumped based on their calculated vapor pressure (8 groups) and aerosol phase reactivity (6 groups). UNIPAR then determines the SOA formation of each lumping group from both partitioning and aerosol phase reactions (oligomerization, acid catalyzed reactions, and organosulfate formation) assuming a single homogeneously mixed organic-inorganic phase as a function of inorganic composition and VOC/NO_x. The model is validated using isoprene photooxidation experiments performed in the dual, outdoor UF APHOR chambers. UNIPAR is able to predict the experimental SOA formation of isoprene without seed, with H_2SO_4 seed gradually titrated by ammonia, and with the acidic seed generated by SO_2 oxidation. Oligomeric mass is predicted to account for more than 65% of the total OM formed in all cases and over 85% in the presence of strongly acidic seed. The model is run to determine the sensitivity of Y_{SOA} to [H^+], LWC, and VOC/NO_x, and it is determined that the SOA formation of isoprene is most

strongly related to [H^+] but is dynamically related to all three parameters. For VOC/NO_x > 10, with increasing NO_x both experimental and simulated Y_{SOA} increase and are found to be more sensitive to [H^+] and LWC. For atmospherically relevant conditions, Y_{SOA} is found to be more than 150% higher in partially titrated acidic seeds (NH_4HSO_4) than in effloresced inorganics or in isoprene only.

1 Introduction

Volatile organic compounds (VOCs) are emitted into the atmosphere from both biogenic and anthropogenic sources. Once emitted, these compounds react with atmospheric oxidants and radicals to form semi-volatile products that may self-nucleate or partition onto pre-existing particulate matter to form secondary organic aerosol (SOA). Isoprene (2-methyl-1,3-butadiene) is a biogenic VOC with the largest emission of all non-methane hydrocarbons (Guenther et al., 2006), and yet it was initially thought to form insignificant amounts of SOA due to the volatility of its principal oxidation products. This conclusion was supported by early chamber investigations that found isoprene only forms SOA at concentrations much higher than ambient conditions (Pandis et al., 1991; R. M. Kamens et al., 1982). However, recent chamber (Edney et al., 2005; Kroll et al., 2005, 2006; Limbeck et al., 2003) and field studies (Claeys et al., 2004; Edney et al., 2005) found that the large emission rate of isoprene makes the contribution to global SOA formation significant even at low yields, and it is estimated that isoprene is the largest single source of global organic aerosol (Henze and Seinfeld, 2006). The proposal of new SOA formation mechanisms, primarily the classical equilibrium partitioning theory by Pankow (1994) and the discovery of aerosol phase oligomerization reactions in the presence of inorganic acids (Jang et al., 2002, 2003), led to the re-examination of the SOA formation potential of isoprene. More recent studies have found the SOA yield of isoprene and its oxidation products to be highly sensitive to aerosol acidity ([H^+], mol/L aerosol) (Jang et al., 2002; Kuwata et al., 2015; Limbeck et al., 2003; Surratt et al., 2010) and aerosol liquid water content (LWC).

The ~~sensitivity of the SOA yield of isoprene to LWC and [H^+] is~~tendency of isoprene photooxidation products to engage in aerosol phase oligomerization reactions is primarily due to the reactivity of its secondary products. The presence of two double bonds makes isoprene highly reactive and allows for rapid OH initiated oxidation in the atmosphere. The ~~speciation~~ distribution of isoprene photooxidation products and the resultant SOA yields are dependent

on NO_x concentrations and atmospheric aging. When NO_x concentrations are low, RO_2 radicals react with HO_2 radicals to form hydroxyperoxides (ROOH) at high yield. Then, ROOH further react with OH radicals to form dihydroxyepoxides (IEPOX) (Paulot et al., 2009). IEPOX has been found to undergo rapid reactive uptake onto wet ammonium sulfate (AS) inorganic aerosol and acidic inorganic seeds at all RH leading to the formation of tetrols, organosulfates (OS) and other ~~lowly~~ low volatility~~e~~ oligomers. In the presence of high NO_x, SOA formation will depend on the ratio of NO_2 to NO with isoprene SOA yields being be ~~higher~~ lower at ~~large~~ low NO_2/NO due to RO2 reacting with NO to produce more volatile products (Kroll et al., 2006; Surratt et al., 2010)~~(Surratt et al., 2010)~~.

~~However, the presence of any significant amounts of NO_x will lead to SOA at lower yields and with less sensitivity to $[H^+]$ and LWC than photooxidation under low NO_x conditions.~~

In order to quantify and understand the impact of SOA on climate and human health, the prediction of SOA formation of isoprene is essential. SOA models have been developed and utilized to predict the SOA formation of various VOC systems. The two-product model was developed based on classical partitioning theory (Pankow, 1994) and represents SOA formation through use of two or more representative secondary products of varying vapor pressure (Odum et al., 1996). By fitting the stoichiometric and partitioning coefficients of each representative semi-volatile organic compound (SVOC) to experimental data, the SOA yield of a VOC is predicted as a function of the absorbing organic mass (OM) concentration without considering the numerous gas phase products. The simple and efficient handling of SOA mass formation from partitioning by the two-product model led to its widespread use in regional and global models. Nevertheless, the two-product model and its predecessors are limited in their ability to predict SOA formation from aerosol phase reactions in the presence of inorganic aerosol due to the loss of individual product structures, which determine reactivity in the aerosol phase, and the need to fit new parameters for variations in atmospheric conditions. Many regional models have already incorporated different sets of parameters for each VOC under high and low NO_x regimes, but cannot handle the variations seen in ambient aerosol LWC and $[H^+]$ that enhance SOA formation via aerosol phase reactions (Carlton et al., 2009).

More recent studies have modeled aqueous phase SOA production using empirically determined uptake coefficients or effective Henry's constants (when available) to estimate reactive uptake of major isoprene products, such as IEPOX and glyoxal, in the inorganic

Field Code Changed

Formatted: German (Germany)

Formatted: Normal

aqueous phase (Marais et al., 2016; McNeill et al., 2012; Pye et al., 2013; Woo and McNeill, 2015). For example, McNeill et al. (2012) developed the box model GAMMA to predict the aqueous SOA production of isoprene in the presence of deliquesced ammonium sulfate. Pye et al. (2013) modified the regional Community Multi-scale Air Quality model to include the heterogeneous uptake of IEPOX and methacrylic acid epoxide. While these models greatly improve the predictions of isoprene SOA formation over classical partitioning models, SOA formation of these known products via aqueous phase reactions is not fully representative of total isoprene SOA formation. Edney et al. (2005) measured the composition of isoprene SOA in the presence of acidic inorganic seed, and methylglyceric acid and 2-methyltetrols, which are tracer species for aqueous phase reactions, made up only 6% of the total SOA mass with the majority of the products being unidentified. Furthermore, highly oxidized oligomers comprise the majority of isoprene SOA even in the absence of an inorganic aqueous phase (Nguyen et al., 2010; Surratt et al., 2006) due to aerosol phase reactions in organic-only aerosol. The photooxidation of isoprene produces a large number of highly reactive products (epoxides, carbonyls) that will react even in the absence of an inorganic aqueous phase to produce the large fraction of high molecular weight (MW) species. Therefore, while the high contribution of the aqueous phase products of IEPOX and similar compounds make them ideal tracers, they are not fully representative of isoprene SOA as is demonstrated by the large number of high MW products and lack of mass closure in isoprene composition studies even in the absence of an inorganic aqueous phase.

In this study, the Unified Partitioning-Aerosol Phase Reaction (UNIPAR) model, which was previously developed and applied to aromatic VOCs (Im et al., 2014), was updated and expanded to model the SOA formation of isoprene in the presence of low VOC/NO_x (due to the high sensitivity to $[H^+]$ in the low NO_x regime) and aerosol acidity ~~under ambient temperature (T) and relative humidity (RH)~~using natural sunlight. UNIPAR predicts SOA formation from gas-particle partitioning, and ~~only~~ oligomerization reactions in both organic-only aerosol and the inorganic aqueous phase using a lumping structure that was developed to be representative of the thermodynamic properties and chemical reactivity of oxidized products in the aerosol phase. The model was validated using outdoor chamber ~~experimental~~ data from ~~from outdoor chamber runs~~ isoprene photooxidation experiments with and without acidic inorganic seeds.

~~and the results and conclusions are discussed.~~

Formatted: Subscript

Formatted: Not Highlight

2 Experimental Methods

Isoprene SOA photooxidation experiments were performed in the University of Florida Atmospheric PHotochemical Outdoor Reactor (UF-APHOR) chambers over the period of a day. The dual 52 m^3 Teflon film chambers were operated simultaneously to allow for investigation of two different experimental conditions under the same ambient, diurnal profiles of sunlight, RH, and T. The chamber air was cleaned using air purifiers (GC Series, IQAir) for 48 hours prior to each experiment. In the experiments in which inorganic seeds were used, a 0.01 M aqueous solution of H_2SO_4 (SA) was atomized using a nebulizer (LC STAR, Pari Respiratory Equipment) with clean air flow. Next, the desired volume of NO (2% in N_2, Airgas) was injected into the chamber and finally, isoprene (99%, Sigma Aldrich) and CCl_4 (>99.9%, Sigma Aldrich) were injected using a glass manifold with clean air. CCl_4 was used as a tracer for dilution. All chemical species were injected early enough to allow for stabilization and measurement before reactions begun with sunrise. The experimental conditions for each of the chamber runs is shown in Table 1.

To allow for gas and aerosol phase characterization, chamber air is pumped through a number of sampling lines into the lab that is located directly below the roof. Gas phase concentrations of NO_x, O_3, and SO_2 were measured using a Teledyne Model 200E Chemiluminescence NO-NO_x Analyzer, Model 400E Photometric O_3 Analyzer, and Model 102E Fluorescence TRS Analyzer, respectively. A HP 5890 Gas Chromatography-Flame Ionization Detector was employed with an oven temperature of 40 °C to measure isoprene and CCl_4 concentrations. A semi-continuous OC/EC carbon aerosol analyzer (Sunset Laboratory, Model 4) following the NIOSH 5040 method was utilized to measure organic carbon (OC) mass concentration (µgC m^{-3}), and then converted to OM using an OM/OC ratio of 2.2 (Aiken et al., 2008; Kleindienst et al., 2007). Particle number and volume concentrations were measured with a scanning mobility particle sizer coupled with a condensation nuclei counter (TSI, Model 3025A and Model 3022). Particle wall loss was corrected using size-dependent first order rate constants determined by a chamber characterization with inorganic seed.

A Particle into Liquid Sampler (Applikon, ADI 2081) coupled to Ion Chromatography (Metrohm, 761Compact IC) (PILS-IC) was used to quantify aerosol phase inorganic ions. The Colorimetry integrated with Reflectance UV-Visible spectrometer (C-RUV) technique (Jang et al., 2008; Li et al., 2015; Li and Jang, 2012) was used to measure [H^+] (mol L_a^{-1} aerosol) ~~throughout the~~in experiment SA2~~ experiment~~. The C-RUV technique utilizes a dyed filter to

Formatted: Superscript

collect aerosol and act as an indicator for particle acidity. The change in color is measured using a UV-Visible spectrometer in absorbance mode and allows for determination of $[H^+]$ using a calibration curve. Then the amount of $[SO_4^{2-}]$ that forms organosulfates (OS) ($[SO_4^{2-}]_{OS}$) is estimated by comparing the actual particle $[H^+]$ measured by the C-RUV technique to the $[H^+]$ predicted using the inorganic composition from PILS-IC by the inorganic thermodynamic model, E-AIM II (Clegg et al., 1998). OS are reversible in the high temperature water droplets of the PILS system and so the measured $[SO_4^{2-}]$ is the total sulfate including OS. Therefore, by reducing the amount of $[SO_4^{2-}]$ input into E-AIM II until the predicted $[H^+]$ matches the actual value measured by C-RUV, the amount of $[SO_4^{2-}]_{OS}$ can be estimated. A more detailed explanation of the use of the C-RUV technique to estimate OS in SOA can be found in Li et al. (2015). A more complete description of the experimental design and chamber operation can be found in Im et al. (2014).

3 Model Description

UNIPAR simulates the SOA formation of the VOC/NO_x photooxidation products from both partitioning and aerosol phase reactions. The photooxidation of the VOC is predicted explicitly offline, and products are lumped using their volatility and reactivity in aerosol phase reactions (Sect. 3.1). SOA formation is then predicted for the lumped species dynamically as a function of the inorganic aerosol composition ($[H^+]$, LWC). The inputs of the model are the consumption of isoprene (ΔISO), VOC/NO_x, the change in aerosol phase sulfate ($\Delta[SO_4^{2-}]$) and ammonium ions (ΔNH_4^+), T and RH at each time step (Δt = 3 min).

The overall model schematic is shown in Fig. 1. In order to account for effects of inorganic aerosol, isoprene SOA formation is approached in two ways: SOA formation in the presence of deliquesced inorganic seed (SO_4^{2-} > 0 and RH > ERH), and either isoprene only (SO_4^{2-} = 0) or effloresced inorganic seed (SO_4^{2-} > 0 and RH < ERH) (Sect. 3.2 and 3.3). First, the total ~~products~~ mass originating from ΔVOC in each Δt ~~are~~ is split among the lumping groups ($i_{m,n}$~~i~~) and combined with the remaining gas phase concentrations from previous steps to get the total gas phase concentration of each $i_{m,n}$ ($C_{g,i}$, μg m^{-3}) (Sect. 3.1). Then the concentrations in the aerosol phase ($C_{mix,i}$, μg m^{-3}) are calculated based on the aerosol phase state. Using the estimated $C_{mix,i}$ and inorganic aerosol composition, the OM formation from aerosol phase reactions (OM_{AR}, μg m^{-3}) is calculated (Sect. 3.3.1). OM_{AR} includes SOA formation from organic-only oligomerization reactions, aqueous phase reactions and acid-catalyzed reactions, and OS formation (Sect. 3.3.2). OM_{AR} is assumed to be non-volatile and irreversible. Finally,

Formatted: Subscript
Formatted: Superscript
Formatted: Not Superscript/ Subscript
Formatted: Subscript
Formatted: Not Superscript/ Subscript
Formatted: Superscript

the OM from partitioning (OM_P, μg m^{-3}) is predicted using the module developed by Schell et al. (2001) modified to account for the assumed non-volatility and irreversibility of OM_{AR} (Sect. 3.3.3).

3.1 Gas phase photooxidation and lumping structure

The photooxidation of isoprene was simulated using the Master Chemical Mechanism v3.2 (Saunders et al., 1997, 2003) within the Morpho kinetic solver (Jeffries, H.E. et al., 1998). Simulations were performed under varying VOC/NO_x ratios (ppbC/ppb) using the sunlight, temperature, and RH data from 23 April 2014. All of the simulations began with NO and begin with sunrise. The sunlight, RH, and temperature profiles used can be seen in the supplemental information (SI) as well as an example gas phase simulation with corresponding experimental data (Sect. S1).

The predicted photooxidation products are then lumped in UNIPAR using vapor pressure (m, 8 bins) and reactivity (n, 6 bins). The lumping structure is shown in ~~Figure~~ Fig. S3 in the SI including the structure of the product which contributes most to each lumping group. The subcooled liquid vapor pressure of each product ($p^o_{L,i}$) is estimated using a group contribution method (Joback and Reid, 1987; Stein and Brown, 1994; Zhao et al., 1999), which is explained in detail in Im et al. (2014). The reactivity of each product is estimated based on the number of reactive functional groups. The reactivity bins used in UNIPAR are very fast (VF, α-hydroxybicarbonyls and tricarbonyls), fast (F, 2 epoxides or aldehydes,), medium (M, 1 epoxide or aldehyde), slow (S, ketones), partitioning only (P), and organosulfate precursors (OS_P, 3 or more alcohols). The reactivity bins were developed based on previous work in which the measured gas-particle partitioning coefficients (K_p) of toluene and α-pinene SOA products were found to deviate from the theoretical value due to higher than expected particle concentrations. The degree of deviation was found to depend on the functionalization of the SOA product (Jang et al., 2002; Jang and Kamens, 2001). The experimental log(K_p) of ketones (S reactivity bin) were found to be only slightly higher than the theoretical value, while the experimental log(K_p) of conjugated aldehydes (M reactivity bin) and the products associated with F and VF reactivity bins were found to be 10-40 times higher and 2 to 3 orders higher, respectively.

In order to account for their unique reactivity, glyoxal was allocated to group 6F instead of 8F and methylglyoxal was moved from 8M to 6M based on their apparent Henry's constant (Ip et

Formatted: Subscript

Formatted: Subscript

al., 2009). In addition to these reactivity bins, isoprene required the designation of a medium reactivity, multi-alcohol (M-OS_P) bin due to the large number of secondary products which contain both three or more alcohols and reactive functional groups (epoxide or aldehyde). Tetrol precursors (IEPOX), which are produced at high concentrations in the gas phase under low VOC/NO_x, were also given a separate reactivity bin in order to more easily quantify the SOA formation of these products predicted by the model. The concentrations of each lumping group were set at the peak HO_2/NO ratio, which generally corresponds with the time of majority of SOA formation and represents a shift from less oxidized to more oxidized products. The corresponding stoichiometric mass coefficients ($\alpha_{m,n,i}$) of each $i_{m,n}$ were then fit to the initial VOC/NO_x ratio. At higher NO, it takes longer to reach the peak HO_2/NO ratio and SOA formation is also slower. ~~Figure~~ Fig. 2 shows the filled lumping structure at VOC/NO_x of 25 illustrating the high volatility and reactivity of the majority of isoprene products.

Formatted: Font: Italic
Formatted: Font: Italic
Formatted: Subscript
Formatted: Font: Italic

3.2 Aerosol composition and phase state

Tropospheric aerosols have been shown to be primarily composed organic compounds and inorganic sulfate partially or wholly titrated with ammonia (Bertram et al., 2011; Murphy et al., 2006). Under ambient diurnal patterns of RH, these aerosols may effloresce and deliquesce, and can be liquid-liquid phase separated (LLPS) or a single homogeneously mixed phase (SHMP) influencing the amount and composition of SOA formed. While dry, effloresced inorganic salts simply act as a seed for organic coating by SOA, deliquesced seeds contain liquid water into which reactive, soluble compounds can dissolve and further react producing ~~lowly~~ low volati~~l~~lity SOA (Hennigan et al., 2008; Lim et al., 2010; Volkamer et al., 2007). Furthermore, the type of SOA products will determine the phase state of wet aerosol. In LLPS aerosol, hydrophobic SVOC will partition primarily into the organic liquid phase, while a significant fraction of hydrophilic SVOC may dissolve into the salted liquid phase. The RH at which these transitions occur depends on the concentration and composition of the inorganic and organic components of the aerosol.

Bertram et al. (2011) semi-empirically predicted the efflorescence RH (ERH), deliquescence RH (DRH), and the RH of LLPS (SRH) by fitting experimental data of a number of oxygenated organic-AS systems to the oxygen to carbon atomic ratio (O:C) and to the organic to sulfur mass ratio (org:sulf) of the bulk aerosol. UNIPAR utilizes these parameterizations to predict ERH and DRH at each time step ($t = j$) using modeled O:C and org:sulf from the

previous time step ($t = j - 1$). In regards to phase state, UNIPAR is run assuming a SHMP for all of the isoprene simulations due to literature O:C values of isoprene ranging from 0.69 to 0.88 (Bertram et al., 2011; Chen et al., 2011; Kuwata et al., 2013), which corresponds to a SRH of zero.

The interaction of organics and inorganics in SHMP SOA may alter the dissociation of inorganic acids and the resulting $[H^+]$ (mol L_a^{-1} aerosol). In order to estimate the impact of organics on $[H^+]$ in SHMP isoprene SOA, the percent dissociation of H_2SO_4 was determined using AIOMFAC in the presence of varying amounts of tetrol and hexane, which represent polar and non-polar organic species, under controlled RH. The change in percent dissociation was less than 15% when compared to inorganic only aerosol at the same RH (details in supplemental information, Sect. S2). Based on these results, it was assumed that presence of organics in isoprene SHMP SOA does not significantly influence the $[H^+]$ from inorganic acids. Therefore, $[H^+]$ is estimated for each time step by E-AIM II (Clegg et al., 1998) corrected for the ammonia rich condition (Li and Jang, 2012) as a function of inorganic composition measured by PILS-IC ($[SO_4^{2-}]$, $[NH_4^+]$), and RH. Then, $[H^+]$ is diluted using the ratio of the inorganic volume to the total aerosol volume. The inorganic associated LWC is also calculated using E-AIM II. The LWC of isoprene SOA is estimated in AIOMFAC using the hygroscopic growth factor of a representative isoprene SOA: 20% sucrose by mass (Hodas et al., 2015) as a surrogate for tetrol and 80% isoprene derived oligomers (Nguyen et al., 2011). The estimated growth factor is approximately 30% of that of AS and so, in the model the LWC of isoprene is estimated to be 0.3 of the LWC of AS without an ERH.

$[H^+]$ is used to describe particle acidity and has units of mol H^+/L of aerosol. Therefore, $[H^+]$ will change with variation in inorganic composition, LWC and total aerosol mass (SOA). The particle pH is simply the negative log of $[H^+]$.

3.3 SOA formation

In simulating the total OM (OM_T) from isoprene photooxidation, UNIPAR predicts the SOA formation for each $i_{m,n}$~~i~~ from both partitioning ($OM_{P,i}$) and aerosol phase reactions ($OM_{AR,i}$). In the previous applications of UNIPAR for aromatic VOC (Im et al., 2014), SOA formation was modeled under the assumption of LLPS aerosol because aromatic SOA is relatively non-polar, and thus aerosol phase concentrations of $i_{m,n}$ ~~i~~ were calculated by means of a mass balance between the concentrations in the gas phase, the inorganic aerosol phase, and the

Formatted: Superscript

Field Code Changed

Formatted: Superscript

organic aerosol phase. In modeling isoprene SOA formation in the presence of a SHMP aerosol, the total concentration (μg m^{-3} of air) of each lumping species ($C_{T,i}$) was split solely between $C_{g,i}$ and $C_{mix,i}$ by a single gas-particle partitioning coefficient, $K_{mix,i}$ (m^3 μg^{-1}),

$$C_{T,i} = C_{g,i} + C_{mix,i}, \quad (1)$$

$$K_{mix,i} = \frac{C_{mix,i}}{C_{g,i} M_{mix}}, \quad (2)$$

where M_{mix} is the total suspended matter and is the sum of the inorganic mass (M_{in}) and OM_T. ~~$C_{mix,i}$ and $C_{g,i}$ can be determined by combining Eq. 1 and Eq. 2 as follows,~~

~~$$C_{mix,i} = C_{T,i}\left(\frac{K_{mix,i} M_{mix}}{1 + K_{mix,i} M_{mix}}\right) \quad (3)$$~~

~~$$C_{g,i} = C_{T,i}\left(\frac{1}{1 + K_{mix,i} M_{mix}}\right) \quad (4)$$~~

Calculation of $K_{mix,i}$ follows the gas-particle absorption model (Pankow, 1994).

$$K_{mix,i} = \frac{7.501\,RT}{10^9 MW_{mix} \gamma_{mix,i} p^o_{L,i}}, \quad (5)$$

where R is the gas constant (8.314 J K^{-1} mol^{-1}), T is the temperature (K), MW_{mix} is the average molecular weight (g mol^{-1}) of the SHMP aerosol, $\gamma_{mix,i}$ is the activity coefficient of the lumping species in the SHMP aerosol, and $p^o_{L,i}$ is the sub-cooled liquid vapor pressure (mmHg) of $i_{m,n}$~~i~~. $\gamma_{mix,i}$ accounts for the non-ideality in the SHMP aerosol and allows for more realistic representation of the differences in solubility in the aerosol phase. $\gamma_{mix,i}$ will vary between partitioning species due to differences in polarity and molar volume ($V_{mol,i}$), and also over time due to changes in LWC and aerosol composition.

In order to handle the range of possible $\gamma_{mix,i}$ in SHMP isoprene SOA, the AIOMFAC model was run using the highest concentration product of each $i_{m,n}$ (Fig. S3) ~~lumping group~~ in the presence of a mixed isoprene SOA/AS aerosol. The representative isoprene SOA composition was chosen based on the results of Nguyen et al. (2011). The bulk organic to sulfur mass ratio (*org:sulf*), concentration of $i_{m,n}$~~i~~, and the RH were varied to cover the range of experimental values, and the resulting $\gamma_{mix,i}$ were fit to the bulk aerosol *org:sulf*, *ln(RH)*, and ~~lumping species~~the $V_{mol,i}$ and $O{:}C_i$ ~~u~~of each $i_{m,n}$ using a polynomial equation. The resulting

Formatted: Border: Top: (No border), Left: (No border)

Formatted: Font: Italic

Formatted: Font: Italic

Formatted: Font: Not Italic

parameterizations are shown in the SI along with the predicted $\gamma_{mix,i}$ plotted against $\gamma_{mix,i}$ from AIOMFAC (Sect. ~~S3~~S4). In the absence of inorganic aerosol ($[SO_4^{2-}]=0$) or in the presence of dry inorganic aerosol, partitioning is assumed to be ideal with organic only partitioning coefficient ($K_{or,i}$) calculated using $\gamma_{mix,i}$ of 1 (Jang and Kamens, 1998) (~~Figure~~ Fig. 1).

3.3.1 OM from aerosol phase reactions (OM_{AR})

Once $C_{mix,i}$ (µg m^{-3}) is determined for each Δt, the OM_{AR} formation of $i_{m,n}$ ~~i~~ is estimated in UNIPAR assuming a second-order self-dimerization reaction as is shown in Eq. (~~5~~4),

$$\frac{dC'_{mix,i}}{dt} = -k_{AR,i}C'^{2}_{mix,i} \quad (45)$$

where $C'_{mix,i}$ is the aerosol phase concentration of $i_{m,n}$ ~~i~~ in mol L^{-1} of ~~medium~~ aerosol and $k_{AR,i}$ (L mol^{-1} s^{-1}) is the aerosol phase reaction rate of each $i_{m,n}$ ~~i (L mol^{-1} s^{-1})~~. $k_{AR,i}$ (Eq. ~~6~~5) is calculated each time step using the semi-empirical model developed by Jang et al. (2005) as a function of the reactivity, ~~H~~ R (VF, F, M, S; Sect. 3.1), and pK_{BH+} of $i_{m,n}$ ~~i~~ in the aerosol phase, $[H^+]$ and LWC (activity of water, a_w) from the inorganic thermodynamic model (Sect. 3.2), and the excess acidity, X (Im et al., 2014; Jang et al., 2006).

$$k_{AR,i} = 10^{(0.0005*pK_{BH^+}+y*X+1.3*R+\log(a_w)+\log([H^+])-5.5)} \quad k_{AR,i} = 10^{(0.0005*pK_{BH^+}+y*X+1.3*H+\log(a_w[H^+])-5.5)} \quad (56)$$

All of the coefficients of Eq. ~~6~~5 were fit using the flow reactor experimental sets for aerosol growth of model organic compounds (various aldehydes) on acidic aerosol (SO_4^{2-} – NH_4^+ – H_2O) within the LLPS module and tested for LLPS aerosol (toluene SOA and 1,3,5-trimethylbenzene SOA) by Im et al. (2014), except for the factor y for X. In the presence of deliquesced inorganics, $k_{AR,i}$ is a function of X, which represents the effect of an acidic inorganic medium on the reaction of the protonated organics that act as an intermediate for acid-catalysed reactions. For LLPS aerosol, the protonated organic compounds are in highly concentrated inorganic liquid with high X. The mixture of organic and inorganic species in SHMP aerosol will lead to a modification of X and thus the reaction rate of protonated organics. To account for this change in isoprene SOA, y was determined to be 0.49 by fitting the OM_T of experimental set SA1 (Table 1). In the absence of deliquesced inorganic species, the terms associated with the inorganic aqueous phase ($[H^+]$ and X) approach zero making $k_{AR,i}$ primarily a function of the reactivity (~~H~~R) of $i_{m,n}$ allowing for the prediction of oligomerization reactions in the organic only aerosol. ~~i.~~

Then by assuming that OM_{AR} is non-volatile and irreversible, $\Delta OM_{AR,i}$ can be calculated as the reduction in $C_{T,i}$ for each time step. ~~(Eq. 6),~~

~~$$\Delta OM_{AR} = -\sum_i \Delta C_{T,i} = -\sum_i \int \frac{dC_{T,i}}{dt}. \quad (7)$$~~

~~Combining Eq. 1-6 and solving the second-order ODE provides the analytical solution utilized in UNIPAR (Eq. 7),~~

~~$$\Delta OM_{AR} = \sum_i \frac{k_{AR,i}\beta_{3,i}C_{T,i}^2\Delta t}{1+k_{AR,i}\beta_{3,i}C_{T,i}\Delta t}, \quad (8)$$~~

~~where $\beta_{3,i}$ is equal to~~

~~$$\beta_{3,i} = \frac{K_{mix,i}^2 M_{mix}\rho_{mix}10^3}{MW_i(1+K_{mix,i}M_{mix})^2}. \quad (9)$$~~

The full derivation of the equations used to predict OM_{AR} is shown in the SI (Sect. S3).

Formatted: Border: Top: (No border), Left: (No border)

Formatted: German (Germany)

3.3.2 OS formation

Sulfuric acid produced from the photooxidation of SO_2 influences aerosol phase state and hygroscopicity (Sect. 3.2), and acts as a catalyst in OM_{AR} formation. It can be wholly or partially titrated by ammonia, or it can react with reactive organic compounds to form OS. The formation of OS from the esterification of $[SO_4^{2-}]$ with reactive organic functional groups leads to a reduction in $[H^+]$ and LWC influencing subsequent OM_{AR} formation (Im et al., 2014). Therefore, the formation of OS must be estimated in order to accurately predict SOA growth. Of the total $[SO_4^{2-}]$ present in the SHMP aerosol, we assume that the sulfate which is not associated with ammonium ($[SO_4^{2-}]_{free}=[SO_4^{2-}]-0.5[NH_4^+]$) can form OS. The fraction of $[SO_4^{2-}]_{free}$ that forms OS is calculated using Eq. ~~10~~6,

$$\frac{[SO_4^{2-}]_{OS}}{[SO_4^{2-}]_{free}} = 1 - \frac{1}{1+f_{OS}\frac{N_{OS}}{[SO_4^{2-}]_{free}}}. \quad (~~10~~6)$$

where f_{OS} is a semi empirical parameter determined to be 0.07 by Im et al. (2014) by fitting the $[H^+]$ predicted by UNIPAR to the measured $[H^+]$ in toluene SOA, as a measure of OS formation, using the method of Li et al. (2015). The experimentally determined f_{OS} was validated for isoprene SOA using the experimental data of this study (Sect. 4.1). N_{OS} is the number of OS forming functional groups present in the aerosol phase. The functional groups

that have been shown to form *OS* are alcohols (Eddingsaas et al., 2012; Li et al., 2015; Minerath et al., 2008; Zhang et al., 2012), aldehydes (Liggio et al., 2005), and epoxides (Surratt et al., 2010). Alcohols and aldehydes can react with [SO_4^{2-}] in a single position, while epoxides ~~open in the aerosol phase and~~ react with [SO_4^{2-}] in two positions following ring opening in the aerosol phase. The average number of [SO_4^{2-}] reaction positions is determined for each $i_{m,n}$~~i~~, and then N_{OS} is calculated as the product of the molar concentration ~~of i~~ and the reaction positions of $i_{m,n}$~~i~~. Finally, $[SO_4^{2-}]_{OS}$ is removed from $[SO_4^{2-}]_{free}$ so that LWC and [H^+] can be recalculated for the next time step. As OS forms, both LWC and [H^+] are reduced.

3.3.3 OM from partitioning (OM_P)

After OM_{AR} formation, $OM_{P,i}$ is calculated using the module developed by Schell et al. (2001) modified to account for the assumed non-volatility and irreversibility of OM_{AR}. After OM_{AR} formation, the amount of the remaining $C_{T,i}$ of each lumping group that partitions between the gas and the SHMP aerosol is calculated as a function of the effective gas-phase saturation concentration of $i_{m,n}$~~i~~ ($C^*_{g,i}=1/K_{mix,i}$) using a mass balance following Eq. ~~10~~7,

$$OM_{P,i} = \left[(C_{T,i} - OM_{AR,i}) - C^*_{g,i} \frac{\frac{C_{mix,i}}{MW_i}}{\sum_i \left(\frac{C_{mix,i}}{MWi} + \frac{OM_{AR,i}}{MW_{oli,i}} \right) + OM_o} \right], \qquad (~~10~~7)$$

where MW_k and MW_{oli} are the molecular weight (g mol^{-1}) of the lumping species and the dimer of the lumping species, respectively, and OM_o is the pre-existing organic mass (mol m^{-3}). The system of non-linear equations solved iteratively and the calculated $OM_{P,i}$ are summed to get the total OM_P for each Δt. Unlike when $i_{m,n}$~~i~~ partitions into an organic only phase (γ=1), $\gamma_{mix,i}$ is used in calculating $C^*_{g,i}$ to account for the non-ideality of $i_{m,n}$~~i~~ partitioning into the SHMP aerosol (Sect. 3.2). The remaining concentration ($C_{T,i}$– $OM_{AR,i}$) are passed to the next time step and combined with the newly formed $i_{m,n}$~~i~~ (ΔVOC* $\alpha_{i_{m,n}}$).

Formatted: Font: Italic

4 Results and discussion

4.1 Model evaluation: SOA yield, O:C, and organosulfate formation

The ability of UNIPAR to simulate the SOA formation from isoprene photooxidation in the presence and absence of acidic inorganic seeds under low initial VOC/NO_x was determined through comparison of the simulated OM_T and experimental OM formation (OM_{exp}). All

OM_{exp} were corrected for particle wall loss. ~~Figure~~ Fig. 3 shows measured and predicted SOA formation in the presence and absence of SA at initial VOC/NO_x of ~17 for ISO1 and SA1 and 32 for ISO2 and SA2. The experiments performed ~~In~~ in the absence of inorganic seed (ISO1 and ISO2~~),~~) are used to test the prediction of organic-only oligomerization by UNIPAR. SOA formation is reasonably predicted in the absence of an inorganic aqueous phase for ~~by UNIPAR at~~ both experimental conditions with a maximum SOA yield (Y_{SOA} = $\Delta OM_{exp}/\Delta Iso$) of 0.025 and 0.007 for ISO1 and ISO2, respectively. These SOA yields are similar to those of reported literature values for isoprene in the absence of acidic seeds (Dommen et al., 2006). The model marginally overestimates the SOA formation in beginning of each chamber run, but the modeled OM_T falls within the range of error of OM_{exp} once the rate of SOA formation stabilizes and reaches a maximum. OM_{AR} makes up the majority of OM_T (>65% in ISO1 and ISO2). This is in agreement with the work of Nguyen et al. (2010) and Surratt et al. (2006) who analyzed the composition of isoprene SOA formed in the absence of an inorganic aqueous phase and found that the majority of SOA mass was from oligomeric structures. Furthermore, UNIPAR predicts that the approximately 70% of the OM_T is from lumping group $3OS_p$-M, of which more than 93% of the mass contribution is organic peroxides (MCM products C510OOH (~40%), C57OOH (~27%), C58OOH (~15%) and HMACROOH(11%), structures shown in Fig. S7 of the SI). This is close to the measurements of Surratt et al. (2006), in which 61% of the total mass in the absence of seeds is from organic peroxides.

The presence of SA seeds (shown in orange in ~~Figure~~ Fig. 3) greatly increases yields under both experimental conditions resulting in Y_{SOA} of ~~8.5%~~ 0.085 and ~~4.8%~~0.048 for SA1 and SA2, respectively, due to the dissolution of $i_{m,n}$~~i~~ into a larger M_{mix} resulting from increased LWC and increased $k_{AR,i}$ attributed to ~~the presence of~~ lower particle pH (higher $[H^+]$). Using the factor y that was fit using exp. SA1 in Table 1 (Eq. ~~6~~ 5 in Sect 3.3.1), the model accurately predicts the OM_T of ~~set~~ exp. SA2 at a lower VOC/NO_x in the presence of SA seed. Overall, OM_{AR} is the dominant contributor to OM_T for both sets contributing more than 65% and 85% in the absence and presence of SA, respectively. Also, the higher VOC/NO_x (lower NO_x) of both ISO2 and SA2 resulted in lower Y_{SOA} than ISO1 and SA1 which is discussed further in Sect. 4.3. In experiment SO2 (Table 1), SO_2(g) was introduced to the chamber instead of SA seed so that the model could be further tested under a situation more representative on the ambient atmosphere in which SO_2 is oxidized to SA ~~leading to dynamic changes in $[H^+]$ and LWC~~. As can be seen in Fig 3, (shown in green), the model also reasonably predicts the OM_T.

Formatted: Subscript

Formatted: Subscript

Formatted: Font: Italic

Formatted: Subscript

Formatted: Subscript

In addition to OM_T, O:C and $[SO_4^{2-}]_{OS}$ were also predicted using the model. The predicted $[SO_4^{2-}]_{OS}$ is important due to ~~both the formation of additional OM_{AR} and for~~ the consumption of SO_4^{2-} that leads to an ~~reduction in $[H^+]$~~increase in particle pH and a reduction in LWC. In ~~the presence of SA seed (~~exp. SA2~~)~~, $[SO_4^{2-}]_{OS}$ ~~was determined~~ measured using the C-RUV method allowing for comparison to the model (refer to Sect. 2 for C-RUV method description). Fig. 4 shows time series of the model predicted and measured $[SO_4^{2-}]_{OS}$ along with the total $[SO_4^{2-}]$ and $[NH_4^+]$ measured by the PILS-IC, the measured RH, and the predicted particle pH. Once SOA formation starts, OS quickly forms. The measured $[SO_4^{2-}]_{OS}$ is reasonably well predicted by the model with the predicted value being within the range of error once SOA mass stabilizes. The predicted pH is relatively stable in the first hour of the experiment because the effects of decreasing RH (and LWC) and increasing $[NH_4^+]$ counteract each other, but once SOA formation starts pH increases rapidly due to titration by NH_3 produced from the chamber walls, the consumption of $[SO_4^{2-}]$ by OS formation, and the dilution of $[H^+]$ by SOA mass. Overall, the predicted pH starts at -0.73 and increases to 0.65 at the end of the experimental run, which is within the range of ambient aerosol pH measured by Guo et al. (2015) in the S.E. U.S (mean: 0.94, min: -0.94, max: 2.23).

~~The measured and predicted $[SO_4^{2-}]_{OS}$ / $[SO_4^{2-}]$ were 0.32 ± 0.06 and 0.36, respectively.~~ While the O:C of the experimental SOA were not measured, the simulated O:C can be compared to literature values which range from 0.69 to 0.88 (Bertram et al., 2011; Chen et al., 2011; Kuwata et al., 2013). UNIPAR estimates the O:C ratio using $O:C_i$ and mole fraction of each species in the aerosol phase not accounting for changes that may result from oligomerization, hydration or OS formation. In the presence of untitrated SA, the modeled O:C is 0.69 which is the lower end of the range of literature values. With increasing titration changes in composition lead to higher overall predicted O:C. In SA1, SA is partially titrated by NH_3^+ over the course of the experiment and the resulting O:C is 0.84. For ISO1 and ISO2, the O:C are 0.92 and 0.98, which is higher than the reported values. This is due to the predicted SOA being comprised of a few compounds with O:C near 1 without considering the change of molecular structures via aerosol phase reactions. Chen et al. (2011) showed a similar result in that the O:C ratio of monomeric products in isoprene SOA is higher that of oligomers.

Formatted: Not Superscript/ Subscript

Formatted: Superscript

Formatted: German (Germany)

4.2 Isoprene SOA yield and the influence of VOC/NO_x and inorganic composition

In the following sections the model is used to investigate the influence of VOC/NO_x, LWC, and [H+] on isoprene Y_{SOA} and composition. The experimental conditions of SA1 (RH, T, ΔISO) are used in all of these simulations unless otherwise specified.

Recent studies have investigated the effect of NO_x on the SOA formation of isoprene for the high NO_x regime (VOC/NO_x < 5.5) and in the absence of NO_x (Chan et al., 2010a; Kroll et al., 2006; Xu et al., 2014), and found that in the Y_{SOA} of isoprene ~~isoprene will be higher when formed in the absence of NOx than in the presence of high NO_x concentrations~~is non-linearly related to VOC/NO_x ~~–~~with Y_{SOA} being highest at intermediate NO_x conditions (VOC/NO_x = ~2). However, very little investigation has been performed on isoprene SOA formation within ~~in~~ the low NO_x regime (VOC/NO_x > 5.5 and NO_x > 0 ppb) of this study, which is typical of rural areas downwind of urban centers (Finlayson-Pitts and Pitts, Jr., 1993). To investigate the influence of the NO_x level on Y_{SOA} in this range, simulations were performed in which the VOC/NO_x ratio was increased incrementally from 10 to 100 with SA seeded SOA without titration and isoprene only SOA. The Y_{SOA} of each simulation are plotted in Fig. 45. Overall, ~~with decreasing VOC/NO_x (increasing~~ increasing NO_x within this range (decreasing VOC/NO_x~~)~~, increases Y_{SOA} both with and without acidic seeds ~~increases in all cases~~, which agrees with the general trend of Kroll et al. (2006) where intermediate NO_x conditions had higher Y_{SOA} than no-NO_x conditions. However, the degree of the increase in Y_{SOA} with increasing NO_x is different for the isoprene only SOA and the SOA formed in the presence of SA seeds, which has not previously been shown to the best of our knowledge.

Y_{SOA} increases much more rapidly with increasing NO_x in the presence of SA seeds, which is due to an increase in the relative contribution of reactive species. ~~as opposed to the high NO_x regime where increases in NO_x lead to reduction in Y_{SOA}.~~ RO radicals produced from the reaction of RO_2 radicals with NO ~~and NO~~ can lead to multifunctional carbonyls via reaction with oxygen and also simple carbonyls such as ~~or~~ glyoxal and methylglyoxal through fragmentation of RO radicals. These products~~, which~~ are all highly reactive in the aerosol phase and produce OM_{AR}. ~~This is illustrated by the more drastic reduction in Y_{SOA} of SA seeded SOA due to the sensitivity of these compounds to acid catalyzed reactions.~~ Furthermore, some late generation RO_2 radicals, whose precursors are formed from the RO pathway (High NO), react with HO_2 ~~and~~ to form low ~~volatile~~ volatility ~~peroxynitrate~~ organic

Formatted: Subscript
Formatted: Subscript
Formatted: Subscript
Formatted: Subscript
Formatted: Not Superscript/ Subscript
Formatted: Not Superscript/ Subscript
Formatted: Subscript
Formatted: Subscript
Formatted: Font: Not Italic
Formatted: Font: Not Italic, Subscript
Formatted: Subscript

peroxides with alcohol functional groups and an aldehyde (3OS$_p$-M: C510OOH, C57OOH, C58OOH, HMACROOH in MCM, Sect S7). Therefore, ~~increases~~ increases in NO_x within the~~in VOC/NO_x within the~~ simulation condition (VOC/NO_x 10~100) of this study leads to increases Y_{SOA} with higher sensitivity to VOC/NO_x in the presence of inorganic seed. Fig~~ure~~ S5 shows the stoichiometric mass coefficients ($\alpha_{i,m,n}$) of important products as a function of VOC/NO_x.

Y_{SOA} is also dynamically related to inorganic compositions. SOA formation in the absence of inorganic seed is primarily a function of the characteristics of $i_{m,n}$~~i~~ and the impact of LWC on isoprene SOA is minimal. However, under ambient conditions SOA will typically be formed in the presence of inorganic aerosol. Variations in the ~~composition of the~~ inorganic aerosol composition ($[SO_4^{2-}]$ and $[NH_4^+]$) and RH lead to significant~~ly~~ changes in LWC and ~~[H$^+$]~~pH. At high LWC, the total volume of absorptive mass (M_{mix}) increases allowing for hydrophilic $i_{m,n}$~~i~~ to partition into the aerosol in significant amounts and engage in aerosol phase reaction. Additionally, highly reactive species such as IEPOX will react to rapidly form SOA in the presence of $[H^+]$ (Gaston et al., 2014). In Fig ~~5~~ 6 the simulated Y_{SOA} is plotted as a function of the fractional free sulfate (FFS), ($[SO_4^{2-}]$-0.5$[NH_4^+]$)/$[SO_4^{2-}]$), and RH. Unlike pH, which is very difficult to measure, $[SO_4^{2-}]$, $[NH_4^+]$, and RH data are widely available and easy to measure, which is why FFS and RH were used in Fig 6. Using an ion balance such as FFS alone has been shown to be not representative of actual particle pH (Guo et al., 2015), but providing both FFS and RH allow for estimation of pH within an inorganic thermodynamic model and ease of use by future studies.

It is difficult to decouple the effects of $[SO_4^{2-}]$, LWC and pH since $[SO_4^{2-}]$ ultimately influences both LWC and pH, but Fig 6 can be used to help elucidate the influence of these effects in UNIPAR. For AS seed (FFS=0.0), SO_4 is entirely titrated by ammonia and the lowest Y_{SOA} occurs below the ERH. As the RH increases, AS becomes deliquesced and the LWC gradually rises leading to an increase in Y_{SOA}. This is true for the predictions at all small values of FFS due to the increase in the total volume of absorptive mass (M_{mix}) associated with increasing LWC, allowing for hydrophilic $i_{m,n}$ to partition into the aerosol in significant amounts and engage in aerosol phase reactions. However, as the amount of $[NH_4^+]$ decreases (FFS < 0.7, highly acidic), the effect of increasing LWC reverses, and Y_{SOA} decreases with increasing LWC due to the dilution of $[SO_4^{2-}]$ and the resulting increase in pH. If RH is held constant, varying FFS allows for investigation of the effect of pH on Y_{SOA}. Increasing FFS or

Formatted: Subscript
Formatted: Subscript
Formatted: Font: Italic
Formatted: Font: Not Italic
Formatted: Font: Not Italic

decreasing pH at constant RH leads to a rapid increase in Y_{SOA} at all RH due to an increase in the SOA formation from the acid catalyzed reactions of species such as IEPOX. Therefore, $[SO_4^{2-}]$ modulates Y_{SOA} within UNIPAR by controlling LWC and $[H^+]$ which influence $k_{AR,i}$ (Eq. 5). The consumption of $[SO_4^{2-}]$ by OS formation is accounted for in UNIPAR through a reduction in acidity and LWC, but the role of $[SO_4^{2-}]$ in reactive uptake as a nucleophile is not directly accounted for.

~~The lowest Y_{SOA} occur below the ERH. For AS seeded SOA (FFS=0.0), simulated Y_{SOA} gradually increases with increasing RH due to the rise in LWC. As FFS increases (the aerosol becomes more acidic), Y_{SOA} dramatically increases at a given RH, e.g. Y_{SOA} increases from 0.033 to 0.138 when FFS changes from 0 (AS) to 1.0 (SA) at 60% RH. At a high FFS Y_{SOA} falls with increases in RH as a result of the reduction in $[H^+]$ from the higher LWC. Therefore, Y_{SOA} of isoprene SOA is concluded to be much more sensitive to $[H^+]$ than to LWC but dynamically related to both.~~

4.3 Simulated composition of isoprene SOA

Analysis of the contributions of each $i_{m,n}$~~i~~ to the overall OM_T allows for a determination of the species that are significant in isoprene SOA for various inorganic compositions. Four simulations were performed at 60% RH with AS and SA seeds at org:sulf of 0.5 and 1.5 to capture the differences in composition as a result of changes in LWC, $[H^+]$, and M_{mix}.

The aerosol mass fraction of each $i_{m,n}$~~i~~ (MF_i) under the simulated conditions are shown in Fig ~~6~~7. IEPOX has been demonstrated to be an important precursor to ambient (Budisulistiorini et al., 2015; Chan et al., 2010b) and laboratory generated (Lin et al., 2012; Paulot et al., 2009) isoprene SOA leading to the formation of 2-methyltetrols (Surratt et al., 2010), OS (Liao et al., 2015), and other species through aerosol phase reactions in which IEPOX products contribute up to 33% of ambient OM in Southeast U.S. (Budisulistiorini et al., 2013). The formation of IEPOX derived SOA has been shown to be primarily from the reactive uptake in the presence of LWC and $[H^+]$, but is most highly correlated with aerosol acidity (Gaston et al., 2014). In ~~Figure~~ Fig. ~~6~~7, it can be seen that the MF_i of IEPOX derived SOA is higher in the presence of $[H^+]$. When accounting for the yield of each system, the total formation of IEPOX derived SOA is much greater in the presence of SA seed than AS seed. Additionally, the MF_i of IEPOX derived SOA falls within the range measured in literature. When org:sulf increases from 0.5 to 1.5 in the presence of SA, the reduction of MF_i of IEPOX products is

Formatted: Font: Not Italic, Not Superscript/ Subscript
Formatted: Superscript
Formatted: Font: Not Italic
Formatted: Subscript

due to the increasing contribution of other $i_{m,n}$ (7MA and OTHER) while the mass contribution of IEPOX remains similar. The MF_i of glyoxal (GLY) is significant for all four simulations, but increases with growth of M_{mix} due to its high aqueous solubility and tendency to form hydrates that can form oligomers.

In the absence of acidity, $k_{AR,i}$ are relatively small and the MF_i are primarily a function of the gas phase concentration, volatility and solubility of *i*. For example, in the AS seeded SOA simulations, $3OS_p$-M (products organic peroxides with both reactive groups an aldehyde and alcohols, Figures S3 and S7) contributes more than half of the total mass (Fig. ure 67) due to its high gas phase concentration and low volatility. As LWC and $k_{AR,i}$ increase (AS to SA seed aerosol and org:sulf 1.5 to 0.5), more volatile and reactive $i_{m,n}$ are able to contribute to MF_i. Therefore, the MF_i of $3OS_p$-M is significantly reduced in SA seeded SOA as other $i_{m,n}$ contribute in larger fractions. Overall, OM_P only contributes a small fraction of the total OM_T, and the MF_i of the partitioning species generally decreases with increasing contribution of other species at higher LWC and $[H^+]$.

4.4 Model sensitivity, uncertainty, and limitations

UNIPAR utilizes the chemical structures provided by MCM to estimate the thermodynamic properties of the gas phase products, which are lumped based on their calculated vapor pressure (8 groups) and aerosol phase reactivity (6 groups). However, since not all atmospheric reactions have been studied in detail, MCM determines the products and kinetics of unstudied reactions using the known degradation mechanisms of similar chemical species. Pinho et al. (2005) evaluated the isoprene mechanism of MCM v3 by comparing the oxidation of isoprene and its products methacrolein and methylvinyl ketone to chamber data. The model performed reasonably well for these limited products, but a large amount of uncertainty remains in regards to the prediction of the hundreds of other isoprene derived products. Furthermore, the lumping approach of UNIPAR uses a fixed gas phase composition set at the maximum HO_2/NO for each VOC/NO_x ratio. This approach does not account for changes to the gas phase composition that occur due to continued oxidation.

Deviation of the estimated $p^o_{L,i}$ from the actual $p^o_{L,i}$ due to the uncertainty of the group contribution method (Sect. 3.1) can change the lumping assignment affecting both OM_P and OM_{AR}. The uncertainty associated with the group contribution method used for $p^o_{L,i}$ estimation is a factor of 1.45 (Joback and Reid, 1987; Stein and Brown, 1994; Zhao et al.,

1999). The temperature dependency of each lumping group as is calculated as a function of the enthalpy of vaporization (ΔH_{vap}) and also has associated uncertainty that can affect the model prediction. The error of this method is 2.6% (Kolská et al., 2005). To determine the model sensitivity to these parameters, simulations of SA1 were performed by increasing and decreasing $p^{o}_{L,i}$ and ΔH_{vap} by a factor of 1.5 and 1.1, respectively. The change in OM_T from the baseline for each simulation is shown in ~~Figure~~ Fig. S6. Increasing and decreasing $p^{o}_{L,i}$ by a factor of 1.5 results in a 32.03% and -26.41% change, respectively, while modifying ΔH_{vap} only leads to ±0.27% change.

The thermodynamic model AIOMFAC was employed to generate a simplified parameterization to estimate $\gamma_{mix,i}$ in the SHMP isoprene SOA as a function of O:C, org:sulf, RH, and V_{mol}. AIOMFAC is a valuable tool for predicting the activity coefficients of complex mixtures, but it has substantial uncertainty resulting from limitations of the database used in development and the error associated with the underlying modules. Moreover, the expected accuracy is limited further by the regression performed in UNIPAR. For the condition simulated by UNIPAR, $\gamma_{mix,i}$ are all near unity (0.65-1.75). Considering the characteristics of a SHMP aerosol, a factor of 1.5 was applied to the predicted $\gamma_{mix,i}$ and the resulting change in OM_T is -16.22%/+32.00% (Fig S6), which is similar to the model sensitivity to $p^{o}_{L,i}$.

The other parameter largely affecting the simulated SOA formation in UNIPAR is $k_{AR,i}$, which is calculated primarily as a function of LWC, $[H^+]$, and reactivity of $i_{m,n}$~~i~~ (Sect. 3.3.1). Estimations of LWC and $[H^+]$ are performed by the inorganic thermodynamic model E-AIM. Similar to AIOMFAC, the accuracy of E-AIM will depend on the underlying assumptions and the database used in development. For LWC, the predictions of E-AIM are consistent with other inorganic thermodynamic models and are based on widely used, critically reviewed water activity data (Zhang et al., 2000). However, inorganic thermodynamic models vary widely in predicting $[H^+]$ especially at low RH. This is especially true for ammonia rich inorganic salts at low RH. Corrections for the ammonia rich predictions of $[H^+]$ were applied based on the results of Li and Jang (2012) in which aerosol $[H^+]$ was measured using a filter based colorimetry method coupled with a PILS-IC. The total uncertainty of this method is approximately 18%. There is also uncertainty stemming from the flow chamber study that was used to fit the coefficients used in predicting $k_{AR,i}$. To determine the possible sensitivity of the model to the combined uncertainty of the corrected E-AIM and the function used to

predict $k_{AR,i}$, a factor of 2.0 was applied to simulations and the resulting change in OM_T is approximately ±13% (Fig S6).

Furthermore, not all recent advancements in the understanding of SOA formation mechanisms are accounted for by UNIPAR, including but not limited to SOA viscosity, nighttime chemistry of nitrate radicals (NO_3^*), and SVOC wall loss. Virtanen et al. (2010) reported that biogenic SOA can exist as amorphous solids or glassy state, which can lead to deviations from equilibrium processes, but Song et al. (2015) found that isoprene derived SOA is of low viscosity under the range of ambient RH. Thus, impact of viscosity on isoprene SOA is minimal. The nighttime reaction of isoprene with NO_3^* has been found to lead to significant SOA formation due to the formation of stable primary organonitrate (ON). Ng et al. (2008) measured SOA yields up to 23.8% from the dark chamber reaction of isoprene and NO_3^* under dry conditions (<10% RH), while Rollins et al. (2012) linked NO_3^* chemistry to ambient, nighttime SOA production with 27 to 40% of nighttime OM growth from ON. Under low NO_x conditions, isoprene photooxidation has been shown to produce primarily tertiary ON in both the gas phase and through aerosol phase epoxide reactions (Eddingsaas et al., 2010; Paulot et al., 2009). Darer et al. (2011) investigated the stability of primary and tertiary ON and found the tertiary ON to be highly unstable and to rapidly convert to OS and polyols in both neutral and acidic SOA. Therefore, it is unlikely that ON significantly contribute to the SOA investigated and modeled in this study.

A number of recent studies have found that the loss of gas phase vapors to chamber walls can compete with gas-particle partitioning (Matsunaga and Ziemann, 2010; Zhang et al., 2014, 2015). Vapor wall loss was not accounted for in this study and thus the experimental SOA mass may be low biased. However, based on the conclusions of Zhang et al. (2015), the high volatility of isoprene products likely results in gas-particle partitioning outcompeting vapor wall loss in chambers with a large ratio of volume to surface area.

Another new development in the SOA formation is the discovery of the salting-in and salting-out of glyoxal and methylglyoxal (Waxman et al., 2015). While these effects are very interesting and likely influence the SOA formation of these species, they are not yet included within UNIPAR. The topic will be reconsidered for application within our model once these effects have been more comprehensively investigated for a wider range of relevant water-soluble organic molecules and inorganic aerosol compositions.

Formatted: German (Germany)

In the recent Southern Oxidant and Aerosol Study field campaign, Budisulistiorini et al. (2015) and Xu et al. (2015) found ambient isoprene SOA formation in the SE U.S. to be most highly correlated with [SO_4^{2-}], and insensitive to [H^+] and LWC. However, in the summer months the aerosol of the SE U.S. are highly acidic (pH -1 to 2) and high in LWC due to the high RH (> 50%) (Guo et al., 2015). Under these conditions, the formation of isoprene derived SOA is not likely to be highly correlated with changes in LWC and [H^+] since both are always high. Yet when comparing neutral and acidic conditions, the presence of acidity has repeatedly been shown to lead to increases in Y_{SOA} (Lin et al., 2012; Surratt et al., 2007). Most recently, Lewandowski et al. (2015) found up to a 459% increases in YSOA from the presence inorganic acid [H^+]. Additionally, Xu et al. (2015) found a reduction in isoprene derived SOA with increases RH for the highly acidic aerosol of the campaign. A similar reduction with increasing RH is seen at high FFS in Fig. ~~5~~ 6 due to the dilution of [SO_4^{2-}] and the corresponding [H^+] by increases in LWC.

5 Conclusions and Atmospheric Implications

Under the assumption of SHMP aerosol, UNIPAR was able to simulate the low NO_x SOA formation of isoprene from partitioning and aerosol phase reactions with and without an inorganic acid seed. The data used to validate the model was generated using the UF-APHOR outdoor chamber, which allows for day long experiments under ambient sunlight, T and RH. For the SOA formation of isoprene in the absence of deliquesced inorganic seeds, UNIPAR was able to predict the experimental OM_T using the same approach that was applied to anthropogenic, aromatic VOCs in Im et al. (2014) without any modification. Differences between the SHMP SOA formed by isoprene in the presence of deliquesced inorganic seeds and LLPS SOA of the previous study required a slight reduction in $k_{AR,i}$. After validating the model using the measured SOA formation of outdoor chamber experiments, simulations were performed to elucidate the sensitivity of Y_{SOA} and composition to model parameters. From this analysis it was determined that the Y_{SOA} of isoprene and the resulting SOA composition is primarily a function of VOC/NO_x, [H^+], and LWC. For the range of VOC/NO_x investigated in this study (≥10), increases in NO_x corresponded with increases in Y_{SOA} and a higher sensitivity to [H^+]. This is due to the increased production of highly reactive carbonyls, such as glyoxal, and a more general shift to lower volatility (Figure S6).

Changes in [H^+] and LWC were shown to strongly influence Y_{SOA} (Fig ~~5~~6). At a given RH, increases in [H^+] result in increased OM formation. For titrated acidic aerosol, increases in

RH lead to gradual increases in Y_{SOA}. However for highly acidic aerosol (FFS≥0.75), increases in RH decrease Y_{SOA} due to dilution of $[H^+]$. Overall, isoprene SOA formation was found to be most sensitive to $[H^+]$ with the highest Y_{SOA} occurring at high FFS and low RH.

Due to the pervasiveness of isoprene in the ambient atmosphere, any variation in Y_{SOA} will have a strong influence on the global SOA budget and needs to be accounted for by climate and air quality models. Since the experimental runs and simulations performed in this study were at concentrations beyond those of the ambient atmosphere, additional simulations were performed to estimate Y_{SOA} for conditions more representative of the ambient atmosphere. The ΔISO during each Δt was assumed to be constant and estimated assuming a pseudo first order reaction with OH using an isoprene concentration of 2.4 ppb from the rural measurements of Wiedinmyer et al. (2001) and a OH concentration of 1.0E6 molecules/cm^3. Using a $[SO_4^{2-}]$ of 5.55 μg/m^3 and OM_o of 3 μg/m^3 based on the non-urban continental composition of submicron PM from the review of Heintzenberg (1989), two sets of simulations were performed for AS and AHS at RH of 30% and 60% and VOC/NO_x=10. The simulated Y_{SOA} of AS are 0.01695 (OM_T = 0.329 μg m^{-3}) and 0.0207 (OM_T = 0.402 μg m^{-3}), and of AHS are 0.0446 (OM_T = 0.867 μg m^{-3}) and 0.0449 (OM_T = 0.873 μg m^{-3}) at 30% and 60% RH, respectively. The OM_T formation and associated Y_{SOA} were calculated after an eight hour simulation. AS at 30% RH is the seen as the baseline as it is below the ERH. Increasing the RH to 60% leads to a 22% increase in Y_{SOA} for AS due to the increased LWC. The presence of AHS seeds and the resultant increase in $[H^+]$ leads to an increase of 163% and 165% in Y_{SOA} over the baseline at 30% and 60% RH, respectively. These results support the conclusion that the SOA formation of isoprene is more sensitive to $[H^+]$ than to LWC, but dynamically related to both. Furthermore, while the SOA formation of isoprene may be reasonably predicted as a linear function of $[H^+]$ for a specific RH and VOC/NO_x, as is proposed by Surratt et al. (2007), a single linear relationship will not hold at different RH for a single VOC/NO_x or under the possible range of conditions in the ambient atmosphere. In the application of UNIPAR to the aromatic LLPS SOA system, Im et al. (2014) found the Y_{SOA} of toluene to be higher in the presence AHS than AS at 30% RH, but the same at 60% RH meaning that the SOA formation of toluene is less sensitive to $[H^+]$ but more sensitive to LWC than isoprene. The relationship between Y_{SOA}, LWC, and $[H^+]$ will not only vary dynamically for different VOC/NO_x but also between different VOC systems. Failure to account for these relationships in regional and global scale models may lead to significant underestimation of SOA formation in acidic and humid conditions.

Acknowledgements

This work was supported by the grant from the National Science Foundation (ATM-0852747) and the grant from the National Research Funding of Korea (2014M3C8A5032316).

References

Aiken, A. C., DeCarlo, P. F., Kroll, J. H., Worsnop, D. R., Huffman, J. A., Docherty, K. S., Ulbrich, I. M., Mohr, C., Kimmel, J. R., Sueper, D., Sun, Y., Zhang, Q., Trimborn, A., Northway, M., Ziemann, P. J., Canagaratna, M. R., Onasch, T. B., Alfarra, M. R., Prevot, A. S. H., Dommen, J., Duplissy, J., Metzger, A., Baltensperger, U. and Jimenez, J. L.: O/C and OM/OC Ratios of Primary, Secondary, and Ambient Organic Aerosols with High-Resolution Time-of-Flight Aerosol Mass Spectrometry, Environ. Sci. Technol., 42(12), 4478–4485, doi:10.1021/es703009q, 2008.

Bertram, A. K., Martin, S. T., Hanna, S. J., Smith, M. L., Bodsworth, A., Chen, Q., Kuwata, M., Liu, A., You, Y. and Zorn, S. R.: Predicting the relative humidities of liquid-liquid phase separation, efflorescence, and deliquescence of mixed particles of ammonium sulfate, organic material, and water using the organic-to-sulfate mass ratio of the particle and the oxygen-to-carbon elemental ratio of the organic component, Atmos Chem Phys, 11(21), 10995–11006, doi:10.5194/acp-11-10995-2011, 2011.

Budisulistiorini, S. H., Canagaratna, M. R., Croteau, P. L., Marth, W. J., Baumann, K., Edgerton, E. S., Shaw, S. L., Knipping, E. M., Worsnop, D. R., Jayne, J. T., Gold, A. and Surratt, J. D.: Real-Time Continuous Characterization of Secondary Organic Aerosol Derived from Isoprene Epoxydiols in Downtown Atlanta, Georgia, Using the Aerodyne Aerosol Chemical Speciation Monitor, Environ. Sci. Technol., 47(11), 5686–5694, doi:10.1021/es400023n, 2013.

Budisulistiorini, S. H., Li, X., Bairai, S. T., Renfro, J., Liu, Y., Liu, Y. J., McKinney, K. A., Martin, S. T., McNeill, V. F., Pye, H. O. T., Nenes, A., Neff, M. E., Stone, E. A., Mueller, S., Knote, C., Shaw, S. L., Zhang, Z., Gold, A. and Surratt, J. D.: Examining the effects of anthropogenic emissions on isoprene-derived secondary organic aerosol formation during the 2013 Southern Oxidant and Aerosol Study (SOAS) at the Look Rock, Tennessee ground site, Atmos Chem Phys, 15(15), 8871–8888, doi:10.5194/acp-15-8871-2015, 2015.

Carlton, A. G., Wiedinmyer, C. and Kroll, J. H.: A review of Secondary Organic Aerosol (SOA) formation from isoprene, Atmos Chem Phys, 9(14), 4987–5005, doi:10.5194/acp-9-4987-2009, 2009.

Chan, A. W. H., Chan, M. N., Surratt, J. D., Chhabra, P. S., Loza, C. L., Crounse, J. D., Yee, L. D., Flagan, R. C., Wennberg, P. O. and Seinfeld, J. H.: Role of aldehyde chemistry and NOx concentrations in secondary organic aerosol formation, Atmos Chem Phys, 10(15), 7169–7188, doi:10.5194/acp-10-7169-2010, 2010a.

Chan, M. N., Surratt, J. D., Claeys, M., Edgerton, E. S., Tanner, R. L., Shaw, S. L., Zheng, M., Knipping, E. M., Eddingsaas, N. C., Wennberg, P. O. and Seinfeld, J. H.: Characterization and Quantification of Isoprene-Derived Epoxydiols in Ambient Aerosol in the Southeastern United States, Environ. Sci. Technol., 44(12), 4590–4596, doi:10.1021/es100596b, 2010b.

Chen, Q., Liu, Y., Donahue, N. M., Shilling, J. E. and Martin, S. T.: Particle-Phase Chemistry of Secondary Organic Material: Modeled Compared to Measured O:C and H:C Elemental Ratios Provide Constraints, Environ. Sci. Technol., 45(11), 4763–4770, doi:10.1021/es104398s, 2011.

Formatted: Bibliography, Widow/Orphan control, Adjust space between Latin and Asian text, Adjust space between Asian text and numbers

Claeys, M., Wang, W., Ion, A. C., Kourtchev, I., Gelencsér, A. and Maenhaut, W.: Formation of secondary organic aerosols from isoprene and its gas-phase oxidation products through reaction with hydrogen peroxide, Atmos. Environ., 38(25), 4093–4098, doi:10.1016/j.atmosenv.2004.06.001, 2004.

Clegg, S. L., Brimblecombe, P. and Wexler, A. S.: Thermodynamic Model of the System H+−NH4+−SO42-−NO3-−H2O at Tropospheric Temperatures, J. Phys. Chem. A, 102(12), 2137–2154, doi:10.1021/jp973042r, 1998.

Darer, A. I., Cole-Filipiak, N. C., O'Connor, A. E. and Elrod, M. J.: Formation and Stability of Atmospherically Relevant Isoprene-Derived Organosulfates and Organonitrates, Environ. Sci. Technol., 45(5), 1895–1902, doi:10.1021/es103797z, 2011.

Dommen, J., Metzger, A., Duplissy, J., Kalberer, M., Alfarra, M. R., Gascho, A., Weingartner, E., Prevot, A. S. H., Verheggen, B. and Baltensperger, U.: Laboratory observation of oligomers in the aerosol from isoprene/NOx photooxidation, Geophys. Res. Lett., 33(13), L13805, doi:10.1029/2006GL026523, 2006.

Eddingsaas, N. C., VanderVelde, D. G. and Wennberg, P. O.: Kinetics and Products of the Acid-Catalyzed Ring-Opening of Atmospherically Relevant Butyl Epoxy Alcohols, J. Phys. Chem. A, 114(31), 8106–8113, doi:10.1021/jp103907c, 2010.

Eddingsaas, N. C., Loza, C. L., Yee, L. D., Chan, M., Schilling, K. A., Chhabra, P. S., Seinfeld, J. H. and Wennberg, P. O.: α-pinene photooxidation under controlled chemical conditions-Part 2: SOA yield and composition in low- and high-NOx environments, Atmospheric Chem. Phys., 12(16), 7413–7427, doi:10.5194/acp-12-7413-2012, 2012.

Edney, E. O., Kleindienst, T. E., Jaoui, M., Lewandowski, M., Offenberg, J. H., Wang, W. and Claeys, M.: Formation of 2-methyl tetrols and 2-methylglyceric acid in secondary organic aerosol from laboratory irradiated isoprene/NOX/SO2/air mixtures and their detection in ambient PM2.5 samples collected in the eastern United States, Atmos. Environ., 39(29), 5281–5289, doi:10.1016/j.atmosenv.2005.05.031, 2005.

Finlayson-Pitts, B. J. and Pitts, Jr., J. N.: Atmospheric Chemistry of Tropospheric Ozone Formation: Scientific and Regulatory Implications, J. Air Waste Assoc., 43(8), 1091–1100, doi:10.1080/1073161X.1993.10467187, 1993.

Gaston, C. J., Riedel, T. P., Zhang, Z., Gold, A., Surratt, J. D. and Thornton, J. A.: Reactive Uptake of an Isoprene-Derived Epoxydiol to Submicron Aerosol Particles, Environ. Sci. Technol., 48(19), 11178–11186, doi:10.1021/es5034266, 2014.

Guenther, A., Karl, T., Harley, P., Wiedinmyer, C., Palmer, P. I. and Geron, C.: Estimates of global terrestrial isoprene emissions using MEGAN (Model of Emissions of Gases and Aerosols from Nature), Atmos Chem Phys, 6(11), 3181–3210, doi:10.5194/acp-6-3181-2006, 2006.

Guo, H., Xu, L., Bougiatioti, A., Cerully, K. M., Capps, S. L., Hite, J. R., Carlton, A. G., Lee, S.-H., Bergin, M. H., Ng, N. L., Nenes, A. and Weber, R. J.: Fine-particle water and pH in the southeastern United States, Atmospheric Chem. Phys., 15(9), 5211–5228, doi:10.5194/acp-15-5211-2015, 2015.

Heintzenberg, J.: Fine particles in the global troposphere A review, Tellus B, 41B(2), 149–160, doi:10.1111/j.1600-0889.1989.tb00132.x, 1989.

Hennigan, C. J., Bergin, M. H., Dibb, J. E. and Weber, R. J.: Enhanced secondary organic aerosol formation due to water uptake by fine particles, Geophys. Res. Lett., 35(18), L18801, doi:10.1029/2008GL035046, 2008.

Henze, D. K. and Seinfeld, J. H.: Global secondary organic aerosol from isoprene oxidation, Geophys. Res. Lett., 33(9), L09812, doi:10.1029/2006GL025976, 2006.

Hodas, N., Zuend, A., Mui, W., Flagan, R. C. and Seinfeld, J. H.: Influence of particle-phase state on the hygroscopic behavior of mixed organic–inorganic aerosols, Atmos Chem Phys, 15(9), 5027–5045, doi:10.5194/acp-15-5027-2015, 2015.

Im, Y., Jang, M. and Beardsley, R. L.: Simulation of aromatic SOA formation using the lumping model integrated with explicit gas-phase kinetic mechanisms and aerosol-phase reactions, Atmos Chem Phys, 14(8), 4013–4027, doi:10.5194/acp-14-4013-2014, 2014.

Ip, H. S. S., Huang, X. H. H. and Yu, J. Z.: Effective Henry's law constants of glyoxal, glyoxylic acid, and glycolic acid, Geophys. Res. Lett., 36(1), L01802, doi:10.1029/2008GL036212, 2009.

Jang, M. and Kamens, R. M.: A Thermodynamic Approach for Modeling Partitioning of Semivolatile Organic Compounds on Atmospheric Particulate Matter: Humidity Effects, Environ. Sci. Technol., 32, 1237–1243, doi:10.1021/es970773w, 1998.

Jang, M. and Kamens, R. M.: Characterization of Secondary Aerosol from the Photooxidation of Toluene in the Presence of NOx and 1-Propene, Environ. Sci. Technol., 35, 3626–3639, doi:10.1021/es010676+, 2001.

Jang, M., Czoschke, N. M., Lee, S. and Kamens, R. M.: Heterogeneous Atmospheric Aerosol Production by Acid-Catalyzed Particle-Phase Reactions, Science, 298(5594), 814–817, doi:10.1126/science.1075798, 2002.

Jang, M., Carroll, B., Chandramouli, B. and Kamens, R. M.: Particle Growth by Acid-Catalyzed Heterogeneous Reactions of Organic Carbonyls on Preexisting Aerosols, Environ. Sci. Technol., 37(17), 3828–3837, doi:10.1021/es021005u, 2003.

Jang, M., Czoschke, N. M. and Northcross, A. L.: Semiempirical Model for Organic Aerosol Growth by Acid-Catalyzed Heterogeneous Reactions of Organic Carbonyls, Environ. Sci. Technol., 39(1), 164–174, doi:10.1021/es048977h, 2005.

Jang, M., Czoschke, N. M., Northcross, A. L., Cao, G. and Shaof, D.: SOA Formation from Partitioning and Heterogeneous Reactions: Model Study in the Presence of Inorganic Species, Environ. Sci. Technol., 40(9), 3013–3022, doi:10.1021/es0511220, 2006.

Jang, M., Cao, G. and Paul, J.: Colorimetric Particle Acidity Analysis of Secondary Organic Aerosol Coating on Submicron Acidic Aerosols, Aerosol Sci. Technol., 42(6), 409–420, doi:10.1080/02786820802154861, 2008.

Jeffries, H.E., Gary, M. W., Kessler, M and Sexton, K. G.: Morphecule reaction mechanism, Morpho., 1998.

Joback, K. G. and Reid, R. C.: Estimation of Pure-Component Properties from Group-Contributions, Chem. Eng. Commun., 57(1-6), 233–243, doi:10.1080/00986448708960487, 1987.

Kleindienst, T. E., Jaoui, M., Lewandowski, M., Offenberg, J. H., Lewis, C. W., Bhave, P. V. and Edney, E. O.: Estimates of the contributions of biogenic and anthropogenic hydrocarbons to secondary organic aerosol at a southeastern US location, Atmos. Environ., 41(37), 8288–8300, doi:10.1016/j.atmosenv.2007.06.045, 2007.

Kolská, Z., Růžička, V. and Gani, R.: Estimation of the Enthalpy of Vaporization and the Entropy of Vaporization for Pure Organic Compounds at 298.15 K and at Normal Boiling Temperature by a Group Contribution Method, Ind. Eng. Chem. Res., 44(22), 8436–8454, doi:10.1021/ie050113x, 2005.

Kroll, J. H., Ng, N. L., Murphy, S. M., Flagan, R. C. and Seinfeld, J. H.: Secondary organic aerosol formation from isoprene photooxidation under high-NOx conditions, Geophys. Res. Lett., 32(18), L18808, doi:10.1029/2005GL023637, 2005.

Kroll, J. H., Ng, N. L., Murphy, S. M., Flagan, R. C. and Seinfeld, J. H.: Secondary Organic Aerosol Formation from Isoprene Photooxidation, Environ. Sci. Technol., 40(6), 1869–1877, doi:10.1021/es0524301, 2006.

Kuwata, M., Shao, W., Lebouteiller, R. and Martin, S. T.: Classifying organic materials by oxygen-to-carbon elemental ratio to predict the activation regime of Cloud Condensation Nuclei (CCN), Atmospheric Chem. Phys., 13(10), 5309–5324, doi:10.5194/acp-13-5309-2013, 2013.

Kuwata, M., Liu, Y., McKinney, K. and Martin, S. T.: Physical state and acidity of inorganic sulfate can regulate the production of secondary organic material from isoprene photooxidation products, Phys. Chem. Chem. Phys., 17(8), 5670–5678, doi:10.1039/C4CP04942J, 2015.

Lewandowski, M., Jaoui, M., Offenberg, J. H., Krug, J. D. and Kleindienst, T. E.: Atmospheric oxidation of isoprene and 1,3-butadiene: influence of aerosol acidity and relative humidity on secondary organic aerosol, Atmos Chem Phys, 15(7), 3773–3783, doi:10.5194/acp-15-3773-2015, 2015.

Liao, J., Froyd, K. D., Murphy, D. M., Keutsch, F. N., Yu, G., Wennberg, P. O., St. Clair, J. M., Crounse, J. D., Wisthaler, A., Mikoviny, T., Jimenez, J. L., Campuzano-Jost, P., Day, D. A., Hu, W., Ryerson, T. B., Pollack, I. B., Peischl, J., Anderson, B. E., Ziemba, L. D., Blake, D. R., Meinardi, S. and Diskin, G.: Airborne measurements of organosulfates over the continental U.S., J. Geophys. Res. Atmospheres, 120(7), 2014JD022378, doi:10.1002/2014JD022378, 2015.

Liggio, J., Li, S.-M. and McLaren, R.: Heterogeneous Reactions of Glyoxal on Particulate Matter: Identification of Acetals and Sulfate Esters, Environ. Sci. Technol., 39, 1532–1541, doi:10.1021/es048375y, 2005.

Li, J. and Jang, M.: Aerosol Acidity Measurement Using Colorimetry Coupled With a Reflectance UV-Visible Spectrometer, Aerosol Sci. Technol., 46(8), 833–842, doi:10.1080/02786826.2012.669873, 2012.

Li, J., Jang, M. and Beardsley, R. L.: Dialkylsulfate formation in sulfuric acid-seeded secondary organic aerosol produced using an outdoor chamber under natural sunlight, Environ. Chem., doi:10.1071/EN15129, 2015.

Limbeck, A., Kulmala, M. and Puxbaum, H.: Secondary organic aerosol formation in the atmosphere via heterogeneous reaction of gaseous isoprene on acidic particles, Geophys. Res. Lett., 30(19), 1996, doi:10.1029/2003GL017738, 2003.

Lim, Y. B., Tan, Y., Perri, M. J., Seitzinger, S. P. and Turpin, B. J.: Aqueous chemistry and its role in secondary organic aerosol (SOA) formation, Atmospheric Chem. Phys., 10(21), 10521–10539, doi:10.5194/acp-10-10521-2010, 2010.

Lin, Y.-H., Zhang, Z., Docherty, K. S., Zhang, H., Budisulistiorini, S. H., Rubitschun, C. L., Shaw, S. L., Knipping, E. M., Edgerton, E. S., Kleindienst, T. E., Gold, A. and Surratt, J. D.: Isoprene Epoxydiols as Precursors to Secondary Organic Aerosol Formation: Acid-Catalyzed Reactive Uptake Studies with Authentic Compounds, Environ. Sci. Technol., 46(1), 250–258, doi:10.1021/es202554c, 2012.

Marais, E. A., Jacob, D. J., Jimenez, J. L., Campuzano-Jost, P., Day, D. A., Hu, W., Krechmer, J., Zhu, L., Kim, P. S., Miller, C. C., Fisher, J. A., Travis, K., Yu, K., Hanisco, T. F., Wolfe, G. M., Arkinson, H. L., Pye, H. O. T., Froyd, K. D., Liao, J. and McNeill, V. F.: Aqueous-phase mechanism for secondary organic aerosol formation from isoprene: application to the southeast United States and co-benefit of SO2 emission controls, Atmos Chem Phys, 16(3), 1603–1618, doi:10.5194/acp-16-1603-2016, 2016.

Matsunaga, A. and Ziemann, P. J.: Gas-Wall Partitioning of Organic Compounds in a Teflon Film Chamber and Potential Effects on Reaction Product and Aerosol Yield Measurements, Aerosol Sci. Technol., 44(10), 881–892, doi:10.1080/02786826.2010.501044, 2010.

McNeill, V. F., Woo, J. L., Kim, D. D., Schwier, A. N., Wannell, N. J., Sumner, A. J. and Barakat, J. M.: Aqueous-Phase Secondary Organic Aerosol and Organosulfate Formation in Atmospheric Aerosols: A Modeling Study, Environ. Sci. Technol., 46(15), 8075–8081, doi:10.1021/es3002986, 2012.

Minerath, E. C., Casale, M. T. and Elrod, M. J.: Kinetics Feasibility Study of Alcohol Sulfate Esterification Reactions in Tropospheric Aerosols, Environ. Sci. Technol., 42(12), 4410–4415, doi:10.1021/es8004333, 2008.

Murphy, D. M., Cziczo, D. J., Froyd, K. D., Hudson, P. K., Matthew, B. M., Middlebrook, A. M., Peltier, R. E., Sullivan, A., Thomson, D. S. and Weber, R. J.: Single-particle mass spectrometry of tropospheric aerosol particles, J. Geophys. Res. Atmospheres, 111(D23), D23S32, doi:10.1029/2006JD007340, 2006.

Ng, N. L., Kwan, A. J., Surratt, J. D., Chan, A. W. H., Chhabra, P. S., Sorooshian, A., Pye, H. O. T., Crounse, J. D., Wennberg, P. O., Flagan, R. C. and Seinfeld, J. H.: Secondary organic aerosol (SOA) formation from reaction of isoprene with nitrate radicals (NO3), Atmospheric Chem. Phys., 8, 4117–4140, doi:10.5194/acp-8-4117-2008, 2008.

Nguyen, T. B., Bateman, A. P., Bones, D. L., Nizkorodov, S. A., Laskin, J. and Laskin, A.: High-resolution mass spectrometry analysis of secondary organic aerosol generated by ozonolysis of isoprene, Atmos. Environ., 44(8), 1032–1042, doi:10.1016/j.atmosenv.2009.12.019, 2010.

Nguyen, T. B., Roach, P. J., Laskin, J., Laskin, A. and Nizkorodov, S. A.: Effect of humidity on the composition of isoprene photooxidation secondary organic aerosol, Atmos Chem Phys, 11(14), 6931–6944, doi:10.5194/acp-11-6931-2011, 2011.

Odum, J. R., Hoffman, T., Bowman, F., Collins, D., Flagan, R. C. and Seinfeld, J. H.: Gas/Particle Partitioning and Secondary Organic Aerosol Yields, Environ. Sci. Technol., 30(8), 2580–2585, 1996.

Pandis, S. N., Paulson, S. E., Seinfeld, J. H. and Flagan, R. C.: Aerosol formation in the photooxidation of isoprene and β-pinene, Atmospheric Environ. Part Gen. Top., 25(5–6), 997–1008, doi:10.1016/0960-1686(91)90141-S, 1991.

Pankow, J. F.: An absorption model of gas/particle partitioning of organic compounds in the atmosphere, Atmos. Environ., 28(2), 185–188, doi:10.1016/1352-2310(94)90093-0, 1994.

Paulot, F., Crounse, J. D., Kjaergaard, H. G., Kürten, A., Clair, J. M. S., Seinfeld, J. H. and Wennberg, P. O.: Unexpected Epoxide Formation in the Gas-Phase Photooxidation of Isoprene, Science, 325(5941), 730–733, doi:10.1126/science.1172910, 2009.

Pinho, P. G., Pio, C. A. and Jenkin, M. E.: Evaluation of isoprene degradation in the detailed tropospheric chemical mechanism, MCM v3, using environmental chamber data, Atmos. Environ., 39(7), 1303–1322, doi:10.1016/j.atmosenv.2004.11.014, 2005.

Pye, H. O. T., Pinder, R. W., Piletic, I. R., Xie, Y., Capps, S. L., Lin, Y.-H., Surratt, J. D., Zhang, Z., Gold, A., Luecken, D. J., Hutzell, W. T., Jaoui, M., Offenberg, J. H., Kleindienst, T. E., Lewandowski, M. and Edney, E. O.: Epoxide Pathways Improve Model Predictions of Isoprene Markers and Reveal Key Role of Acidity in Aerosol Formation, Environ. Sci. Technol., 47(19), 11056–11064, doi:10.1021/es402106h, 2013.

R. M. Kamens, M. W. Gery, H. E. Jeffries, M. Jackson and E. I. Cole: Ozone-isoprene reactions: Product formation and aerosol potential, Int. J. Chem. Kinet. - INT J CHEM KINET, 14(9), 955–975, doi:10.1002/kin.550140902, 1982.

Rollins, A. W., Browne, E. C., Min, K.-E., Pusede, S. E., Wooldridge, P. J., Gentner, D. R., Goldstein, A. H., Liu, S., Day, D. A., Russell, L. M. and Cohen, R. C.: Evidence for NOx Control over Nighttime SOA Formation, Science, 337(6099), 1210–1212, doi:10.1126/science.1221520, 2012.

Saunders, S. M., Jenkin, M. E., Derwent, R. G. and Pilling, M. J.: World wide web site of a master chemical mechanism (MCM) for use in tropospheric chemistry models, Atmospheric Environ. - ATMOS Env., 31(8), 1249–1249, doi:10.1016/S1352-2310(97)85197-7, 1997.

Saunders, S. M., Jenkin, M. E., Derwent, R. G. and Pilling, M. J.: Protocol for the development of the Master Chemical Mechanism, MCM v3 (Part A): tropospheric degradation of non-aromatic volatile organic compounds, Atmos Chem Phys, 3(1), 161–180, doi:10.5194/acp-3-161-2003, 2003.

Schell, B., Ackermann, I. J., Hass, H., Binkowski, F. S. and Ebel, A.: Modeling the formation of secondary organic aerosol within a comprehensive air quality model system, J. Geophys. Res. Atmospheres, 106(D22), 28275–28293, doi:10.1029/2001JD000384, 2001.

Song, M., Liu, P. F., Hanna, S. J., Li, Y. J., Martin, S. T. and Bertram, A. K.: Relative humidity-dependent viscosities of isoprene-derived secondary organic material and atmospheric implications for isoprene-dominant forests, Atmos Chem Phys, 15(9), 5145–5159, doi:10.5194/acp-15-5145-2015, 2015.

Stein, S. E. and Brown, R. L.: Estimation of normal boiling points from group contributions, J. Chem. Inf. Model., 34(3), 581–587, doi:10.1021/ci00019a016, 1994.

Surratt, J. D., Murphy, S. M., Kroll, J. H., Ng, N. L., Hildebrandt, L., Sorooshian, A., Szmigielski, R., Vermeylen, R., Maenhaut, W., Claeys, M., Flagan, R. C. and Seinfeld, J. H.: Chemical composition of secondary organic aerosol formed from the photooxidation of isoprene, J. Phys. Chem. A, 110(31), 9665–9690, doi:10.1021/jp061734m, 2006.

Surratt, J. D., Lewandowski, M., Offenberg, J. H., Jaoui, M., Kleindienst, T. E., Edney, E. O. and Seinfeld, J. H.: Effect of Acidity on Secondary Organic Aerosol Formation from Isoprene, Environ. Sci. Technol., 41(15), 5363–5369, doi:10.1021/es0704176, 2007.

Surratt, J. D., Chan, A. W. H., Eddingsaas, N. C., Chan, M., Loza, C. L., Kwan, A. J., Hersey, S. P., Flagan, R. C., Wennberg, P. O. and Seinfeld, J. H.: Reactive intermediates revealed in secondary organic aerosol formation from isoprene, Proc. Natl. Acad. Sci. U. S. A., 107(15), 6640–6645, doi:10.1073/pnas.0911114107, 2010.

Virtanen, A., Joutsensaari, J., Koop, T., Kannosto, J., Yli-Pirilä, P., Leskinen, J., Mäkelä, J. M., Holopainen, J. K., Pöschl, U., Kulmala, M., Worsnop, D. R. and Laaksonen, A.: An amorphous solid state of biogenic secondary organic aerosol particles, Nature, 467(7317), 824–827, doi:10.1038/nature09455, 2010.

Volkamer, R., San Martini, F., Molina, L. T., Salcedo, D., Jimenez, J. L. and Molina, M. J.: A missing sink for gas-phase glyoxal in Mexico City: Formation of secondary organic aerosol, Geophys. Res. Lett., 34(19), L19807, doi:10.1029/2007GL030752, 2007.

Waxman, E. M., Elm, J., Kurtén, T., Mikkelsen, K. V., Ziemann, P. J. and Volkamer, R.: Glyoxal and Methylglyoxal Setschenow Salting Constants in Sulfate, Nitrate, and Chloride Solutions: Measurements and Gibbs Energies, Environ. Sci. Technol., 49(19), 11500–11508, doi:10.1021/acs.est.5b02782, 2015.

Wiedinmyer, C., Friedfeld, S., Baugh, W., Greenberg, J., Guenther, A., Fraser, M. and Allen, D.: Measurement and analysis of atmospheric concentrations of isoprene and its reaction products in central Texas, Atmos. Environ., 35(6), 1001–1013, doi:10.1016/S1352-2310(00)00406-4, 2001.

Woo, J. L. and McNeill, V. F.: simpleGAMMA v1.0 – a reduced model of secondary organic aerosol formation in the aqueous aerosol phase (aaSOA), Geosci. Model Dev., 8(6), 1821–1829, doi:10.5194/gmd-8-1821-2015, 2015.

Xu, L., Kollman, M. S., Song, C., Shilling, J. E. and Ng, N. L.: Effects of NOx on the Volatility of Secondary Organic Aerosol from Isoprene Photooxidation, Environ. Sci. Technol., 48(4), 2253–2262, doi:10.1021/es404842g, 2014.

Xu, L., Guo, H., Boyd, C. M., Klein, M., Bougiatioti, A., Cerully, K. M., Hite, J. R., Isaacman-VanWertz, G., Kreisberg, N. M., Knote, C., Olson, K., Koss, A., Goldstein, A. H., Hering, S. V., Gouw, J. de, Baumann, K., Lee, S.-H., Nenes, A., Weber, R. J. and Ng, N. L.: Effects of anthropogenic emissions on aerosol formation from isoprene and monoterpenes in the southeastern United States, Proc. Natl. Acad. Sci., 112(1), 37–42, doi:10.1073/pnas.1417609112, 2015.

Zhang, H., Worton, D. R., Lewandowski, M., Ortega, J., Rubitschun, C. L., Park, J.-H., Kristensen, K., Campuzano-Jost, P., Day, D. A., Jimenez, J. L., Jaoui, M., Offenberg, J. H., Kleindienst, T. E., Gilman, J., Kuster, W. C., de Gouw, J., Park, C., Schade, G. W., Frossard, A. A., Russell, L., Kaser, L., Jud, W., Hansel, A., Cappellin, L., Karl, T., Glasius, M., Guenther, A., Goldstein, A. H., Seinfeld, J. H., Gold, A., Kamens, R. M. and Surratt, J. D.: Organosulfates as Tracers for Secondary Organic Aerosol (SOA) Formation from 2-Methyl-3-Buten-2-ol (MBO) in the Atmosphere, Environ. Sci. Technol., 46(17), 9437–9446, doi:10.1021/es301648z, 2012.

Zhang, X., Cappa, C. D., Jathar, S. H., McVay, R. C., Ensberg, J. J., Kleeman, M. J. and Seinfeld, J. H.: Influence of vapor wall loss in laboratory chambers on yields of secondary organic aerosol, Proc. Natl. Acad. Sci., 111(16), 5802–5807, doi:10.1073/pnas.1404727111, 2014.

Zhang, X., McVay, R. C., Huang, D. D., Dalleska, N. F., Aumont, B., Flagan, R. C. and Seinfeld, J. H.: Formation and evolution of molecular products in α-pinene secondary organic aerosol, Proc. Natl. Acad. Sci., 112(46), 14168–14173, doi:10.1073/pnas.1517742112, 2015.

Zhang, Y., Seigneur, C., Seinfeld, J. H., Jacobson, M., Clegg, S. L. and Binkowski, F. S.: A comparative review of inorganic aerosol thermodynamic equilibrium modules: similarities, differences, and their likely causes, Atmos. Environ., 34(1), 117–137, doi:10.1016/S1352-2310(99)00236-8, 2000.

Zhao, L., Li, P. and Yalkowsky, S. H.: Predicting the Entropy of Boiling for Organic Compounds, J. Chem. Inf. Model., 39(6), 1112–1116, doi:10.1021/ci990054w, 1999.

Table 1. Experimental conditions and resulting SOA data of the isoprene photooxidation experiments performed with and without inorganic acidic seed in the dual, outdoor UF APHOR chambers. [a] SOA yield ($Y_{SOA} = \Delta OM/\Delta Iso$) is calculated at the point of maximum organic mass (OM). [b] In Exp. SO2, SO_2 (g) was injected into the chamber to generate acidic seeds instead of directly injecting H_2SO_4 (aq).

Exp.	Date	RH (%)	Temp (K)	$[ISO]_0$ (ppb)	$[NO_x]_0$ (ppb)	VOC/NO_x (ppbC/ppb)	$[H_2SO_4]$ (µg m^{-3})	Y_{SOA}[a] (%)
ISO1	2015-01-27	27-66	279-298	839	241	17.4	0	2.5
SA1	2015-01-27	20-54	279-299	850	253	16.8	53	8.5
ISO2	2014-12-14	19-49	282-303	852	131	32.7	0	0.7
SA2	2014-12-14	14-40	284-305	857	130	32.5	40	4.8
SO2	2014-01-18	48-91	273-292	627	91	34.6	26[b]	3.0

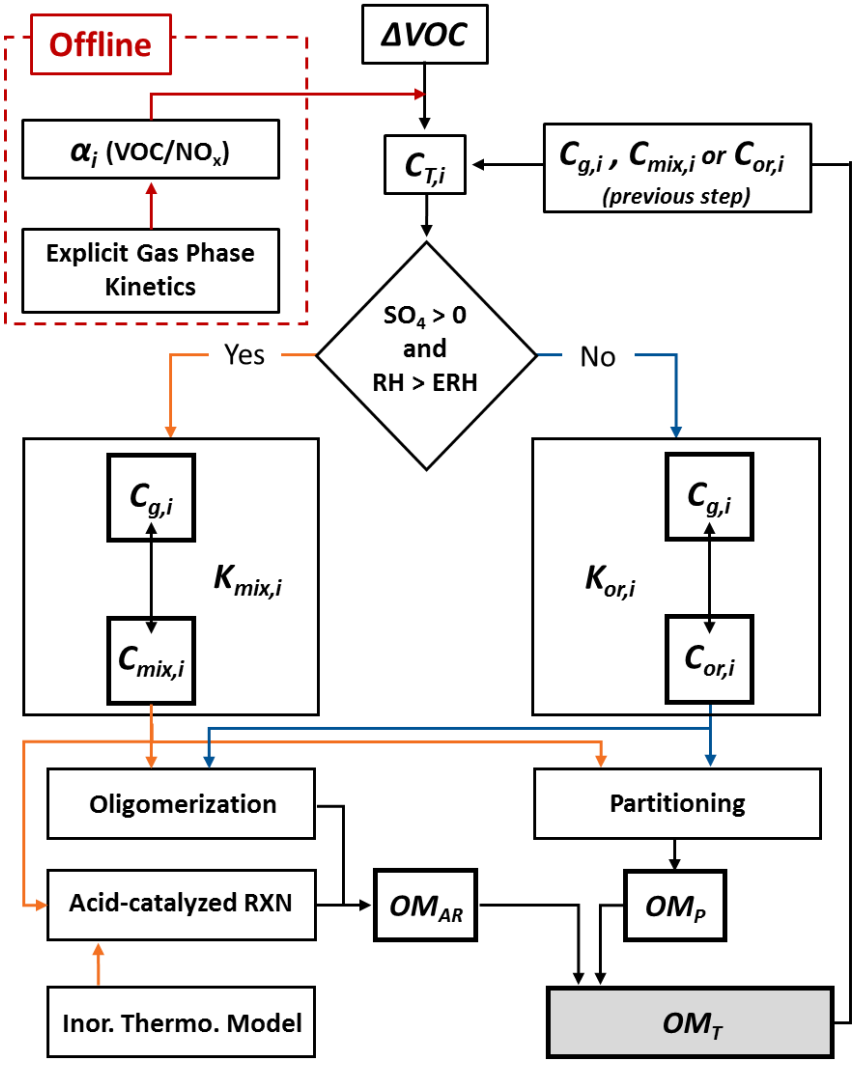

Figure 1. The overall schematic of the model applied to simulate isoprene SOA within UNIPAR. ~~$C_{T,i}$~~ $C_{T,i}$ is the total concentration of each lumping species, i, and $C_{g,i}$, $C_{mix,i}$, and $C_{or,i}$ are the concentrations of ~~of~~ each ~~lumping species, i,~~ within the gas, single homogenously mixed (SHMP) aerosol, and organic-only aerosol, repestively. ΔVOC is the consumption of the volatile organic compound of interest in each time step. α_i is the stoichiometric mass ratio

Formatted: Font: Not Italic

Formatted: Font: Italic

Formatted: Font: Italic, Subscript

of each *i*, which is calculated offline as a function of VOC/NO_x based on explicit gas phase simulations, and is used to distribute the total ΔVOC between each *i*. $K_{mix,i}$ and $K_{or,i}$ are the equilibrium partitioning coefficients for the SHMP and organic-only aerosol, respectively. OM_T, OM_P and OM_{AR} are the total organic mass and the organic mass from aerosol phase reactions and partitioning, respectively.

Formatted: Font: Italic
Formatted: Subscript
Formatted: Font: Italic
Formatted: Subscript
Formatted: Subscript
Formatted: Subscript

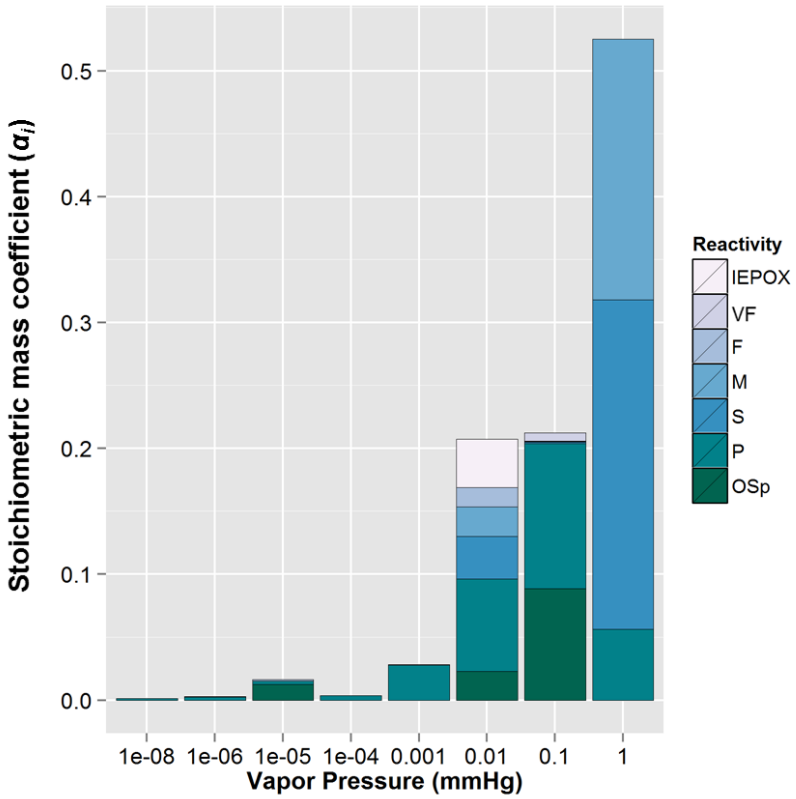

Figure 2. The stoichiometric mass coefficients (α_i) of each lumping group at a VOC/NO_x (ppbC/ppb) of 25. The photooxidation products predicted by an explicit gas phase chemical mechanism are lumped as a function of vapor pressure (x-axis, 8 bins) and aerosol phase reactivity (y-axis, 6 bins). The aerosol phase reactivity bins are very fast (VF, α-hydroxybicarbonyls and tricarbonyls), fast (F, 2 epoxides or aldehydes,), medium (M, 1 epoxide or aldehyde), slow (S, ketones), partitioning only (P), organosulfate precursors (OS_P, 3 or more alcohols) and IEPOX products, which were lumped separately to more easily quantify their contribution.

Formatted: Left

Formatted: Font: Italic

Formatted: Font: Italic, Subscript

1

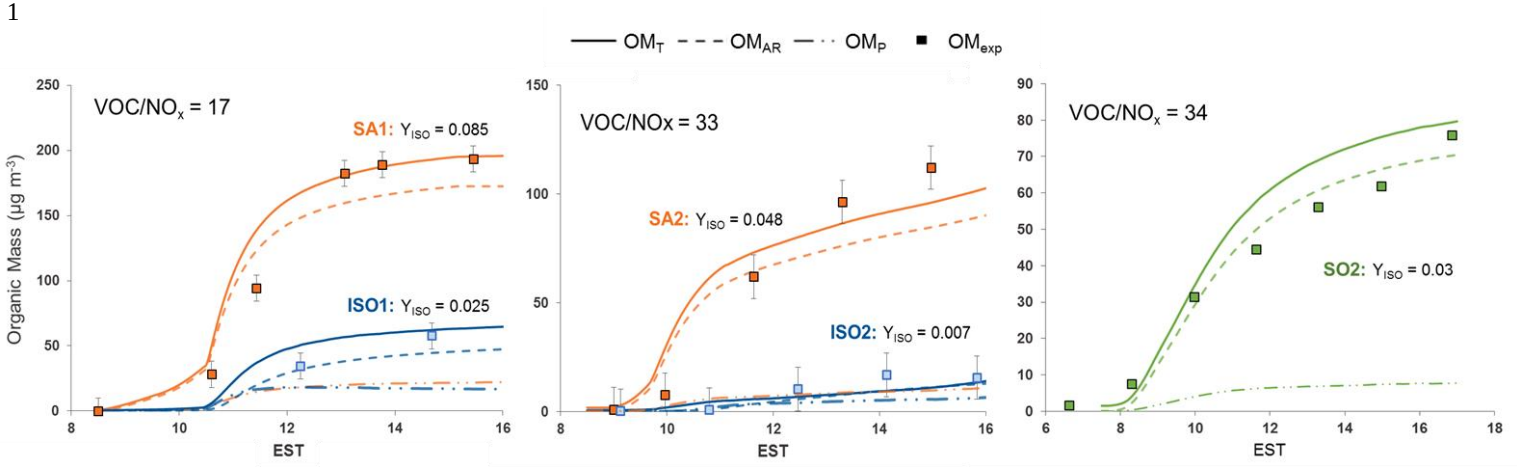

Figure 3. Time profiles of the experimentally measured and simulated SOA mass concentrations resulting from the photooxidation of isoprene. Data from experiments peformed in the absence of inoroganic seed is shown in blue, in the presence of sulfuric acid in orange, and in the presence of inorganic seed generated from SO_2 photooxidation in green. Solid, dashed, and dashed-dotted lines represent the simulated total organic mass (OM_T), organic mass from aerosol phase reactions (OM_{AR}), and organic mass from partitioning (OM_P), respectively. The experimental measured organic mass (OM_{exp}) is shown with square markers and is corrected for particle wall loss. The VOC/NO_x (ppbC/ppb) are shown for each experiment.

Formatted: Left: 1.38", Right: 0.79", Top: 0.98", Bottom: 0.98", Width: 11.69", Height: 8.27", Header distance from edge: 0.59", Footer distance from edge: 0.98"

Formatted: Left

Formatted: Left, Tab stops: 1.92", Left

1

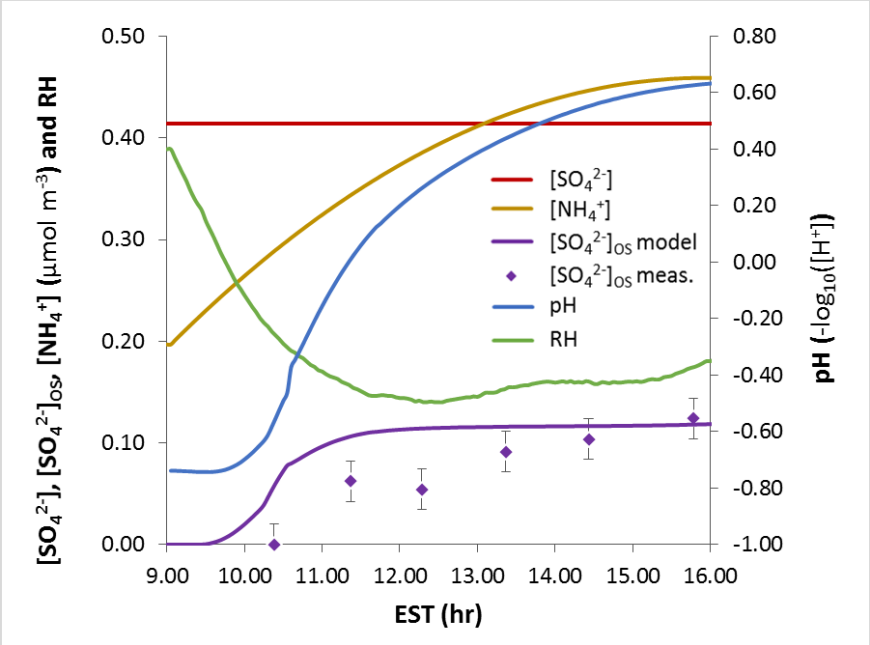

Figure 4. Time profiles of the total inorganic sulfate ($[SO_4^{2-}]$) and ammonium ($[NH_4^+]$) concentrations, and RH from Experiment SA2, along with the measured and model predicted concentrations of the sulfate associated with organosulfates (OS) ($[SO_4^{2-}]_{OS}$), and the predicted particle pH.

\

Formatted: Left

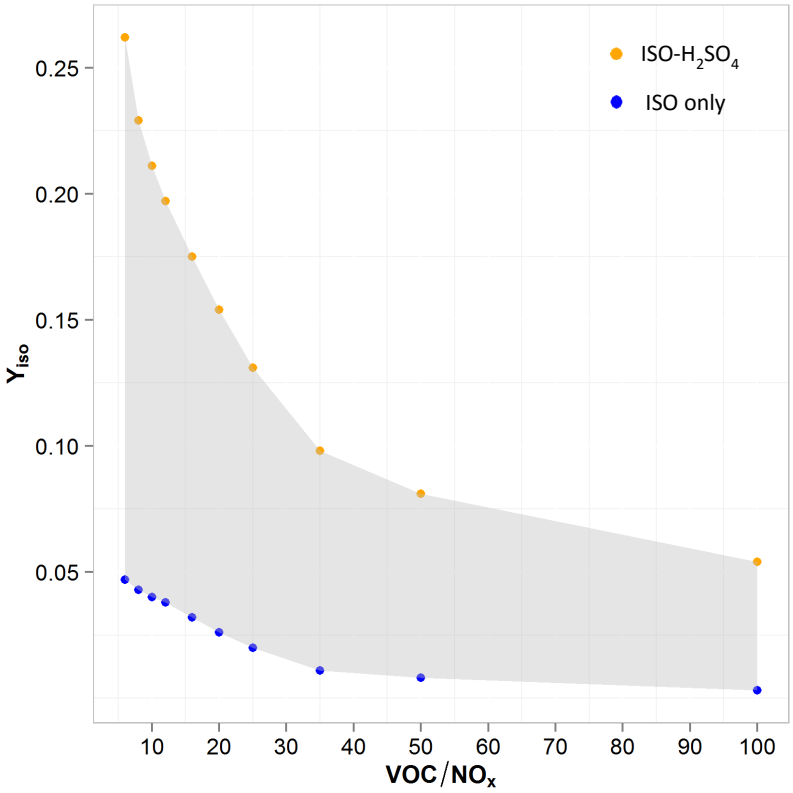

Figure 45. Simulated isoprene SOA yields (Y_{SOA} = $\Delta OM/\Delta Iso$) as a function of VOC/NO_x (ppbC/ppb) for values 10 to 100. The simulations were performed using the experimental conditions of SA1 (Table 1) without inorganic seed (blue) and in the presence of untitrated sulfuric acid (orange).

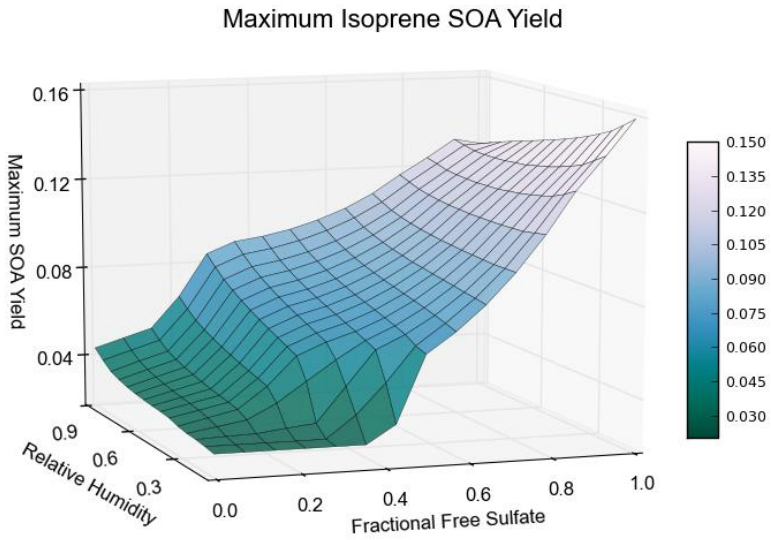

Figure ~~5~~6. Simulated isoprene SOA yields (Y_{SOA} = $\Delta OM/\Delta Iso$) as a function of relative humidity (RH) and fractional free sulfate (FFS= $([SO_4^{2-}]-0.5[NH_4^+])/[SO_4^{2-}]$). Using the experimental conditions of SA1, the RH and FFS were varied to determine the impact of acidity and aerosol liquid water content on Y_{SOA}.

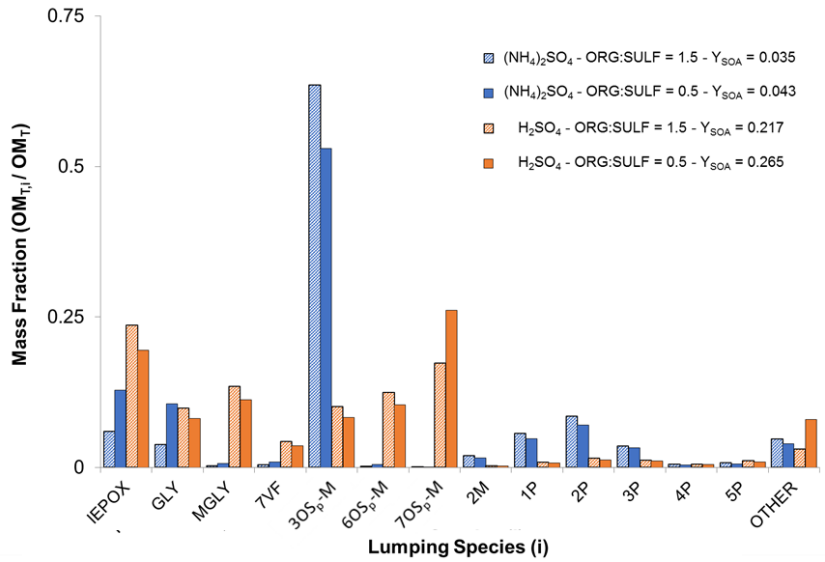

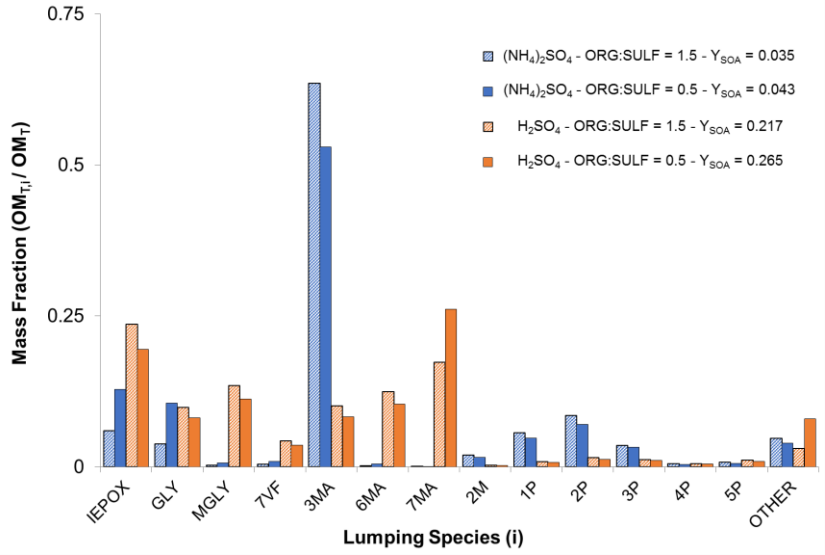

Figure ~~6~~7. The mass fraction ($MF_i = OM_{T,i}/ OM_T$) of each lumping species, *i*, that contribute significantly to the simulated isoprene SOA in the presence of ammonium sulfate, $(NH_4)_2SO_4$, and sulfuric acid seeds, H_2SO_4, at organic to sulfur mass ratios of 0.5 and 1.5. The MF_i of the remaining lumping groups are summed and included in 'OTHER.' The MF_i, Y_{SOA}, and

org:sulf are calculated at the point of maximum SOA mass with an initial VOC/NO_x ratio of ~17 (Exp. SA1 in Table 1).

Formatted: Subscript

Cover Sheet for Supplemental Information (SI)

Simulating the SOA formation of isoprene from partitioning and aerosol phase reactions in the presence of inorganic acid

R. L. Beardsley[1] and M. Jang[1,*]

[1]Department of Environmental Engineering Sciences, University of Florida, P.O. Box 116450, Gainesville, FL 32611, USA

Correspondence to: M. Jang (mjang@ufl.edu)

Number of Figures: 7

Number of Tables: 2

Section S1: Gas phase simulations and lumping

Gas phase oxidation. The Master Chemical Mechanism v3.2 (Saunders et al., 1997, 2003) was employed within the Morpho Kinetc Solver (Jeffries, H.E. et al., 1998) to simulate isoprene photooxidation for the range of VOC/NO_x shown in Table S1. The simulations were run using the temperature (T), relative humidity (RH) and total ultra-violet radiation (UV) data measured on 23 April 2014 measured in the UF APHOR chamber (Figure S1). Then, the predicted gas phase concentrations of each species at the maximum HO_2/NO were used for lumping as a function of VOC/NO_x.

Table S1. Concentrations of isoprene and NO_x used in gas phase photooxidation simulations of isoprene used in lumping as a function of VOC/NO_x

ISO (ppb)	500	500	500	500	500	500	500	500	500	500	500
NOx (ppb)	25	40	50	75	100	150	200	300	400	500	625
VOC/NOx	**100**	**62.5**	**50**	**33.33**	**25**	**16.67**	**12.5**	**8.33**	**6.25**	**5**	**4**

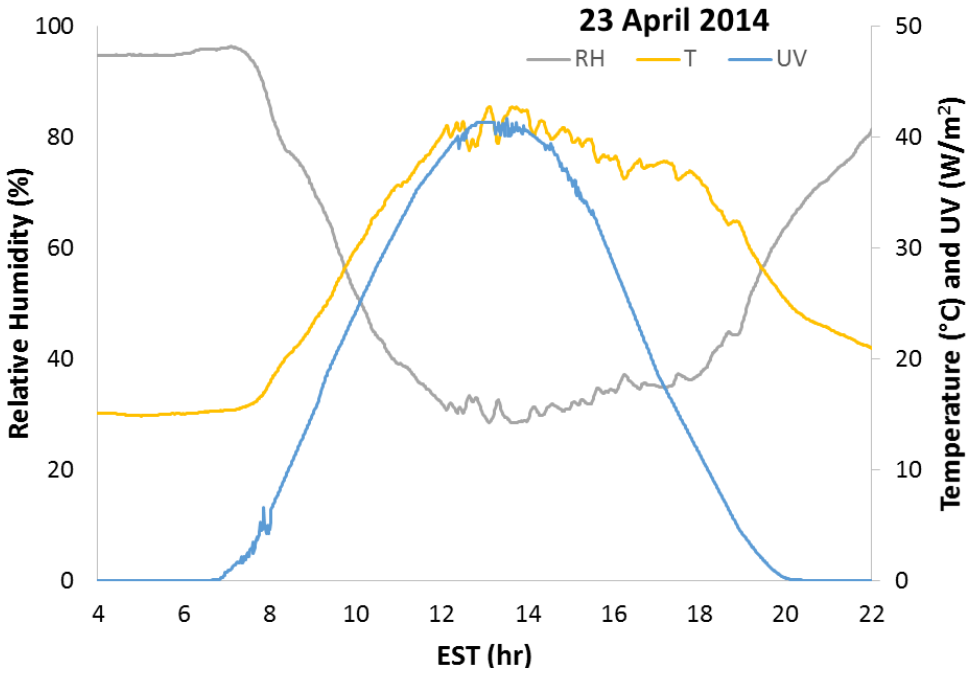

Figure S1. Time profile of relative humidity, temperature, and total ultra-violet radiation measured in the UF-APHOR chambers on 23 April 2014.

MCM and Morpho were also used to provide the ΔISO required by UNIPAR for each experimental simulation. It was determined that the MCM is reasonably representative of the actual

photooxidation by comparing the measured and predicted concentrations of isoprene, NO, NO_2 and O_3 in each experiment. Figure S2 shows the measured and modeled concentrations from the east chamber of experiment A on 27 January 2015 as an example. The major discrepancies in each simulation occur between the model and experimental values for O_3 and NO_2 as can be seen in Fig. S2. MCM predicts a higher O_3 concentration than reality and that it forms more quickly. On the other hand, while the predicted and measured peak NO_2 match reasonably well the measured NO_2 is higher than the predicted late in the experiment. This is likely due to organonitrates being detected as NO_2 by the chemiluminescence NO_x analyzer.

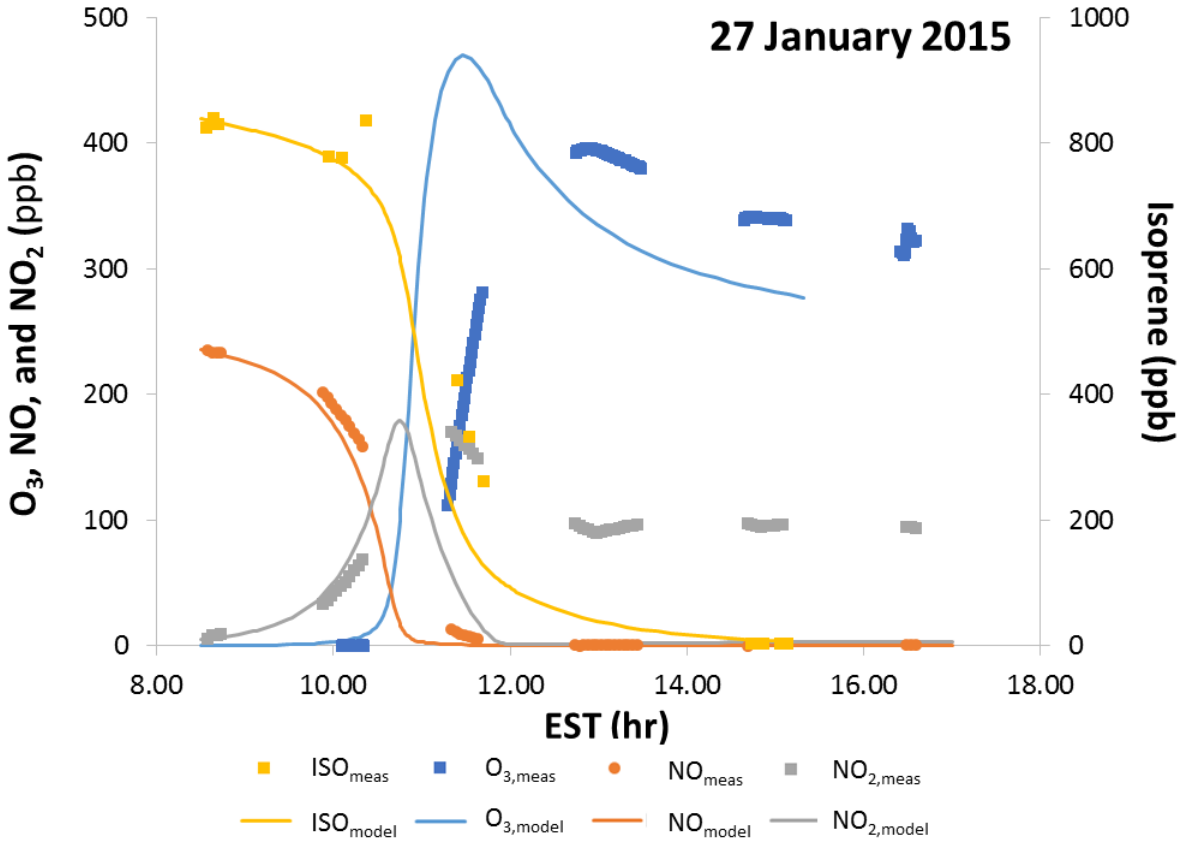

Figure S2. Time profile of the measured and predicted isoprene, NO, NO_2, and O_3 from 27 January, 2015 in the east UF-APHOR chamber.

Lumping. As is described in detail in Sect. 3.1, the products from MCM are lumped based on their vapor pressure and reactivity in aerosol phase reactions. Figure S3 shows the product of highest concentration in each lumping group when VOC/NO_x is 25. The empty groups are those for which isoprene has no photooxidation products.

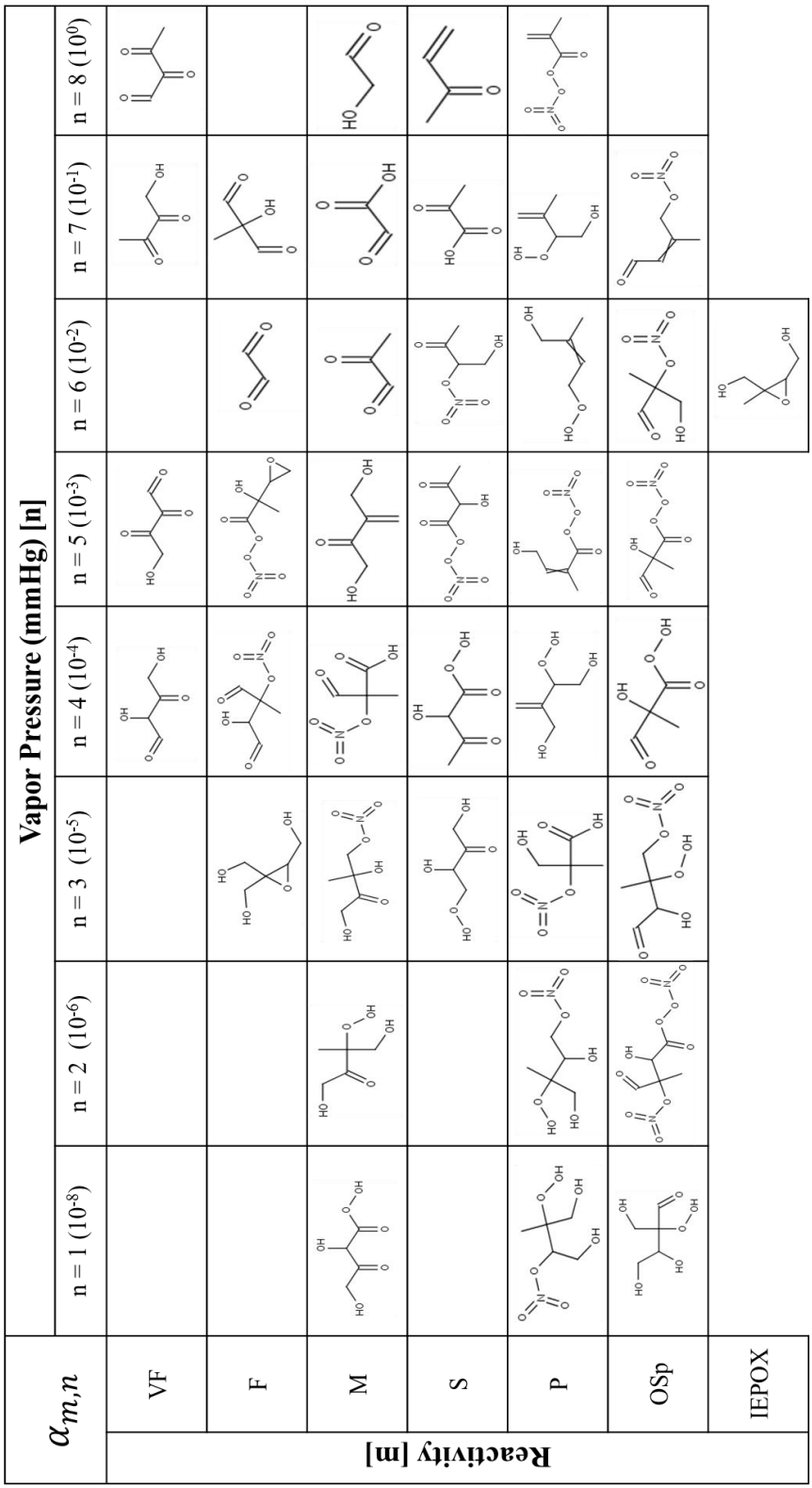

Figure S3. The lumping structure of UNIPAR filled with the product of highest concentration in each lumping group at a VOC/NO_x of 25. Empty bins represent lumping groups for which isoprene has no photooxidation products.

Section S2: Estimation of aerosol acidity([H^+])

In UNIPAR, the aerosol liquid water content (LWC) and acidity ([H^+]) are predicted using the inorganic thermodynamic model E-AIM II (Clegg et al., 1998) as a function of [SO_4^{2-}] and [$NH4^+$], corrected for the ammonia rich condition based on the results of Li and Jang (2012). Since isoprene are SHMP SOA, the interaction of organics and inorganics in the mixed phase may influence the dissociation of inorganic acids potentially leading to large deviations from the predicted [H^+]. AIOMFAC was employed to determine whether not this influence is significant. Table S2 shows the fractional dissociation of H_2SO_4 in the presence of varying amounts of tetrol and hexane, which represent polar and non-polar organic species. Although there is a reduction in the dissociation of sulfuric acid due to the presence of both tetrol and hexane, the maximum percent differencein these simulations is less than 12%. Based on these results, it was assumed that protonation is not significantly impacted by the presence of organics, and the [H^+] predicted by the inorganic composition is simply diluted by the concentration of organics in each time step. This assumption introduces uncertainty into the prediction of aerosol phase reactions, but there is not currently an approach with little uncertainty to predict [H^+] of mixed inorganic/organic aerosol composed of a large number of species.

Table S2. Output from AIOMFAC simulations performed to determine the impact of the presence of organics on the protonation of sulfuric acid. Tetrol and hexane were used to represent polar and non-polar organics.

organic	RH(%)	X_{org}	X_{H+}	X_{SO4}	X_{HSO4}	H/(H+SO4+HSO4)
tetrol	46.35	0.000	0.150	0.039	0.072	0.575
tetrol	44.04	0.194	0.120	0.005	0.110	0.510
tetrol	47.66	0.114	0.125	0.011	0.103	0.523
tetrol	20.06	0.000	0.202	0.042	0.118	0.558
tetrol	20.51	0.366	0.169	0.003	0.164	0.504
tetrol	19.71	0.204	0.216	0.012	0.192	0.514
hexane	49.98	0.000	0.143	0.038	0.067	0.577
hexane	51.98	0.210	0.125	0.018	0.090	0.538
hexane	50.97	0.089	0.114	0.026	0.063	0.563
hexane	20.06	0.000	0.202	0.042	0.118	0.558
hexane	21.05	0.204	0.203	0.008	0.187	0.510
hexane	22.56	0.382	0.185	0.022	0.141	0.531

Section S3. Derivation of the model equations used to predict the organic mass from aerosol phase reactions (OM_{AR})

In modeling isoprene SOA formation in the presence of a SHMP aerosol, the total concentration ($C_{T,i}$, μg m^{-3} of air) of each lumping species ($i_{m,n}$) is split solely between $C_{g,i}$ and $C_{mix,i}$ (Eq. S1) by a single gas-particle partitioning coefficient, $K_{mix,i}$ (m^3 μg^{-1}),

$$C_{T,i} = C_{g,i} + C_{mix,i}, \tag{S1}$$

$$K_{mix,i} = \frac{C_{mix,i}}{C_{g,i} M_{mix}}, \tag{S2}$$

where M_{mix} is the mass of the total suspended matter and is the sum of the inorganic mass (M_{in}) and the total organic mass (OM_T).

$C_{mix,i}$ and $C_{g,i}$ can be determined by combining Eq. S3 and Eq. S4 as follows,

$$C_{mix,i} = C_{T,i}\left(\frac{K_{mix,i} M_{mix}}{1 + K_{mix,i} M_{mix}}\right) \tag{S3}$$

$$C_{g,i} = C_{T,i}\left(\frac{1}{1 + K_{mix,i} M_{mix}}\right) \tag{S4}$$

Calculation of $K_{mix,i}$ (Eq. S5) follows the gas-particle absorption model (Pankow, 1994).

$$K_{mix,i} = \frac{7.501\,\mathrm{RT}}{10^9\, MW_{mix} \gamma_{mix,i}\, p^o_{L,i}}, \tag{S5}$$

where R is the gas constant (8.314 J K^{-1} mol^{-1}), T is the temperature (K), MW_{mix} is the average molecular weight (g mol^{-1}) of the SHMP aerosol, $\gamma_{mix,i}$ is the activity coefficient of the lumping species in the SHMP aerosol, and $p^o_{L,i}$ is the sub-cooled liquid vapor pressure (mmHg) of $i_{m,n}$.

Once $C_{mix,i}$ is determined for each Δt, the OM_{AR} formation of $i_{m,n}$ is estimated in UNIPAR assuming a second-order self-dimerization reaction as is shown in Eq. S6,

$$\frac{dC'_{mix,i}}{dt} = -k_{AR,i} C'^{\,2}_{mix,i}. \tag{S6}$$

where $C^{'}_{mix,i}$ is the aerosol phase concentration of $i_{m,n}$ in mol L^{-1} of medium and $k_{AR,i}$ (L mol^{-1} s^{-1}) is the aerosol phase reaction rate of each $i_{m,n}$. $k_{AR,i}$ (Eq. S7) is calculated each time step using the semi-empirical model developed by Jang et al. (2005) as a function of the reactivity, R (VF, F, M, S; Sect. 3.1), and pK_{BH+} of $i_{m,n}$ in the aerosol phase, $[H^+]$ and LWC (activity of water, a_w) from the inorganic thermodynamic model (Sect. 3.2), and the excess acidity, X (Im et al., 2014; Jang et al., 2006).

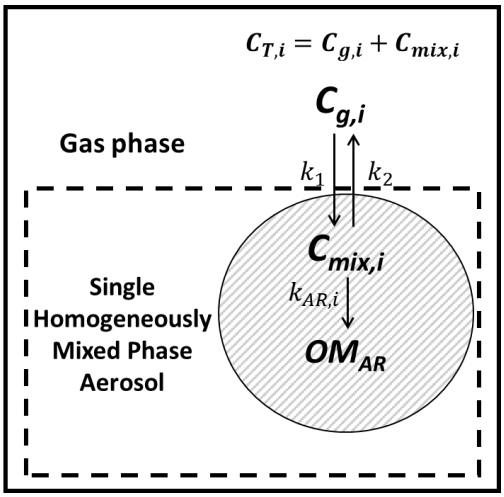

$$k_{AR,i} = 10^{(0.0005*pK_{BH^+}+y*X+1.3*R+\log(a_w)+\log([H^+])-5.5)} \quad \text{(S7)}$$

Then by assuming that OM_{AR} is non-volatile and irreversible, $\Delta OM_{AR,i}$ can be calculated as the reduction in $C_{T,i}$ for each time step (Eq. S8),

$$\Delta OM_{AR} = -\sum_i \Delta C_{T,i} = -\sum_i \int \frac{dC_{T,i}}{dt}. \quad \text{(S8)}$$

Where,

$$\frac{dC_{T,i}}{dt} = \frac{dC_{g,i}}{dt} + \frac{dC_{mix,i}}{dt} \quad \text{(S9)}$$

$$\frac{dC_{g,i}}{dt} = k_2 C_{mix,i} - k_1 C_{g,i} \quad \text{(S10)}$$

$$\frac{dC_{mix,i}}{dt} = k_1 C_{g,i} - k_2 C_{mix,i} - k_{AR,i} C_{mix,i}^2 f_{mix,i} \quad \text{(S11)}$$

$$\frac{dC_{T,i}}{dt} = k_2 C_{mix,i} - k_1 C_{g,i} + k_1 C_{g,i} - k_2 C_{mix,i} - k_{AR,i} C_{mix,i}^2 f_{mix,i} \quad \text{(S12)}$$

$$\frac{dC_{T,i}}{dt} = -k_{AR,i} {C_{mix,i}}^2 f_{mix,i} \quad \text{(S13)}$$

$C_{mix,i}$ is the concentration in μg/m^3 and $C^{'}_{mix,i}$ is the aerosol phase concentration of $i_{m,n}$ in mol L^{-1} of aerosol. $f_{mix,i}$ is the conversion factor from $C^{'}_{mix,i}$ to $C_{mix,i}$

$$C_{mix,i} = C_{T,i}\left(\frac{K_{mix,i}M_{mix}}{1+K_{mix,i}M_{mix}}\right) \text{ and } f_{mix,i} = \frac{C_{mix,i}}{C'_{mixi}} = \left(\frac{MW_i * M_{mix}}{\rho_{mix} 10^3}\right) \quad \text{(S14)}$$

$$\frac{dC_{T,i}}{dt} = -k_{AR,i}C_{T,i}^2\left(\frac{K_{mix,i}M_{mix}}{1+K_{mix,i}M_{mix}}\right)^2\left(\frac{MW_i * M_{mix}}{\rho_{mix}10^3}\right) \quad \text{(S15)}$$

Then, combining equations S8 and S15 and solving the second-order ODE provides the analytical solution utilized in UNIPAR (Eq. S16),

$$\Delta OM_{AR} = -\sum_i \frac{k_{AR,i}\beta_{3,i}C_{T,i}^2\Delta t}{1+k_{AR,i}\beta_{3,i}C_{T,i}\Delta t}, \quad \text{(S16)}$$

where $\beta_{3,i}$ is equal to

$$\beta_{3,i} = \frac{K_{mix,i}^2 M_{mix}\rho_{mix}10^3}{MW_i(1+K_{mix,i}M_{mix})^2}. \quad \text{(S17)}$$

Section S4: Prediction of the activity coefficients of organic species in SHMP isoprene SOA

As is described in Sect 3.3 of the manuscript, the non-ideality of each lumping species in the SHMP aerosol is accounted for by the acitivity coefficient $\gamma_{mix,i}$. $\gamma_{mix,i}$ will vary between each species due to differences in polarity and molar volume, and over time due to changes in aerosol phase composition. In order to estimate $\gamma_{mix,i}$ for the lumped isoprene photooxidation products,

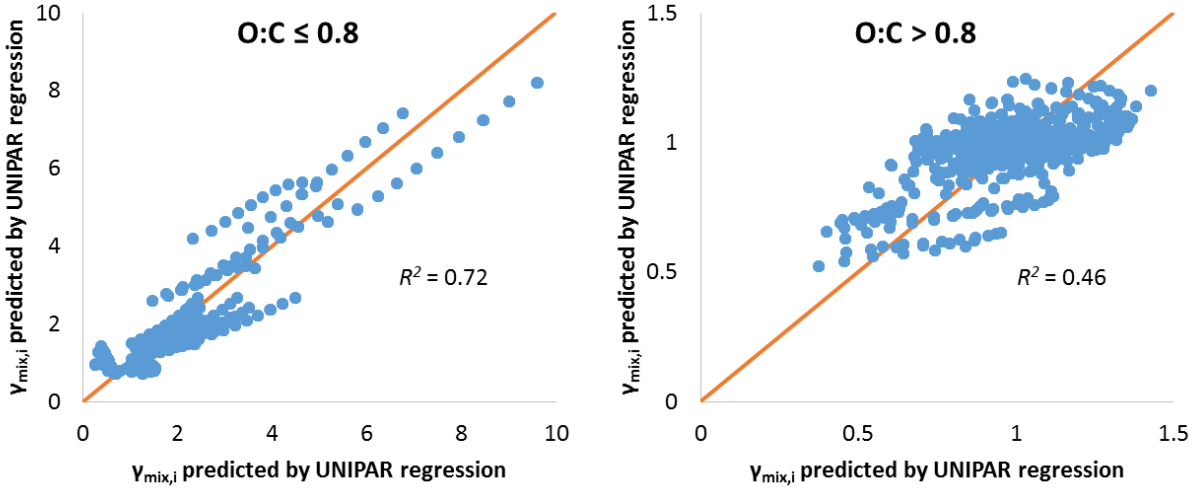

Figure S4. The $\gamma_{mix,i}$ predicted by AIOMFAC plotted against the $\gamma_{mix,i}$ predicted by the regressions in Eq. S18 and S19 along with a y=x line and the R^2.

AIOMFAC was run for the highest concentration product of each lumping group in the presence of a mixed isoprene SOA-ammonium sulfate aerosol with the SOA composition based on the results of Nguyen et al. (2011). The bulk organic to sulfur mass ratio (org:sulf), concentration of i, and RH were varied to cover the range of experimental values. The resulting $\gamma_{mix,i}$ were fit to the bulk org:sulf, ln(RH), the oxygen to carbon molar ratio ($O:C_i$) of i and molar volume($V_{mol,i}$) of i for two ranges of O:C. The parameterizations are shown in equations S18 and S19 below.

O:C ≤ 0.8

$$\ln(\gamma_{mix,i}) = 2.354 + 0.146 * \ln(RH) + 0.128 * org:sulf - 3.195 * O:C \quad \text{(S18)}$$

O:C > 0.8

$$\ln(\gamma_{mix,i}) = -0.229 + 0.050 * \ln(RH) - 0.011 * org:sulf - 0.252 * O:C + 0.007 * V_{mol,i} \quad \text{(S19)}$$

The regressions for $\gamma_{mix,i}$ have R^2 of 0.72 and 0.46 for O:C less than or equal to 0.8 and greater than 0.8, respectively, as is shown in Figure S4. The polar compounds used in fitting Eq S18 have AIOMFAC predicted $\gamma_{mix,i}$ that range from 0.5 to 5.5, while those of O:C greater than 0.8 only range from 0.5 to 1.5. The small range of $\gamma_{mix,i}$ for Eq. S14 leads to higher residuals and a lower R^2, but all of the values predicted by AIOMFAC and the regressions generated are close to unity minimizing the impact of error on model output.

Section S5. Concentration of isoprene SOA products as a function of VOC/NO_x

In both the simulated and experimental SOA formation of isoprene, there is an increase in SOA yield with increasing NO_x (decreasing VOC/NO_x), and the influence of NOx is stronger in the presence of acidity. The mass stoichiometric coefficients of products that contribute significantly to the simulated isoprene SOA are shown in Figure S5 below. The stochiometric coefficients are

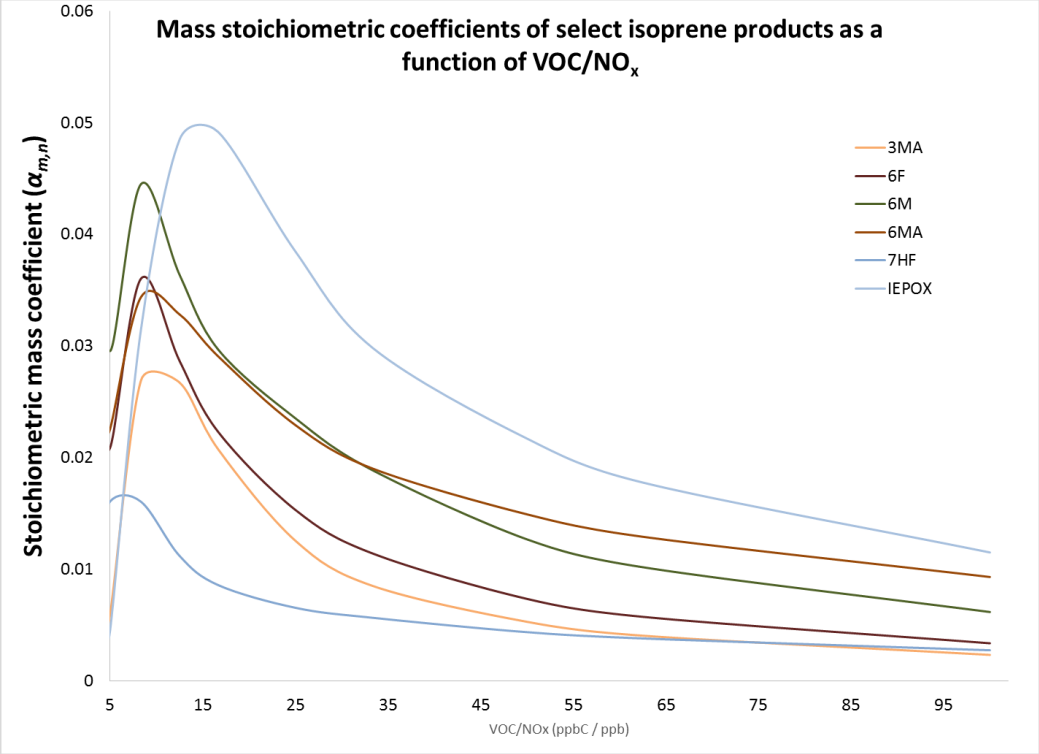

Figure S5. The stoichiometric mass coefficients ($\alpha_{m,n}$) of selected products which contribute significantly to isoprene SOA as a function of VOC/NO_x.

calculated using simulations based on the Master Chemical Mechanism within the Morpho Kinetc Solver (Sect. S1). As can be seen, all of the products are lower in concentration with a reduction in NOx under the conditions of this study (VOC/NO_x: 10 to 100). The reduction in products that are highly reactive in aerosol phase reactions, such as glyoxal (6F, in Figure S5) explains the increased sensitivity to VOC/NO_x in the presence of acidic seed.

Section S6. Model Sensitivity and Uncertainity

In order to determine the impact of the uncertainty of the underlying modules and parameterizations applied in UNIPAR, sensitivity tests were performed in which vapor pressure ($p^o_{L,i}$), enthalpy of vaporization (ΔH_{vap}), activity coefficient of i in the SHMP aerosol ($\gamma_{mix,i}$), and the aerosol phase reaction rate of i ($k_{AR,i}$) were increased and decreased by a factor chosen to exceed

the possible error of the method. After applying the factors, simulations of Exp. SA1 were performed and the resulting percent change in OM_T is shown in Figure S5.

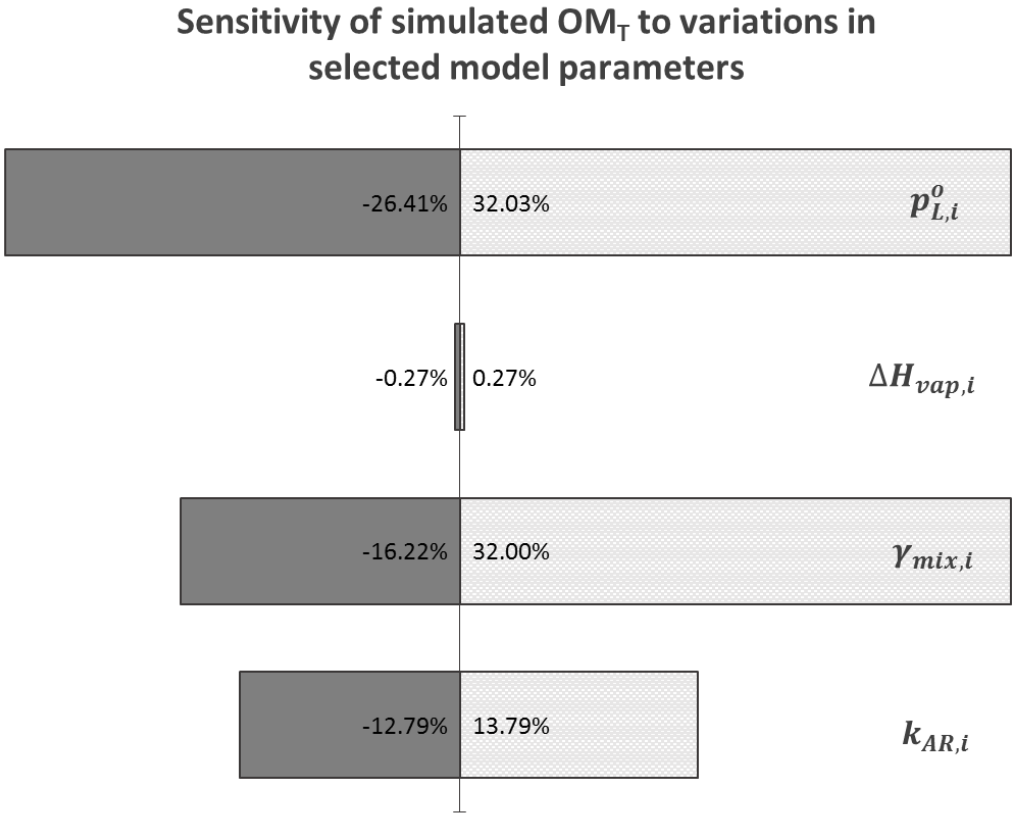

Figure S6. The percent change in the model predicted OM_T from experiment SA1 after each parameter was increased and decreased by a factor chosen to exceed the uncertainty of the underlying methods used for estimating each variable.

Section S7. Product structures of $3OS_p$-M

In the absence of inorganic aqueous phase, 70% of the total organic mass is predicted to be from lumping group $3OS_p$-M, which is comprised almost entirely of the organic peroxides, with the MCM products C510OOH (~40%), C57OOH (~27%), C58OOH(~15%) and HMACROOH(11%) making up approximately 93% (structures shown in Fig. S7)

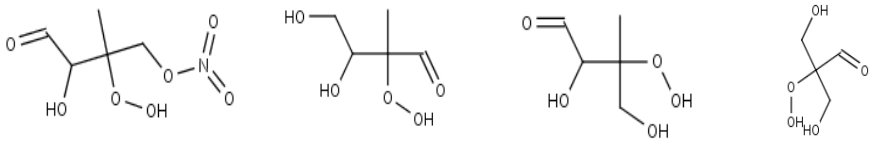

C510OOH C57OOH C58OOH HMACROOH

Figure S7. The structures of the organic peroxides that comprise lumping group $3OS_p$-M.

References:

Clegg, S. L., Brimblecombe, P. and Wexler, A. S.: Thermodynamic Model of the System H+−NH4+−SO42-−NO3-−H2O at Tropospheric Temperatures, J. Phys. Chem. A, 102(12), 2137–2154, doi:10.1021/jp973042r, 1998.

Im, Y., Jang, M. and Beardsley, R. L.: Simulation of aromatic SOA formation using the lumping model integrated with explicit gas-phase kinetic mechanisms and aerosol-phase reactions, Atmos Chem Phys, 14(8), 4013–4027, doi:10.5194/acp-14-4013-2014, 2014.

Jang, M., Czoschke, N. M. and Northcross, A. L.: Semiempirical Model for Organic Aerosol Growth by Acid-Catalyzed Heterogeneous Reactions of Organic Carbonyls, Environ. Sci. Technol., 39(1), 164–174, doi:10.1021/es048977h, 2005.

Jang, M., Czoschke, N. M., Northcross, A. L., Cao, G. and Shaof, D.: SOA Formation from Partitioning and Heterogeneous Reactions: Model Study in the Presence of Inorganic Species, Environ. Sci. Technol., 40(9), 3013–3022, doi:10.1021/es0511220, 2006.

Jeffries, H.E., Gary, M. W., Kessler, M and Sexton, K. G.: Morphecule reaction mechanism, Morpho., 1998.

Li, J. and Jang, M.: Aerosol Acidity Measurement Using Colorimetry Coupled With a Reflectance UV-Visible Spectrometer, Aerosol Sci. Technol., 46(8), 833–842, doi:10.1080/02786826.2012.669873, 2012.

Nguyen, T. B., Roach, P. J., Laskin, J., Laskin, A. and Nizkorodov, S. A.: Effect of humidity on the composition of isoprene photooxidation secondary organic aerosol, Atmos Chem Phys, 11(14), 6931–6944, doi:10.5194/acp-11-6931-2011, 2011.

Saunders, S. M., Jenkin, M. E., Derwent, R. G. and Pilling, M. J.: World wide web site of a master chemical mechanism (MCM) for use in tropospheric chemistry models, Atmospheric Environ. - ATMOS Env., 31(8), 1249–1249, doi:10.1016/S1352-2310(97)85197-7, 1997.

Saunders, S. M., Jenkin, M. E., Derwent, R. G. and Pilling, M. J.: Protocol for the development of the Master Chemical Mechanism, MCM v3 (Part A): tropospheric degradation of non-aromatic volatile organic compounds, Atmos Chem Phys, 3(1), 161–180, doi:10.5194/acp-3-161-2003, 2003.